

UNIVERSITY OF HAWAII LIBRARY

TOWARD ADVANCED ANALYSIS IN STEEL FRAME DESIGN

**A DISSERTATION SUBMITTED TO THE GRADUATE DIVISION OF THE
UNIVERSITY OF HAWAII IN PARTIAL FULFILLMENT OF THE
REQUIREMENTS FOR THE DEGREE OF**

DOCTOR OF PHILOSOPHY

IN

CIVIL ENGINEERING

MAY 2003

By

Ken Hwa

Dissertation Committee:

Wai-Fah Chen, Chairperson

Phillip S. K. Ooi

H. Ronald Riggs

Ian N. Robertson

Ronald H. Knapp

ACKNOWLEDGEMENTS

I would like to express my deepest appreciation to my advisor and committee chairperson, Professor Wai-Fah Chen, for his guidance and motivation during my learning career at Purdue University and University of Hawaii at Manoa. Whether through our numerous meetings and e-mails I have learned a lot from Professor Chen. His patience and encouragement gave me the confidence and willingness to overcome the many difficulties encountered while doing this research. He has shown concerns for my academic career at graduate level and also for my future. I believe his valuable advice *will benefit me throughout my future endeavors.*

I am grateful to Professor Ronald H. Knapp, Professor Phillip Ooi, Professor H. Ronald Riggs, and Professor Ian Robertson for serving on my graduate advisory committee. They have enriched my knowledge during the courses of my study at UH Manoa. The time they spent on reviewing my dissertation drafts and helpful comments are also very thankful. I would also like to acknowledge Professor Edmond D. H. Cheng, chairperson of the Department of Civil and Environmental Engineering, UH Manoa, for providing me with the valuable teaching opportunities and for creating a pleasant environment to further my studies.

I would also like to thank all my friends especially Tai-Kuang Lee, Yeon-Kang Wang, Chien-Lung Tien, Yan Liu, Linlin Huang, Stephanie Fung and Alison Agapay both for their friendship and for their help during my research.

Finally, I would like to present special thanks to my parents, for their consideration and support that made this work possible.

ABSTRACT

The trends for analysis and design of steel frames are indicated in this dissertation. The current practice consists of applying the first-order elastic analysis with amplification factors or second-order elastic analysis in combination with the AISC-LRFD interaction equations. Determination of the effective length factors and individual member capacity checks are necessary to select adequate structural member sizes. The direct analysis method is a second-order elastic analysis approach that eliminates the determination of effective length factors from the current AISC-LRFD method. Unsupported member length is used to calculate the axial strength of a member. Equivalent notional loads and/or modified stiffness are applied together with the external loads to account for the effects of initial out-of-plumbness and inelastic softening. For both AISC-LRFD and direct analysis methods, a structure is analyzed as a whole, but the axial and flexural strength of each member is examined individually. Inelastic redistribution of internal forces in the structural system cannot be considered. As a result, determined member forces are not correct and more conservative member sizes will be obtained. Moreover, member-based approaches cannot predict structural behaviors such as failure mode and overstength factor.

The advanced analysis method considered in this work is a second-order refined plastic hinge analysis in which both effective length factors and individual member capacity checks are not required. In addition, advanced analysis is a structure system-based analysis/design method that can overcome the difficulties of using member-based

design approaches. Thus, advanced analysis is a state-of-the-art method for steel structure design.

Several numerical examples are provided to show the design details of all three methods. The design requirements corresponding to each analysis approach are illustrated in these examples. The pros and cons of each method are discussed by comparing the design results.

Advanced analysis is also a computer-based analysis and design procedure consistent with the features of performance-based design. Applying advanced analysis to performance-based fire resistance and seismic design are proposed. This dissertation shows advanced analysis is efficient in predicting the duration that structures could support load under elevated temperature and capable of determining the performance level of a structure subjected to seismic forces.

TABLE OF CONTENTS

ACKNOWLEDGEMENTS	iii
ABSTRACT	iv
LIST OF TABLES	xii
LIST OF FIGURES	xv
CHAPTER 1: INTRODUCTION	1
1.1 Design Trends of Steel Framed Structures	1
1.2 Motivation	3
1.3 Objective.....	4
1.4 Scope.....	5
CHAPTER 2: LOAD AND RESISTANCE FACTOR DESIGN	7
2.1 Introduction.....	7
2.2 Overview of AISC-LRFD Method	8
2.2.1 Interaction Equations	8
2.2.2 Effective Length Factor K	9
2.2.3 Required Flexural Strength M_u	11
2.2.4 Column Strength P_n	13
2.2.5 Flexural Strength M_n	14
2.3 Two-Story Unbraced Steel Frame Example	16
2.3.1 Structural Configuration	16
2.3.2 Analysis	17
2.3.3 Adequacy Checks of Members	17

2.4 The Difficulties of Using AISC-LRFD Method	24
2.4.1 Effective Length Factors	24
2.4.2 Separate Member Capacity Checks	27
2.5 Summary	28
CHAPTER 3: DIRECT ANALYSIS METHOD	29
3.1 Introduction	29
3.2 Beam-Column Design with Unsupported Member Length by LRFD Method	30
3.3 Direct Analysis Method with Notional Load (DAM-NL Method)	34
3.3.1 The Application of DAM-NL Method to Steel Frame Analysis	36
3.3.2 Design Guidelines	37
3.3.3 Two-Story Unbraced Frame Example	38
3.4 Direct Analysis Method with Modified Stiffness (DAM-MS Method)	40
3.4.1 The Application of DAM-MS Method to Steel Frame Analysis	40
3.4.2 Design Guidelines	42
3.4.3 Two-Story Unbraced Frame Example	43
3.5 The Difficulties of Using Direct Analysis Method	45
3.5.1 Determination of the Directions of Notional Loads	45
3.5.2 Leaned Column Effects	46
3.6 Summary	46
CHAPTER 4: PRACTICAL ADVANCED ANALYSIS METHOD	48
4.1 Introduction	48
4.2 First-Order Hinge-by-Hinge Analysis	49
4.2.1 Assumptions	49
4.2.2 Analysis Procedures	50

4.2.3	Redistribution of Internal Forces	51
4.3	Second-Order Elastic-Plastic Hinge Model	54
4.3.1	Stability Functions	54
4.3.2	Incremental Force-Displacement Relationship	56
4.3.3	Modeling of Plastic Hinges	59
4.3.3.1	Cross-Section Plastic Strength	59
4.3.3.2	Modification of Element Stiffness for the Formation of Plastic Hinges	60
4.4	Second-Order Refined Plastic Hinge Method	63
4.4.1	Tangent Modulus Model Associated with Residual Stresses	64
4.4.2	Two-Surface Stiffness Degradation Model Associated with Flexure	66
4.4.3	Connection Nonlinearity	69
4.4.4	Initial Geometric Imperfections	71
4.4.4.1	Explicit Imperfection Modeling Method	71
4.4.4.2	Equivalent Notional Load Method	72
4.4.4.3	Further Reduced Tangent Modulus Method	75
4.5	Advantages of Advanced Analysis in Steel Design	76
4.6	Two-Story Unbraced Frame Example	78
4.6.1	Structural Modeling	78
4.6.2	Program Execution	79
4.6.3	Output Interpretation	82
4.6.4	Ductility Check	83
4.7	Summary	89

CHAPTER 5: GUIDELINES FOR PRACTICAL STEEL FRAME DESIGN USING ADVANCED ANALYSIS	91
5.1 Introduction	91
5.2 Design Format	91
5.3 Analysis and Design Procedures	92
5.3.1 Load Combinations	94
5.3.2 Preliminary Member Sizing	96
5.3.3 Modeling of Elements	96
5.3.4 Serviceability Checks	97
5.3.5 Modeling of Initial Geometric Imperfection	97
5.3.6 Determination of Incremental Loads	98
5.3.7 Preparation of Input Data	99
5.3.8 Execution of the Analysis Program	99
5.3.9 Ultimate Load Carrying Capacity Checks	103
5.3.10 Ductility Checks	103
5.3.11 Adjustment of Member Size	104
5.4 Summary	105
CHAPTER 6: NUMERICAL EXAMPLES	106
6.1 Introduction	106
6.2 Six-Story Frame	107
6.2.1 AISC-LRFD Method	107
6.2.2 Direct Analysis Method	119
6.2.2.1 Notional Load Method	119
6.2.2.2 Modified Stiffness Method	123

6.2.3	Advanced Analysis Method	125
6.2.4	Comparison of the Analysis/Design Results	126
6.3	Braced Frame	133
6.3.1	AISC-LRFD Method	135
6.3.2	Direct Analysis Method	137
6.3.3	Advanced Analysis Method	138
6.3.4	Comparison of the Analysis/Design Results	139
6.4	Leaned Column Frame	144
6.4.1	AISC-LRFD Method	145
6.4.2	Direct Analysis Method	148
6.4.2.1	Notional Load Method	148
6.4.2.2	Modified Stiffness Method	149
6.4.3	Advanced Analysis Method	150
6.4.4	Comparison of the Analysis/Design Results	151
6.5	Summary	155
CHAPTER 7: PERFORMANCE-BASED DESIGN		157
7.1	Introduction	157
7.2	Fire Resistance Design	158
7.2.1	Overview	159
7.2.2	Basic Assumptions	161
7.2.3	Verification	162
7.2.3.1	Simply Supported Beams	165
7.2.3.2	Steel Frames	167
7.2.4	Analysis Procedures	171

7.2.5 Multi-Story Frame Example	172
7.3 Seismic Design	179
7.3.1 Overview	180
7.3.1.1 Seismic Base Shear	180
7.3.1.2 Lateral Seismic Force	184
7.3.1.3 Combination of Load Effects	185
7.3.1.4 Drift Limitations	186
7.3.1.5 Spectral Response Acceleration	186
7.3.1.6 Expected Yield Stress	187
7.3.2 Performance-Based Seismic Design	188
7.3.3 Analysis Procedures	189
7.3.4 One-Bay Two-Story Steel Frame Example	189
7.4 Summary	195
CHAPTER 8: CONCLUSIONS	196
REFERENCES.....	199

LIST OF TABLES

	<u>Pages</u>
Table 2.1 Member capacity check of the two-story unbraced frame using AISC-LRFD method.....	23
Table 2.2 Effective length factor and axial capacity of the Column CD of the leaned column frame	27
Table 3.1 Comparison of axial strength of the cantilever beam-column with various slenderness parameters.....	33
Table 3.2 Adequacy check for the members of the two-story unbraced frame using DAM-NL method.....	40
Table 3.3 Sectional properties of the members of the two-story unbraced frame	44
Table 3.4 First-order analysis results and member stiffness reduction factors of the two-story unbraced frame.....	44
Table 3.5 Adequacy check for the members of the two-story unbraced frame using DAM-MS method	45
Table 4.1a Input data of the explicit imperfection modeling for the two-story unbraced frame.....	81
Table 4.1b Input data of the equivalent notional load modeling for the two-story unbraced frame	81
Table 4.1c Input data of the further reduced tangent modulus modeling for the two-story unbraced frame	82
Table 4.2a Final step of the output data of the explicit imperfection modeling for the two-story unbraced frame.....	84
Table 4.2b Final step of the output data of the equivalent notional load modeling for the two-story unbraced frame.....	85
Table 4.2c Final step of the output data of the further reduced tangent modulus modeling for the two-story unbraced frame	87
Table 4.3 Overstrength factors of the two-story unbraced frame	88
Table 5.1 Live load element factor, K_{LL}	95

Table 5.2	Input data format for the program PAAP	100
Table 6.1	Sectional properties of the members of the six-story steel frame.....	108
Table 6.2	Member forces of the six-story frame determined by using direct analysis method.....	122
Table 6.3a	Input data of the explicit imperfection modeling for the six-story frame.....	129
Table 6.3b	Input data of the equivalent notional load modeling for the six-story frame	130
Table 6.3c	Input data of the further reduced tangent modulus modeling for the six-story frame	131
Table 6.4	Member strength and overstrength factors for the six-story frame	133
Table 6.5a	Input data of the explicit imperfection modeling for the braced frame	142
Table 6.5b	Input data of the equivalent notional load modeling for the braced frame....	143
Table 6.5c	Input data of the further reduced tangent modulus modeling for the braced frame	144
Table 6.6	Analysis results of the braced frame using advanced analysis method	144
Table 6.7a	Input data of the explicit imperfection modeling for the leaned column frame	154
Table 6.7b	Input data of the equivalent notional load modeling for the leaned column frame	154
Table 6.7c	Input data of the further reduced tangent modulus modeling for the leaned column frame	155
Table 7.1	Mathematical expressions of yield stress and modulus of elasticity at elevated temperature	167
Table 7.2	Critical temperatures of the simply supported beam in fire.....	169
Table 7.3	Test data of the steel frames	169
Table 7.4	Critical temperatures of the tested frames in fire.....	170
Table 7.5	Sectional properties of the members of the multi-story steel frame.....	178
Table 7.6	Input data of the multi-story steel frame.....	178

Table 7.7 Occupancy important factors	183
Table 7.8 Value of coefficient C_u	183
Table 7.9 Value of F_v	183
Table 7.10 Value of F_a	184
Table 7.11 Allowable story drift, Δ_a	184
Table 7.12 Design criteria for structural performance levels	189
Table 7.13 Distribution of lateral seismic forces	191

LIST OF FIGURES

	<u>Pages</u>
Figure 2.1 Two-story unbraced steel frame	18
Figure 2.2 AISC-LRFD method for the two-story unbraced frame.....	18
Figure 2.3 Member forces of the two-story unbraced frame determined by a first-order analysis.....	19
Figure 2.4 Leaned column frame	26
Figure 3.1 Cantilever beam-column	32
Figure 3.2 Normalized axial force-moment relationship of the cantilever beam-column	32
Figure 3.3 Portal frame	34
Figure 3.4 Normalized axial force-moment relationship of the Column AB of the portal frame	35
Figure 3.5 Comparison of strength curves of the portal frame	35
Figure 4.1 Fixed-end beam	53
Figure 4.2 Beam-column subjected to end moments and axial force	55
Figure 4.3 Degree of freedom numbering for the frame element	58
Figure 4.4 Strength interaction curves of wide flange sections	61
Figure 4.5 Member tangent stiffness degradation.....	67
Figure 4.6 Normalized axial force-strain relationship	67
Figure 4.7 Parabolic plastic hinge stiffness degradation function	68
Figure 4.8 Stiffness degradation for a softening plastic hinge.....	68
Figure 4.9 Frame element with end connections	70
Figure 4.10 Explicit imperfection modeling.....	74
Figure 4.11 Equivalent notional load concept for modeling geometric imperfection of braced member.....	74

Figure 4.12	Equivalent notional load concept for modeling geometric imperfection of unbraced member.....	74
Figure 4.13	Further reduced tangent modulus	76
Figure 4.14	Structural modeling of the two-story unbraced frame.....	79
Figure 4.15	Equivalent loading condition of the two-story unbraced frame	79
Figure 4.16	Three advanced analysis models for the two-story unbraced frame	80
Figure 4.17	Locations and sequence of the formation of plastic hinges of the two-story unbraced frame.....	80
Figure 5.1	Analysis and design procedure for advanced analysis method	93
Figure 5.2	Operating procedures of the advanced analysis programs	102
Figure 6.1	Configuration and load condition of the six-story frame	108
Figure 6.2	First-order analysis for the six-story frame	109
Figure 6.3	Member forces of the six-story frame determined by using a first-order analysis	110
Figure 6.4	Analysis model of DAM-notional load method for the six-story frame by using PAAP program.....	121
Figure 6.5	Analysis model of DAM-modified stiffness method for the six-story frame by using PAAP program.....	121
Figure 6.6	Structural modeling of the six-story frame.....	127
Figure 6.7	Analysis models of advanced analysis for the six-story frame	127
Figure 6.8	Configuration and load condition of the braced steel frame	134
Figure 6.9	Member forces of the braced steel frame determined by using a second-order elastic analysis.....	134
Figure 6.10	Structural modeling of the braced steel frame.....	140
Figure 6.11	Analysis models of advanced analysis for the braced steel frame	140
Figure 6.12	Configuration and load condition of the leaned column frame.....	145

Figure 6.13	Member forces of the leaned column frame determined by using a second-order elastic analysis.....	145
Figure 6.14	Member forces of the leaned column frame determined by using the DAM-NL method.....	150
Figure 6.15	Member forces of the leaned column frame determined by using the DAM-MS method.....	150
Figure 6.16	Structural modeling of the leaned column frame.....	152
Figure 6.17	Analysis models of advanced analysis for the leaned column frame.....	152
Figure 7.1	Effect of temperature on yield strength, tensile strength, and modulus of elasticity of structural steel.....	163
Figure 7.2	Time-temperature curve of standard fire.....	164
Figure 7.3	Influence of natural ventilation on fire severity.....	164
Figure 7.4	Strategy of the advanced analysis method for fire resistance design.....	166
Figure 7.5	Effective yield stress and modulus of elasticity under elevated temperature.....	166
Figure 7.6	Configuration of the simply supported beam for fire tests.....	168
Figure 7.7	Configuration of the steel frames for fire tests.....	168
Figure 7.8	Analysis procedure for the determination of fire resistance duration of steel structures.....	174
Figure 7.9	Configuration and load condition of the multi-story frame under fire.....	175
Figure 7.10	Deformation data of the multi-story frame determined by using a first-order analysis.....	176
Figure 7.11	Failure mode of the multi-story frame under fire.....	177
Figure 7.12	Failure mode of the multi-story frame without fire.....	177
Figure 7.13	Pushover analysis procedure for seismic design using advanced analysis.....	192
Figure 7.14	Two-story frame for the seismic performance-based design example.....	193
Figure 7.15	Performance curves of the two-story frame.....	193
Figure 7.16	Plastic behavior of the two-story frame at different performance level.....	194

CHAPTER 1

INTRODUCTION

1.1 Design Trends of Steel Framed Structures

In the current AISC Load and Resistance Factor Design (AISC-LRFD) Specification [1], a first-order elastic analysis with amplification factors or a direct second-order elastic analysis is recommended for analyzing steel frames. The members are isolated from a structural system and are designed by the member strength curves and interaction equations which include the effects of material and geometric nonlinearities. In current practice, effective length factor K is employed to estimate the influence of the overall structural system on the strength of its individual beam-column members.

Although the effective length concept is one of the most popular methods used to evaluate steel frame strength and has been adopted by many of the structural design codes and specifications [1,2,3], the effective length factor is not constant and varies due to many factors such as structural shape, member end restraint, member geometry, material properties, and loading distribution. The process of calculating the effective length factors for each individual member in a complex steel structure is not straightforward. Because the K -factor approach is not convenient for computer implementation, simpler design approaches for steel frames need to be considered.

The current trend is to avoid the use of effective length factors in the design of steel frames. Second-order elastic analysis can eliminate the need for moment amplification

formulas, which involve two sets of effective length factors in the beam-column interaction equations. However, it is necessary to use a K-factor in the axial resistance term of the interaction equations for accurate prediction of the beam-column capacity. It is conservative and advisable to use effective length factor equaling unity for braced frame members [1]. The error though, is unacceptably large if $K = 1.0$ for beam-column members in unbraced frames [4].

The direct analysis method is a second-order elastic analysis/design approach proposed by the AISC-SSRC Task Group on Stability [5] for the new provisions for frame and member stability. In the direct analysis method, the effects of initial out-of-plumbness and inelastic softening of the members are accounted for during the analysis process by applying *notional loads and/or modified stiffness* to the structure. Member compressive strengths are calculated based on the unsupported member length. Therefore, the need to determine effective length factors is eliminated. However, tedious individual member capacity checks are still required. Although the design results of the direct analysis method and the AISC-LRFD method are close, some problems still remain that need to be considered.

Both AISC-LRFD and direct analysis methods are member-based design approaches. Internal force redistribution is not considered and the failure mode of a structural system at the limit state cannot be predicted. Advanced analysis is a second-order inelastic analysis and design method which captures the strength and stability of a structural system and its individual members so that the separate member capacity checks involving the use of K-factors are not required. Material and geometric nonlinearities are accounted

for in the analysis process and nearly identical member sizes, in relation to those of the AISC-LRFD method, will be produced. The advanced analysis meets the design requirements of “Structural Fuse Concept” and “Performance-Based Design” because it is a structure system-based design approach and the failure mode of a structural system can be predicted.

The trends of steel frame design are:

- from hand calculation to the use of computers
- from first-order elastic analysis to second-order inelastic analysis
- from member-based design to structure system-based design
- from strength limit design to performance-based design

Advanced analysis satisfies these design trends. It is simpler, faster, and easier to use daily in design offices than conventional design approaches.

1.2 Motivation

In the past, linear elastic analysis was used to analyze steel frames so that member capacity checks involving the effects of geometry and material nonlinearities were required for all beam-column members. In recent years, because computer hardware and software were rapidly developed, coupled with growing knowledge of structural behaviors, the advanced analysis method could simultaneously consider nonlinear effects influencing the limit state strength and stability of a steel frame and its individual members in the analysis process. The primary benefit of directly estimating the capacity of a steel frame within the analysis process is that the simplified design procedures

eliminate the tedious checking of certain member specification equations and the determination of design approximations such as effective length factors. However, the advanced analysis method uses a second-order inelastic analysis scheme, which is not common in present practice. Most existing commercial software can implement only first-order and/or second-order elastic analysis. Therefore, an intermediate analysis and design method is required before the advanced analysis method can be adopted in the new generation of design codes in the years to come.

Although the advanced analysis method is powerful for the analysis and design of steel structures, not all structural engineers presently accept it because they are accustomed to the conventional design procedures and have less confidence using advanced analysis. Therefore, there is a necessity to motivate structural engineers and students to implement advanced analysis by making it more practical. This will allow them to see and understand the advantages of advanced analysis so that they will be willing to use it.

1.3 Objective

The objective of this dissertation is to study and clarify the trends of steel frame design from current AISC-LRFD approach to the advanced analysis approach. Since the direct analysis method is a second-order elastic analysis approach that is applicable to current commercial design software, it is introduced as the intermediate method before structural engineers can become familiar with the advanced analysis method.

In order to motivate structural engineers to apply advanced analysis to practical analysis and design of steel structures, the features of advanced analysis will be presented in this dissertation. Design guidelines will be provided to assist the users to execute the advanced analysis program. *The structural engineer's confidence in using advanced analysis will be established by considering several numerical examples.* It is expected that these examples will show that the advanced analysis method is simpler, faster, and easier to implement and it is able to overcome the difficulties of the AISC-LRFD and direct analysis method.

It is a trend towards using performance-based design by many researchers and structural engineers. The strategies and procedures of applying advanced analysis to the performance-based fire resistance and seismic design will be studied in this dissertation.

1.4 Scope

Although the analysis of three-dimensional steel frames [6,7,8] and the consideration of lateral torsional buckling [9,10] and local buckling [11,12] of the members may be feasible in the current advanced analysis program, some limitations are assumed in this dissertation in order to clearly illustrate the theories and implementation of advanced analysis. In this dissertation, two-dimensional steel building frames are considered. This study covers both braced and unbraced frames including leaned-column frames. Compact wide-flange section members are used so that the full plastic moment capacity can be developed without local buckling. It is assumed that lateral torsional buckling of all members is prevented by adequate lateral bracings. The applied loads are limited to in-

plane static loads. If seismic design of steel frames is considered, equivalent static seismic loading will be assumed.

The Practical Advanced Analysis Program (PAAP) developed by Chen and Kim [13] will be used to implement the numerical examples. The PAAP program is an educational version of the FORTRAN-based software that performs planar frame analysis for the prediction of the strength and behavior of structural systems. 3PARA is also a FORTRAN-based program for semi-rigid connection parameter calculations if partial restrained connections are considered.

In the second chapter of this dissertation, the steel frame design using current AISC-LRFD method and its difficulties are introduced. The direct analysis method is presented in chapter three. Its simpler design approach allows effective length factors to be eliminated in the design equations. The features and developing processes of the advanced analysis method is covered in the fourth chapter. The step-by-step design procedures of the advanced analysis method are summarized in chapter five. Numerical examples are shown in chapter six to show the comparison of the analysis/design procedures and results of the three methods. In chapter seven, the applications of advanced analysis method to performance-based fire resistance and seismic design of steel frames are discussed.

CHAPTER 2

LOAD AND RESISTANCE FACTOR DESIGN

2.1 Introduction

In AISC-LRFD, it is high probability that the factored load effects do not exceed the factored nominal resistance of the structural members. In the current LRFD specification, designers can choose either a first-order elastic analysis that estimates the second-order effects by using amplification factors or a second-order elastic analysis that directly determines the member forces. The linear elastic analysis applies superposition technique and requires an unbraced frame to be decomposed into non-sway and sway components. The determination of effective length factors and internal forces for each beam-column member is needed in the design process. In order to correctly predict the member forces, limit-state design equations that implicitly account for the effects of the spread of yielding and member stability are used to check the strength capacity of each structural member. This treatment, however, does not satisfy compatibility requirements between the elastic system as assumed in the structural analysis and the actual inelastic member capacity check [14]. Although steel frames can be well designed by AISC-LRFD method, there are some drawbacks when applying K-factor concept and member capacity checks. In the first part of this chapter, design procedures of steel frames using AISC-LRFD method are briefly reviewed. A two-story unbraced steel frame example is then presented

to illustrate the complexities associated with the AISC-LRFD implementation. In the third part, the difficulties of using AISC-LRFD method are discussed.

2.2 Overview of AISC-LRFD Method

In this section, the current AISC-LRFD method [1] is briefly described because it is the basis of the direct analysis method and it is also used for the calibration of the advanced analysis method.

2.2.1 Interaction Equations

For the design of a steel beam-column, the following bilinear interaction equations must be satisfied:

$$\frac{P_u}{\phi_c P_n} + \frac{8}{9} \frac{M_u}{\phi_b M_n} \leq 1.0 \quad \text{for } \frac{P_u}{\phi_c P_n} \geq 0.2 \quad (2.1a)$$

$$\frac{1}{2} \frac{P_u}{\phi_c P_n} + \frac{M_u}{\phi_b M_n} \leq 1.0 \quad \text{for } \frac{P_u}{\phi_c P_n} < 0.2 \quad (2.1b)$$

where

P_u = required axial compressive strength

P_n = nominal axial compressive strength determined from LRFD column strength curve

M_u = required flexural strength

M_n = nominal flexural strength determined from the LRFD beam strength curve

ϕ_c = resistance factor for compression = 0.85

ϕ_b = resistance factor for flexure = 0.9

Beam-column interaction equations were developed on the basis of a curve-fitting to the plastic-zone solution of 82 beam-columns generated by Kanchanalai [15]. They can accurately estimate the ultimate load carrying capacities of beam-column members when the column effective lengths and amplified moments are evaluated properly.

2.2.2 Effective Length Factor K

The effective length factor is the key factor that has been employed to approximately estimate the influence of the overall structural system on the strength of beam-column members. For a column in a braced frame, $K = 1.0$ can be conservatively chosen. For unbraced frames, a number of methods have been proposed to determine K factors [1,16,17,18,19]. The alignment chart method, which assumes the buckling of an idealized sub-assembly in a frame and that all columns in a story buckle simultaneously, is recommended by the AISC-LRFD Specification Commentary to compute K factors. The relative stiffness factors at the top and bottom of a column can be calculated as followed:

$$G = \frac{\sum \left(\frac{I_c}{L_c} \right)}{\sum \left(\frac{I_g}{L_g'} \right)} \quad (2.2)$$

where

I_c, I_g = moment of inertia of columns and girders, respectively

L_c = unsupported length of column

L_g' = modified unsupported length of girder

τ = inelastic stiffness reduction factor of a column

$$\begin{aligned} &= -7.38 \left(\frac{P_u}{P_y} \right) \log \left(\frac{P_u/P_y}{0.85} \right) && \text{for } \frac{P_u}{P_y} > \frac{1}{3} \\ &= 1.0 && \text{for } \frac{P_u}{P_y} \leq \frac{1}{3} \end{aligned}$$

P_u = required axial compressive strength, sum of axial forces in non-sway and sway components

$$P_y = \text{squash load} = A_g F_y$$

The alignment chart method assumes that all joints in a structure are rigid connections and the buckling deformation of a girder is full-reversed curvature bending. If the girders have different end conditions at their far ends, the girder length needs to be modified as follows:

$$L_g' = L_g \left(2 - \frac{M_F}{M_N} \right) \tag{2.3}$$

where

L_g = unsupported length of girder

M_F, M_N = moment at the far end and near end of the girder, respectively, obtained from a lateral load analysis

M_F/M_N is positive in double curvature bending

In order to include consideration of leaning column effects and allow concentration of lateral stiffness on relatively weak columns, the AISC-LRFD Specification

Commentary recommends that the distribution of column stiffness needs to be adjusted.

The modified K factor of the i-th rigid column of a story is

$$K_i' = \sqrt{\frac{\Sigma P_u}{P_{ui}} \frac{I_i}{\Sigma \left(\frac{I_i}{K_i^2} \right)}} \geq \sqrt{\frac{5}{8}} K_i \quad (2.4)$$

where

K_i = effective length factor for the i-th rigid column based on alignment chart for sway case

ΣP_u = required axial compressive strength of all columns in a story

P_{ui} = required axial compressive strength for the i-th rigid column

I_i = moment of inertia in plane of bending for the i-th rigid column

2.2.3 Required Flexural Strength M_u

For the determination of required flexural strength of beam-column, AISC-LRFD Specification requires that the additional moments due to the axial loads acting on the deformed structure must be considered. M_u can be calculated by either second-order elastic analysis or the following approximate method

$$M_u = B_1 M_{nt} + B_2 M_{tt} \quad (2.5)$$

where

M_{nt} = required flexural strength in member assuming lateral translation of the frame is prohibited

M_u = required flexural strength in member as a result of lateral translation of the frame
only

The magnification factor B_1 accounts for the secondary $P - \delta$ member effect in all frames and B_2 estimates the $P - \Delta$ story effect in unbraced frames. The $P - \delta$ effect is associated with the influence of axial force acting through the displacement with respect to the member deformed chord, whereas the $P - \Delta$ effect is the influence of axial force acting through the relative lateral displacement of the member ends. The expression for B_1 is

$$B_1 = \frac{C_m}{1 - \frac{P_u}{P_{e1}}} \geq 1.0 \quad (2.6)$$

where

P_u = required compressive strength of the member considered

$P_{e1} = \frac{\pi^2 EI}{(KL)^2}$, where K is an effective length factor in the plane of bending based on

sidesway inhibited alignment chart

$$C_m = \text{equivalent moment factor} = 0.6 - 0.4 \frac{M_1}{M_2}$$

M_1/M_2 is the ratio of the smaller to larger end moment in non-sway component. It is positive when the member is bent in reverse curvature and negative when bent in single curvature. B_2 can be expressed as

$$B_2 = \frac{1}{1 - \Sigma P_u \left[\frac{\Delta_{oh}}{\Sigma HL} \right]} \quad (2.7a)$$

or

$$B_2 = \frac{1}{1 - \frac{\Sigma P_u}{\Sigma P_{e2}}} \quad (2.7b)$$

where

ΣP_u = required axial strength of all columns in a story

Δ_{oh} = lateral inter-story deflection

ΣH = sum of all story horizontal forces producing Δ_{oh}

L = story height

$\Sigma P_{e2} = \Sigma \left[\frac{\pi^2 EI}{(KL)^2} \right]$, where K is an effective length factor in the plane of bending based on

sideway uninhibited alignment chart

2.2.4 Column Strength P_n

The column curves implicitly account for second-order effects, residual stresses, and an initial out-of-straightness of 1/1500 [20]. P_n could be calculated as follows for the different types of overall buckling modes

$$P_n = \left(\frac{0.877}{\lambda_c^2} \right) P_y \quad \text{for } \lambda_c > 1.5 \quad (2.8a)$$

$$P_n = \left(0.658 \lambda_c^2 \right) P_y \quad \text{for } \lambda_c \leq 1.5 \quad (2.8b)$$

where

$$\lambda_c = \text{slenderness parameter} = \frac{KL}{\pi r} \sqrt{\frac{F_y}{E}}$$

K = effective length factor

L = unbraced member length

r = radius of gyration

E = modulus of elasticity

F_y = specified minimum yield stress

KL/r is equal to the larger value for strong- and weak-axis buckling

2.2.5 Flexural Strength M_n

When laterally braced compact members with $L_b \leq L_p$ are considered, only the limit state of yielding is applicable for the determination of the nominal flexural strength M_n . For unbraced compact members, only the limit states of yielding and lateral torsional buckling are applicable. For an I-shape member subjected to bending about its strong axis, nominal flexural strength M_n is

$$M_n = M_p \quad \text{for } L_b \leq L_p \quad (2.9a)$$

$$M_n = C_b \left[M_p - (M_p - M_r) \frac{L_b - L_p}{L_r - L_p} \right] \leq M_p \quad \text{for } L_p < L_b \leq L_r \quad (2.9b)$$

$$M_n = C_b \frac{\pi}{L_b} \sqrt{EI_y GJ + \left(\frac{\pi E}{L_b} \right)^2 I_y C_w} \leq M_p \quad \text{for } L_b > L_r \quad (2.9c)$$

where

$M_p =$ plastic moment $= F_y Z$, Z is the plastic section modulus

$M_r = F_L S_x$, $F_L =$ smaller of $(F_{yf} - F_r)$ or F_{yw}

$F_{yf} =$ yield stress of flange

$F_{yw} =$ yield stress of web

$F_r =$ compressive residual stress in flange, 10 ksi for rolled shapes and 16.5 ksi for welded shapes

$I_y =$ moment of inertia about y axis

$C_w =$ warping constant

$L_b =$ unbraced length of the member in the out-of-plane bending

$L_p =$ limiting unbraced length for full plastic bending capacity

$L_r =$ limiting unbraced length of inelastic lateral torsional buckling

$J =$ torsional constant

The limiting unbraced lengths L_p and L_r shall be calculated as follows

$$L_p = \frac{300r_y}{\sqrt{F_{yf}}} \quad (2.10)$$

$$L_r = \frac{r_y X_1}{F_L} \sqrt{1 + \sqrt{1 + X_2 F_L^2}} \quad (2.11)$$

where

$$X_1 = \frac{\pi}{S_x} \sqrt{\frac{EGJA}{2}}$$

$$X_2 = 4 \frac{C_w}{I_y} \left(\frac{S_x}{GJ} \right)^2$$

S_x = section modulus about major axis

C_b is a factor which accounts for the effect of moment gradient on the lateral torsional buckling strength of the member.

$$C_b = \frac{12.5M_{\max}}{2.5M_{\max} + 3M_A + 4M_B + 3M_C} \quad (2.12)$$

where

M_{\max}, M_A, M_B, M_C = absolute values of the maximum moment, quarter-point moment, midpoint moment, and three-quarter point moment along the unbraced length of the member, respectively

2.3 Two-Story Unbraced Steel Frame Example

In this section, a general fixed-supported one-bay two-story steel frame is considered. This example is used to implement the design guidelines of AISC-LRFD method. The same example will be presented when the direct analysis method and the advanced analysis method are compared along with their analysis procedures and design requirements.

2.3.1 Structural Configuration

Figure 2.1 shows the steel frame subjected to the combined factored gravity and lateral loads. The preliminary member sizes are shown in the figure. Yield stress of steel

F_y is 50 ksi. Members are oriented such that all webs are in the plane of the frame and braced in the out-of-plane direction.

2.3.2 Analysis

In the AISC-LRFD method, a first-order elastic analysis is performed and the frame is decomposed into a non-sway and sway component as shown in Figures 2.2a and 2.2b. The corresponding moment diagrams M_m and M_u are shown in Figures 2.3a and 2.3b, respectively. Column EF will be checked for adequacy in detail.

2.3.3 Adequacy Checks of Members

(1) Determine P_u

$$P_u = 72.0 + 3.4 = 75.4 \text{ kips}$$

(2) Determine M_u

① Determine B_1

$$C_m = 0.6 - 0.4 \left(\frac{M_1}{M_2} \right) = 0.6 - 0.4 \left(\frac{316.4}{632.8} \right) = 0.4$$

$G_F = 1.0$ assumed to represent full fixity

$$G_E = \frac{\Sigma \left(\frac{I_c}{L_c} \right)}{\Sigma \left(\frac{I_g}{L_g} \right)} = \frac{2 \times \frac{144}{144}}{\frac{375}{288}} = 1.536$$

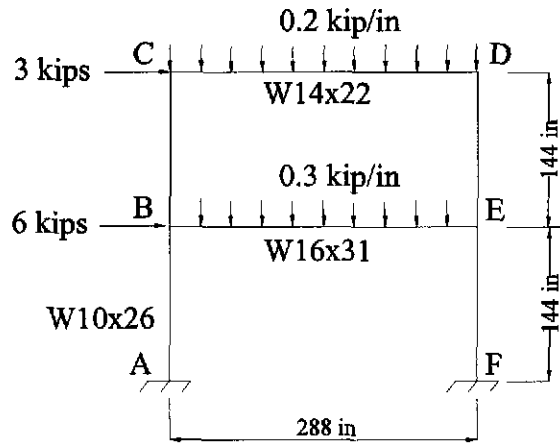
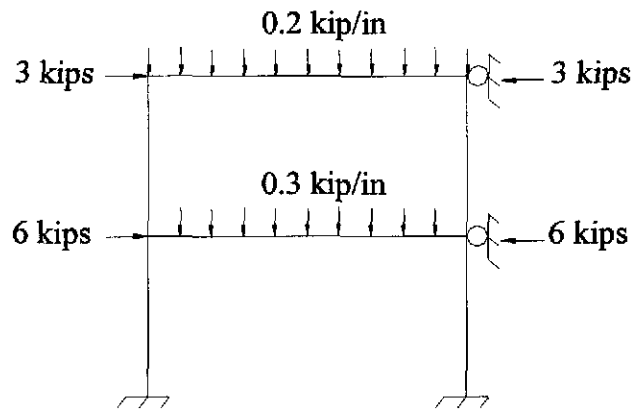
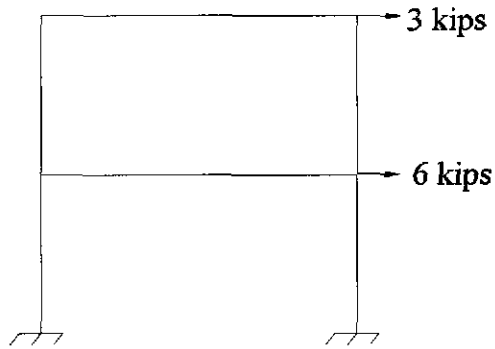


Figure 2.1 Two-story unbraced steel frame

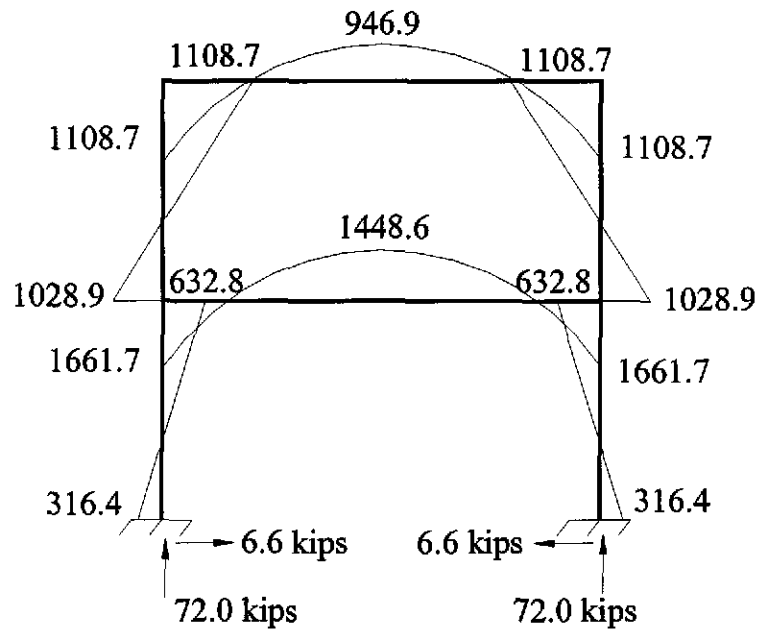


(a) Non-sway component

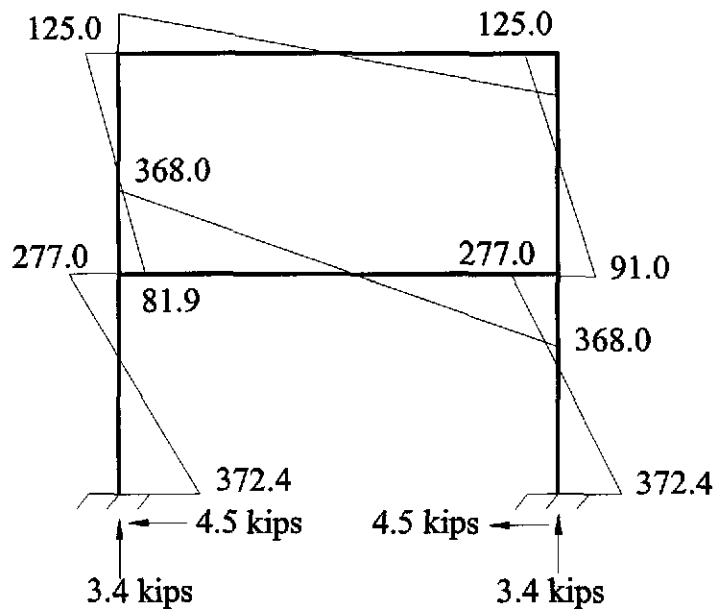


(b) Sway component

Figure 2.2 AISC-LRFD method for the two-story unbraced frame



(a) Non-sway component (unit: kip-in)



(b) Sway component (unit: kip-in)

Figure 2.3 Member forces of the two-story unbraced frame determined by using a first-order analysis

From the alignment chart of sidesway inhibited,

$$K_x = 0.8 \text{ (} K_x \text{ can be unity for simplicity)}$$

$$P_{e1} = \frac{\pi^2 EI}{(K_x L)^2} = \frac{\pi^2 (29000)(144)}{(0.8 \times 144)^2} = 3105.7 \text{ kips}$$

$$B_1 = \frac{C_m}{1 - \frac{P_u}{P_{e1}}} = \frac{0.4}{1 - \frac{75.4}{3105.7}} = 0.41 < 1.0$$

Use $B_1 = 1.0$

② Determine B_2

$$\Sigma P_u = (0.2 + 0.3)(288) = 144 \text{ kips}$$

$$G_F = G_A = 1.0$$

$$G_E = G_B = 1.536$$

From the alignment chart of sidesway uninhibited,

$$K_{EF} = K_{AB} = 1.4$$

$$\Sigma P_{e2} = \Sigma \frac{\pi^2 EI}{(KL)^2} = 2 \times \frac{\pi^2 (29000)(144)}{(1.4 \times 144)^2} = 2028.2 \text{ kips}$$

$$B_2 = \frac{1}{1 - \frac{\Sigma P_u}{\Sigma P_{e2}}} = \frac{1}{1 - \frac{144}{2028.2}} = 1.076$$

③ Calculate M_u

$$M_{u,top} = (1)(632.8) + (1.076)(277.0) = 930.9 \text{ kip-in (govern)}$$

$$M_{u,bot} = (1)(316.4) + (1.076)(372.4) = 717.1 \text{ kip-in}$$

(3) Determine $\phi_c P_n$:

① Determine τ (inelastic stiffness reduction factor)

$$P_y = A_g F_y = (7.61)(50) = 380.5 \text{ kips}$$

$$\frac{P_u}{P_y} = \frac{75.4}{380.5} = 0.198 < \frac{1}{3}$$

$$\tau = 1.0 \text{ (Column EF remains elastic)}$$

② Determine L_g' (end-restrained correction factor)

$$L_g' = L_g \left(2 - \frac{M_F}{M_N} \right) = 288 \left(2 - \frac{368}{368} \right) = 288.0 \text{ in.}$$

③ Determine K_{EF}

$$G_F = 1.0$$

$$G_E = \frac{\sum \left(\frac{\tau I_c}{L_c} \right)}{\sum \left(\frac{I_g}{L_g} \right)} = \frac{2 \times \frac{144}{144}}{\frac{375}{288}} = 1.54$$

From the alignment chart of sidesway uninhibited,

$$K_{EF} = 1.41$$

④ Calculate $\phi_c P_n$

In order to compare the design results of advanced analysis, only strong-axis buckling is considered. In usual AISC-LRFD design, both λ_{cx} and λ_{cy} should be considered and the greater one governs.

$$\lambda_{cx} = \frac{K_x L}{\pi r_x} \sqrt{\frac{F_y}{E}} = \frac{(1.41)(144)}{\pi(4.35)} \sqrt{\frac{50}{29000}} = 0.617 < 1.5$$

$$P_n = (0.658^{\lambda_{cx}^2}) P_y = (0.658^{(0.617)^2}) (380.5) = 324.47 \text{ kips}$$

$$\phi_c P_n = (0.85)(324.47) = 275.8 \text{ kips}$$

(4) Determine $\phi_b M_n$

① Determine L_b

$$L_p = 1.76 r_y \sqrt{\frac{E}{F_y}} = 1.76(1.36) \sqrt{\frac{29000}{50}} = 57.65 \text{ in.}$$

$$L_r = \frac{r_y X_1}{F_L} \sqrt{1 + \sqrt{1 + X_2 F_L^2}} = \frac{(1.36)(2510)}{40} \sqrt{1 + \sqrt{1 + (3760 \times 10^{-6})(40)^2}} = 163.0 \text{ in.}$$

$$L_p < L_b = 144 \text{ in.} < L_r$$

② Determine C_b

$$M_{\max} = 632.8 + 277.0 = 909.8, \quad M_A = 395.5 + 114.7 = 510.2$$

$$M_B = 158.2 - 47.7 = 110.5, \quad M_C = 79.1 + 210.1 = 289.2$$

$$C_b = \frac{12.5 M_{\max}}{2.5 M_{\max} + 3 M_A + 4 M_B + 3 M_C} = \frac{12.5(909.8)}{2.5(909.8) + 3(510.2) + 4(110.5) + 3(289.2)} = 2.22$$

③ Calculate $\phi_b M_n$

$$M_p = Z_x F_y = (31.3)(50) = 1565 \text{ kip-in}$$

$$M_r = S_x F_L = (27.9)(40) = 1116 \text{ kip-in}$$

$$M_n = C_b \left[M_p - (M_p - M_r) \frac{L_b - L_p}{L_r - L_p} \right]$$

$$= (2.22) \left[1565 - (1565 - 1116) \left(\frac{144 - 57.65}{163 - 57.65} \right) \right] = 2657 \text{ kip-in} > M_p$$

use $M_n = M_p = 1565 \text{ kip-in}$

$$\phi_b M_n = 1408.5 \text{ kip-in}$$

(5) Check interaction equation

$$\frac{P_u}{\phi_c P_n} = \frac{75.4}{275.8} = 0.272 > 0.2$$

$$\frac{P_u}{\phi_c P_n} + \frac{8 M_u}{9 \phi_b M_n} = 0.272 + \frac{8 \cdot 930.9}{9 \cdot 1408.5} = 0.859 < 1.0 \quad \therefore \text{O.K.}$$

Table 2.1 Member capacity check of the two-story unbraced frame using AISC-LRFD method

Member	P_u (kips)	M_u (kip-in)	Interaction ratio ΣI	Adequacy
AB	68.6	337.6	0.462	OK
BC	27.9	970.6	0.741	OK
DE	29.7	1229.9	0.928	OK
EF	75.4	930.9	0.859	OK
BE	5.0	2023.4	0.833	OK
CD	16.4	1229.9	0.823	OK

It is required to check the adequacy for all other members in the structure. The interaction ratios of all members of the two-story unbraced frame are summarized in Table 2.1. It shows that the preliminary design of all member sizes is adequate.

2.4 The Difficulties of Using AISC-LRFD Method

Although steel structures can be adequately designed by using the AISC-LRFD method as shown in the previous section, the member capacity checks and the determination of effective length factors and their procedures are often tedious and confusing. Also, since AISC-LRFD method is a member-based design approach, inelastic member forces will not be redistributed and the actual structural behavior and failure mode cannot be predicted.

2.4.1 Effective Length Factors

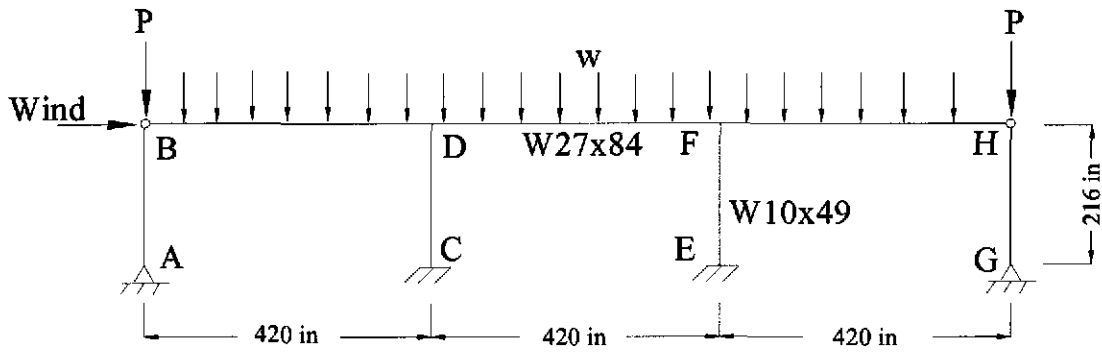
In the current AISC-LRFD method, members are isolated from the structural system. They are analyzed by elastic analysis and designed by member strength curves and interaction equations. The effective length concept provides for the interaction between the structural system and its component members. However, there are several difficulties associated with the use of the effective length approach.

The effective length factors cannot be correctly predicted in practical design process. The development of the effective length approach is based on a number of assumptions and idealizations which seldom exist in real structures [1]. Unexpected errors may arise if those assumptions are violated.

The effective length approach cannot accurately present the actual relationship between a structural system and its members. The determination of effective length factors and column buckling loads may be grouped according to the models associated with [17]: (1) buckling of the subassembly comprised of the considered column and its adjacent members; (2) buckling of the story in which the considered column is contained; and (3) buckling of the overall structural system. The resulting K factor could be quite different if a different model is used. Therefore, the stability calculations based on the effective length approach are complex and often lead to confusion and misunderstanding.

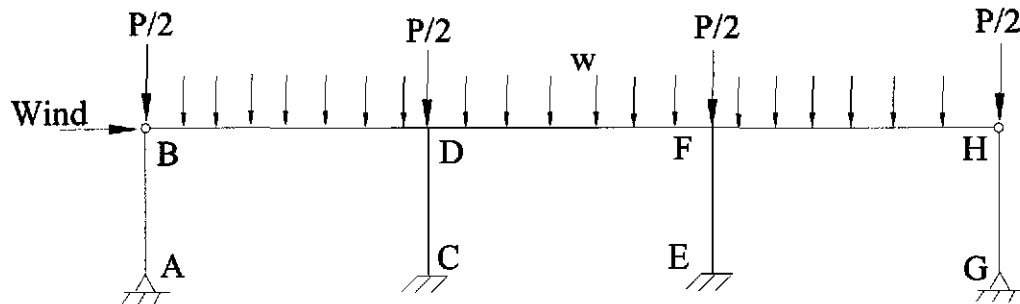
A steel frame with leaned columns is shown in Figure 2.4. The story buckling mode or system buckling mode should be used to determine effective length factors and axial capacities of rigid columns. The determined effective length factors will be much greater and the axial capacities will be much less than those determined by the single column buckling mode or the alignment chart approach. Even when the story buckling mode or system buckling mode is considered, the effective length factor still varies if loading is distributed under different conditions. The column carrying higher axial force has a smaller K factor than the same column carrying the smaller axial force. This is because the columns with low axial forces can help brace the columns that have higher axial forces until story buckling occurs.

In Figure 2.4a, two concentrated loads P are applied on the two leaning columns and uniform load w is applied on all beams. In Figure 2.4b, concentrated load $P/2$ is applied on each column and uniform load w is still applied on all beams. In Figure 2.4c, all gravity loads are uniformly distributed on the beams. Note that the total gravity loads



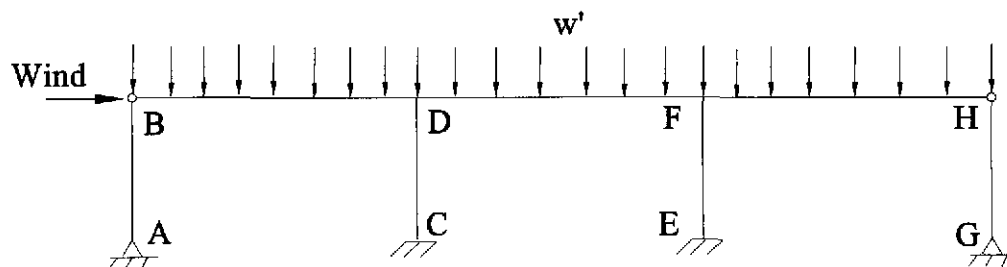
$P=568$ kips, $w=0.3383$ kip/in., Wind=8.19 kips

(a) Case 1



$P=568$ kips, $w=0.3383$ kip/in., Wind=8.19 kips

(b) Case 2



$w'=1.24$ kip/in., Wind=8.19 kips

(c) Case 3

Figure 2.4 Leaned column frame

Table 2.2 Effective length factor and axial capacity of the Column CD of the leaned column frame

Case	Effective Length Factor K	$\phi_c P_n$ (kips)
1	2.64	178.8
2	1.57	391.8
3	1.34	432.2

for all three cases are identical. Table 2.2 shows the effective length factors and axial capacities of rigid column CD in the leaning column frame under different loading conditions.

It is confusing to apply the effective length concept to particular structures. Procedures for determination of the proper K factors for structural system such as steel frames with leaning columns, moment frames connected to shear wall, eccentrically braced frames, or semi-rigid connection frames are confusing and the accuracy of the results are questionable.

2.4.2 Separate Member Capacity Checks

In the design of steel frames for strength and stability, inelastic material behaviors, the flexibility of connections, and second-order effect due to changes in configuration cannot be directly accounted for during the analysis process in the past because computer hardware and software were not sufficient. All these effects must be involved in the member strength terms of interaction equations. In the AISC-LRFD method, elastic analysis is used and each structural member is examined individually through the design

equations to limit the combination of axial and flexural strength, from which some disadvantages arise.

The effects of the inelastic redistribution of internal forces in a structural system cannot be covered through the separate member capacity checks. In this approach, the ultimate strength of the critical member in the considered structure is the design criterion and inelastic redistribution of internal forces will not occur. This will lead to a more conservative design result.

The elastic analysis/design approach cannot predict the failure mode of a structural system. This is because the member capacity checks involving the consideration of inelastic effects is a member-based design approach. The prediction of failure mechanism that must be considered in the limit state of whole structural system cannot be possible.

2.5 Summary

In the AISC-LRFD method, a first-order elastic analysis with amplification factors or a second-order elastic analysis is used. The use of effective length factors and interaction equations was a simple way to estimate the strength and stability of a structural system and its members in a time when computer technology was poor. However, there are several drawbacks when using this analysis/design approach which were discussed in this chapter. To avoid these drawbacks, it is the trend to eliminate the use of K factor in steel frame design. Direct analysis method is a second-order elastic analysis approach without using K factor in the design equations and it will be discussed in the next chapter.

CHAPTER 3

DIRECT ANALYSIS METHOD

3.1 Introduction

It is cumbersome and confusing when calculating the amplification factors involving the determination of effective length factors in a first-order elastic analysis. Therefore, it would be easier and more convenient to use a computer-based method to calculate member forces directly. Instead of using the B1-B2 method, a direct second-order elastic analysis which is common in present practice may be used to estimate the second-order moment for the design of steel structures. Second-order analysis is based on second-order deformation, in which equilibrium conditions are formulated based on the deformed structural geometry. To trace the force-displacement relationship of a structure, the incremental load concept and iterative procedures are required. Although second-order elastic analysis can account for stability effects, it does not provide information on the effects of inelastic nonlinearities of the structure. In addition, a second-order elastic analysis can eliminate the need for moment amplification factors, although, the effective length factor is still required in the axial resistance term of interaction equations for accurate prediction of the beam-column capacity.

The direct analysis method is a second-order elastic analysis/design method for steel structures. In the direct analysis method, member compressive strength in the plane of a frame is obtained by using the unsupported length of the member or $K=1.0$. Notional

loads and/or modified stiffness are used to account for the effects of member initial geometric imperfection and distributed plasticity. Beam-column interaction equations corresponding to the direct analysis method are still needed to provide for the proper strength of each member in the structural system.

In Section 3.2, the AISC-LRFD beam-column design without the use of effective length factors is discussed. It will be shown that the error of using the present AISC-LRFD interaction equations is unacceptably large if the effective length factor is taken as unity for unbraced structures. Second-order elastic analysis combined with the use of notional loads and/or modified stiffness is introduced in Sections 3.3 and 3.4, respectively. Design guidelines for both notional load and modified stiffness methods are proposed. In order to compare with AISC-LRFD method, a two-story unbraced steel frame is analyzed and designed again using these two methods.

3.2 Beam-Column Design with Unsupported Member Length by LRFD

Method

The required flexural strength M_u of a beam-column can be estimated by AISC-LRFD B1-B2 method that uses two sets of effective length factors. The P_{e1} term in the B_1 factor shown in equation (2.6) is based on the effective length factor that is less than one. It is conservative to use $K = 1$ to calculate this term. For an unbraced frame member, the calculation of B_2 using equation (2.7a) does not require the use of the effective length factor. However, if equation (2.7b) is used to determine B_2 , the effective

length factors for the columns in a story are usually greater than one. Using $K = 1$ to estimate the buckling load of an unbraced column P_{e2} is unconservative. Alternatively, if second-order elastic analysis is employed, the use of effective length factors in the calculation of M_u can be waived completely.

For the determination of the P_n term in the beam-column interaction equations shown in equations (2.1a) and (2.1b), the effective length factor K for a braced frame column is usually less than 1.0 and it is advised by AISC-LRFD Specification to use $K = 1$ for conservative evaluation of P_n [1]. For an unbraced column, the use of $K = 1$ may not be adequate.

Figure 3.1 shows a cantilever column fixed at its base. Vertical load P and horizontal load $0.01P$ are applied at the top of the member. The cross section used is W8×31 and the AISC-LRFD slenderness parameter λ_c equals 1.0. Figure 3.2 shows the beam-column behavior curve of the column without considering the design reduction factors. If the current AISC-LRFD method is used, the axial capacity of this member is 215 kips, which is determined by the interaction envelope with $K = 2$. If the unsupported member length is used to calculate the P_n term in the interaction equations, the intersection point of second-order strength curve and interaction envelope with $K = 1$ will give the axial capacity of 255 kips. The difference between using $K = 2$ and $K = 1$ is over 18 percent. Table 3.1 shows the unconservative errors of ultimate axial strength of the considered beam-column for different slenderness parameters if $K = 1$ is used. It is demonstrated that the more slender the member, the greater the error.

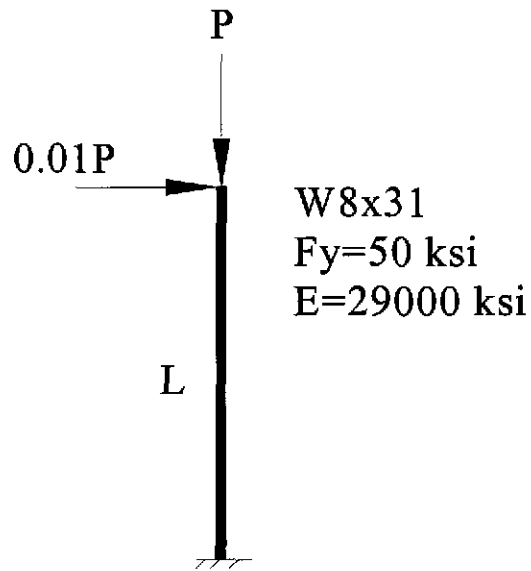


Figure 3.1 Cantilever beam-column

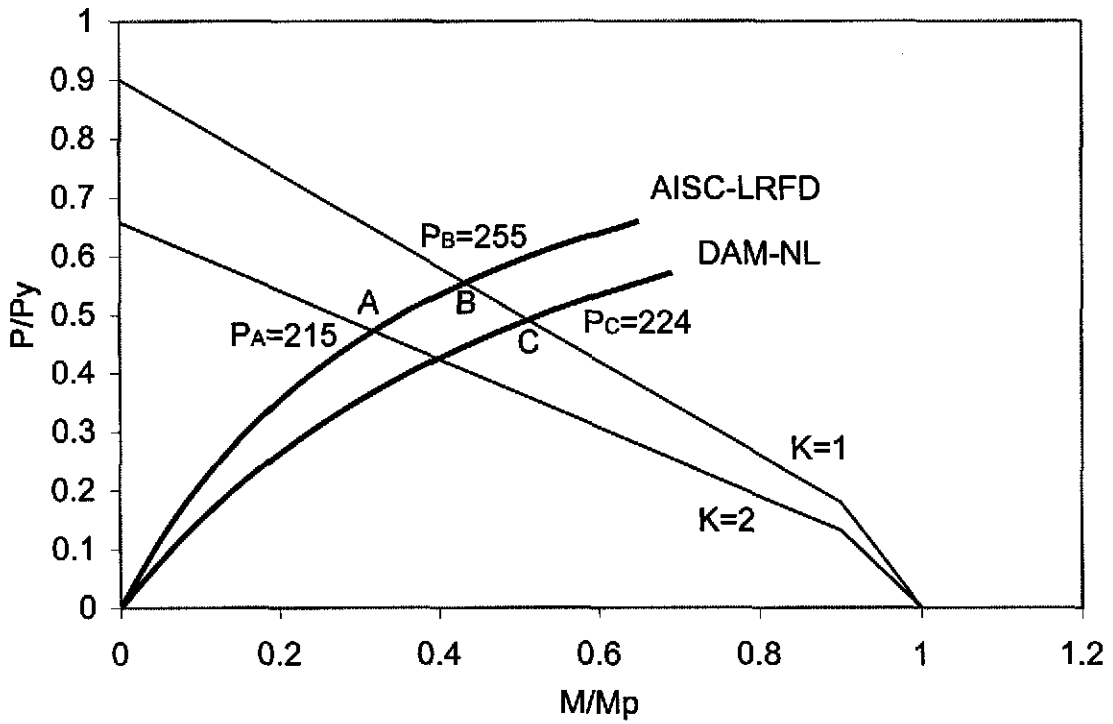


Figure 3.2 Normalized axial force-moment relationship of the cantilever beam-column

Table 3.1 Comparison of axial strength of the cantilever beam-column with various slenderness parameters (unit: kips)

AISC-LRFD λ_c	$K = 2$		$K = 1$		Error in P_u (%)
	P_n	P_u	P_n	P_u	
0	454.0	454.0	454.0	454.0	0.00
0.2	448.4	418.8	454.0	423.3	1.07
0.4	426.5	372.0	448.4	388.0	4.30
0.6	392.2	319.0	439.1	347.6	8.97
0.8	348.4	265.0	426.5	301.4	13.74
1.0	300.1	215.3	410.7	255.0	18.44
1.2	249.6	172.5	390.5	207.0	20.00
1.4	200.8	137.6	371.5	168.3	22.31
1.6	156.2	109.4	348.8	138.0	26.14
1.8	123.4	88.7	324.9	114.1	28.64
2.0	100.0	73.0	300.1	95.7	31.10
3.0	44.4	35.0	177.8	46.0	31.43

Figure 3.3 shows a portal frame subjected to a load combination. The effective length factor of Column AB determined from sidesway uninhibited alignment chart and story buckling approach is 2.0. From the beam-column behavior curve shown in Figure 3.4, the AISC-LRFD method estimates the axial strength of 232 kips in Column AB, while the value is 284 kips if P_n is determined by using $K = 1$. Comparing with AISC-LRFD solution, the unconservative error is about 22 percent if effective length factor is set equal to one. Figure 3.5 shows the beam-column curves of the member AB subjected to various ratios of gravity and lateral loads [15].

It can be seen from the previous two examples that if the unsupported member length is used to determine P_n in the current AISC-LRFD interaction equations, the error is

unacceptably large. The errors associated with $K = 1$ are particularly large for slender members subjected to relatively high axial forces. Based on the research of White and Hajjar [21], the error of using the AISC-LRFD formulae with $K = 1$ may be ignored if the B_2 factor, calculated using equations (2.7a) or (2.7b), is less than or equal to 1.11. It indirectly limits the magnitude of the axial forces which may act on the columns.

3.3 Direct Analysis Method with Notional Load (DAM-NL Method)

Direct analysis method is a second-order elastic analysis method that employs AISC-LRFD design formulae with unsupported member length or $K = 1$ [5]. Notional loads could be used to take into account the effects of changing restrained conditions of the member ends. It is a lateral load that is formulated as a fraction of gravity load acting on a story and applied to the structure to approximate the effects of initial geometric imperfections and/or softening of the structure that may occur due to residual stresses and gradual yielding of members and connections.

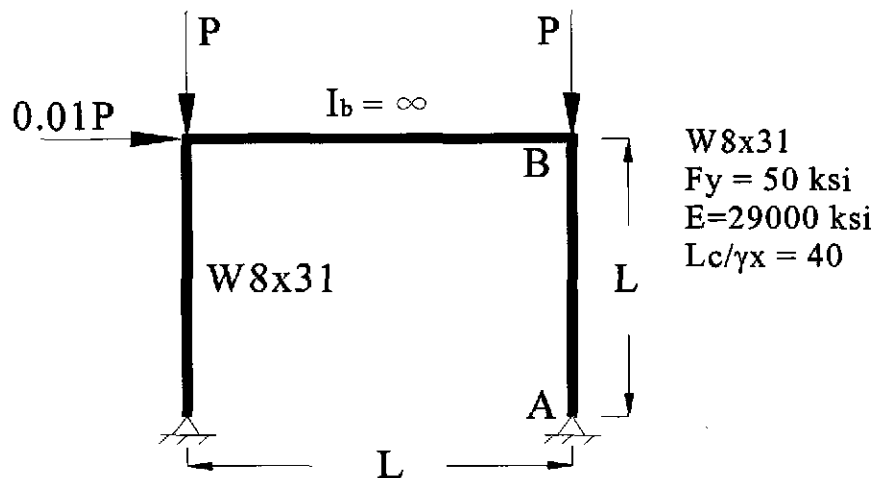


Figure 3.3 Portal frame

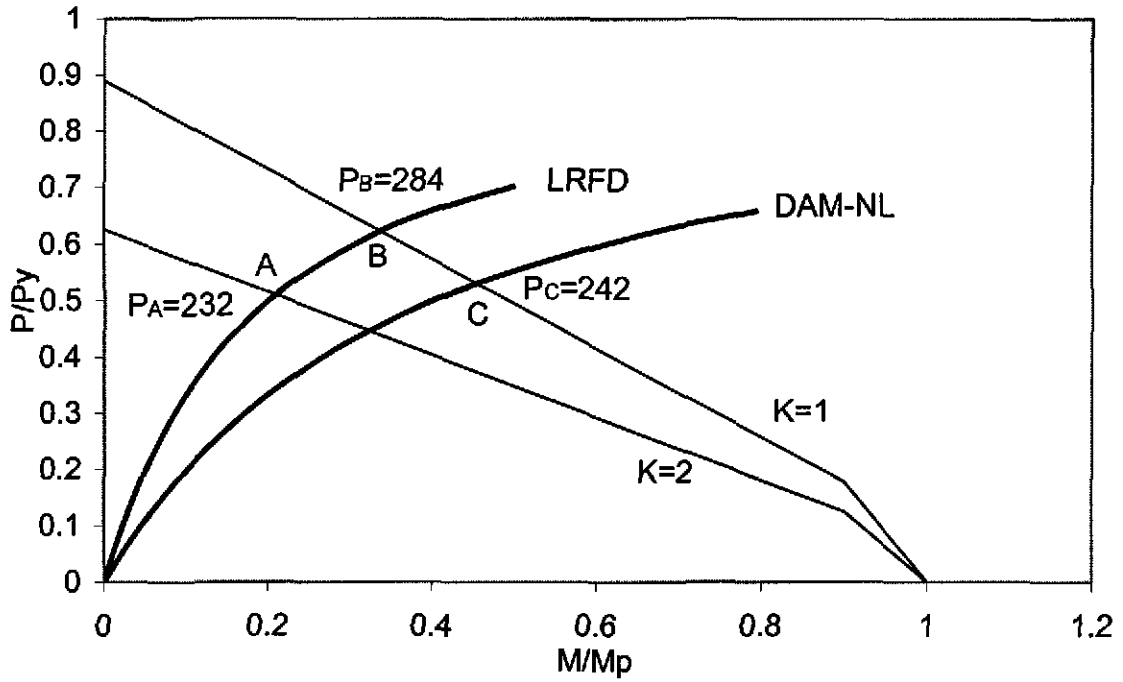


Figure 3.4 Normalized axial force-moment relationship of the Column AB of the portal frame

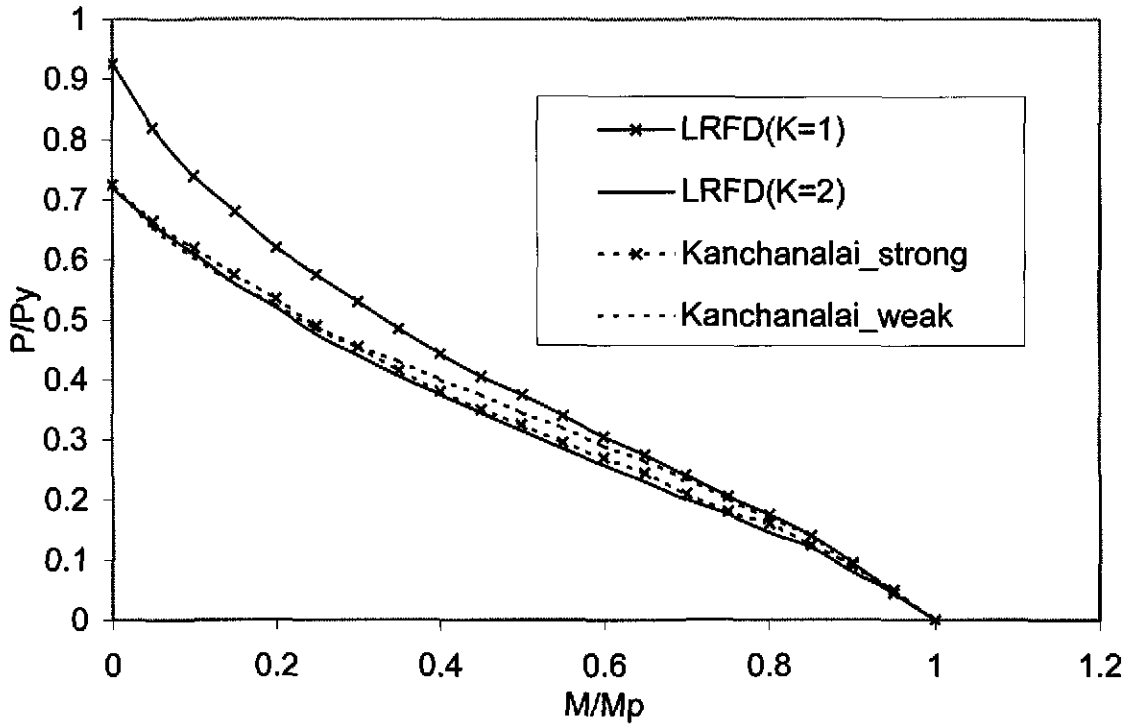


Figure 3.5 Comparison of strength curves of the portal frame

3.3.1 The Application of DAM-NL Method to Steel Frame Analysis

For a braced frame system, the initial geometric imperfection of the frame and its members should be included in the second-order elastic analysis. For the purpose of modeling the destabilizing effects of an $H/500$ erection out-of-plumbness, where H is the story height, notional loads calculated using equation (3.1) should be applied in conjunction with the design loads on the structure [5].

$$NL = 0.002GL \quad (3.1)$$

where

GL = total design gravity loads acting at the considered floor level

NL = notional lateral load applied at the floor level corresponding to GL

A moment frame system should be analyzed by a second-order elastic analysis that includes the effects of initial geometric imperfections of the frame and its members and the loss in stiffness due to material yielding. Required strengths for members and connections shall be determined by applying the design loads combined with notional loads. The notional loads accounting for frame out-of-plumbness and inelastic softening can be expressed as [5]

$$NL = 0.005GL \quad (3.2)$$

where the terms are the same as defined in equation (3.1). In equation (3.2), $0.002GL$ is used to account for the initial out-of-plumbness of $H/500$ and $0.003GL$ is used to take into account the effects of inelasticity.

Consider the cantilever beam-column shown in Figure 3.1. The notional load of $0.005P$ which has the same direction as the external horizontal load is applied at the top

of the member. As shown in Figure 3.2, the direct analysis method gives the ultimate axial strength of 224 kips, which is close to the AISC-LRFD solution of 215 kips. The difference is about 4 percent, which is acceptable. If DAM-NL method is employed to the portal frame shown in Figure 3.3, the beam-column behavior curve is shown in Figure 3.4 and the ultimate axial strength of Column AB is 242 kips. Comparing this with AISC-LRFD solution, the difference is greatly reduced from about 22 percent if no notional load is considered to only 4.3 percent if the notional load equaling $0.005GL$ is applied.

3.3.2 Design Guidelines

The design guidelines of the direct analysis method with notional load are proposed for steel frame design.

Step 1. Select the adequate structural system (braced or unbraced) for its particular purpose.

Step 2. Determine factored load combinations based on adequate design codes.

Step 3. Pre-select the member sizes based on engineers' experiences or simplified analyses.

Step 4. Determine the notional loads $NL = \alpha GL$, where $\alpha = 0.002$ for braced frame and 0.005 for unbraced frames. Note that the directions of notional loads should be adequately specified so that a critical mode of failure would be arrived at.

Step 5. Analyze the structure using any second-order elastic analysis program.

Step 6. Obtain the member required strength P_u and M_u of each member from the results of analysis.

Step 7. Determine the axial capacity P_n for each beam-column based on the AISC-LRFD column strength formula with unsupported member length or $K=1.0$.

Step 8. Determine the flexural strength M_n for each member based on the specified LRFD equations.

Step 9. Check the interaction equations, which have the same form as equation (2.1a) and (2.1b), for all members.

Step 10. Adjust the member sizes for those members which do not satisfy the interaction requirements.

Step 11. Repeat Steps 5 to 10 until the interaction requirements for all members are met.

3.3.3 Two-Story Unbraced Frame Example

The two-story unbraced steel frame shown in Figure 2.1 (Section 2.3) is analyzed and designed again by using direct analysis method with notional load. Column EF will be considered in detail.

(1) Determine notional loads

The notional loads applied at the roof and floor levels are

$$\text{At the roof level: } NL_{roof} = 0.005 \times (0.2 \times 288) = 0.288 \text{ kip}$$

$$\text{At the floor level: } NL_{floor} = 0.005 \times (0.3 \times 288) = 0.432 \text{ kip}$$

(2) Determine P_u and M_u

After applying the notional loads in conjunction with the design loads to the structure and performing a second-order elastic analysis, the axial and flexural strengths required for Column EF are $P_u = 75.8$ kips and $M_u = 963.3$ kip-in, respectively.

(3) Determine $\phi_c P_n$

$$\lambda_{cx} = \frac{L}{\pi r} \sqrt{\frac{F_y}{E}} = \frac{144}{\pi(4.35)} \sqrt{\frac{50}{29000}} = 0.4375 < 1.5$$

$$\phi_c P_n = (0.85) \left[0.658^{(0.4375)^2} \right] (380.5) = 298.5 \text{ kips}$$

(4) Determine $\phi_b M_n$

The determination of $\phi_b M_n$ in the direct analysis method is the same as that in AISC-LRFD method. Therefore, the magnitude of $\phi_b M_n$ is 1408.5 kip-in.

(5) Check interaction equations

$$\frac{P_u}{\phi_c P_n} = \frac{75.8}{298.5} = 0.254$$

$$\frac{P_u}{\phi_c P_n} + \frac{8}{9} \frac{M_u}{\phi_b M_n} = 0.254 + \frac{8}{9} \frac{963.3}{1408.5} = 0.862 < 1.0 \quad \therefore \text{O.K.}$$

The interaction ratio of Column EF determined by direct analysis method with notional load is almost identical to the one determined by AISC-LRFD method. The interaction ratios of all members in the structure using DAM-NL method are summarized in Table 3.2. It shows that preliminary selections of all members are adequate. The design results are the same as the ones of the AISC-LRFD method. It can be seen that the use of

Table 3.2 Adequacy check for the members of the two-story unbraced frame using DAM-NL method

Member	P_u (kips)	M_u (in-kip)	Interaction ratio ΣI	Adequacy
AB	68.2	358.4	0.455	OK
BC	27.8	954.7	0.724	OK
DE	29.8	1254.8	0.941	OK
EF	75.8	963.3	0.862	OK
BE	4.9	2100.9	0.865	OK
CD	16.5	1254.9	0.876	OK

direct analysis method with notional load greatly reduces the effort needed when calculating the terms of M_u and P_u in the interaction equations and good design results will still be obtained.

3.4 Direct Analysis Method with Modified Stiffness (DAM-MS Method)

The modified stiffness approach is a technique which assigns effective stiffness coefficients accounting for softening of the structural system that occurs due to residual stresses and gradual yielding of members and connections under the specified load intensity. In this approach, initial geometric imperfections of the system are still accounted for by notional loads.

3.4.1 The Application of DAM-MS Method to Steel Frame Analysis

The DAM-MS method requires the structure to be analyzed by a second-order elastic analysis and all its members to be checked by using the interaction equations with unsupported member length in the P_u term. Story out-of-plumbness should be included in

the analysis by applying notional loads in conjunction with design loads. The notional load equivalent to the out-of-plumbness of $H/500$ is [5]

$$NL = 0.002GL \quad (3.3)$$

where NL and GL are the same as defined in equation (3.1) and H is the story height.

If the axial compressive force in a column is greater than $0.1P_y$, the flexural rigidity of the column should be reduced to account for the effects of inelastic softening [5]:

$$EI^* = C\tau(EI) \quad (3.4)$$

where

$$C = 1.0 \quad \text{for } M_n \leq 1.2M_y$$

$$= 0.8 \quad \text{for } M_n > 1.2M_y$$

$$\tau = 1.0 \quad \text{for } P \leq 0.5P_y$$

$$= 4 \frac{P}{P_y} \left(1 - \frac{P}{P_y} \right) \quad \text{for } P > 0.5P_y$$

M_n = nominal flexural capacity

M_y = nominal yield moment

E = modulus of elasticity

I = moment of inertia about the axis of bending

EI^* = modified flexural rigidity

P_y = squash load

P = axial compression in a column

The stiffness reduction factor τ is based on the CRC tangent modulus concept [22] and used to account for the effects of residual stresses. It can approximate the plastic-zone solution accurately if appropriate geometric imperfections are incorporated [23]. The parameter C is used to allow for gradual inelastic stiffness reduction of the element associated with material plastification. Essentially, it is a function of the axial force and bending moment in the member. However, the scalar number is approximately chosen to simplify the implementation of the analysis.

3.4.2 Design Guidelines

The design guidelines of the direct analysis method with modified stiffness are proposed for steel frame design as follow:

Steps 1 to 3 are the same as the steps 1 to 3 of DAM-NL method in Section 3.3.2.

Step 4. Perform an elastic analysis to determine the axial forces of all members in the structure.

Step 5. Modify the flexural rigidities for members with axial forces greater than $0.1P_y$, by multiplying the stiffness reduction factors shown in Section 3.4.1.

Step 6. Determine the notional load $NL = 0.002GL$ at each floor level.

Step 7. Analyze the structure using a second-order elastic analysis with the consideration of modified stiffness and notional loads.

Steps 8 to 13 are the same as the steps 6 to 11 of DAM-NL method.

3.4.3 Two-Story Unbraced Frame Example

In this section, the two-story unbraced steel frame shown in Figure 2.1 (Section 2.3) is analyzed and designed by using DAM-MS method. Column EF will be considered in detail.

(1) Determine stiffness reduction factors

An elastic analysis is implemented to determine the axial force in each member. The cross sectional properties of the members are given in Table 3.3. The results and calculated stiffness reduction factors are shown in Table 3.4. In this example, no inelastic effect needs to be considered.

(2) Determine notional loads

At the roof level: $NL_{roof} = 0.002 \times (0.2 \times 288) = 0.1152$ kip

At the floor level: $NL_{floor} = 0.002 \times (0.3 \times 288) = 0.1728$ kip

(3) Determine P_u and M_u

A second-order elastic analysis is performed under the consideration of flexural stiffness reduction and notional loads. The determined axial and flexural strengths, P_u and M_u , are 75.7 kips and 925.3 kip-in, respectively.

(4) Determine $\phi_c P_n$ and $\phi_b M_n$

The design strength $\phi_c P_n$ and $\phi_b M_n$ are identical to the ones calculated by using DAM-NL method. Therefore, the axial capacity of Column EF is 298.5 kips and the flexural capacity is 1408.5 kip-in.

(5) Check interaction equations

$$\frac{P_u}{\phi_c P_n} = \frac{75.7}{298.5} = 0.254$$

$$\frac{P_u}{\phi_c P_n} + \frac{8 M_u}{9 \phi_b M_n} = 0.254 + \frac{8 \cdot 925.3}{9 \cdot 1408.5} = 0.836 < 1.0 \quad \therefore \text{O.K.}$$

The analysis results are shown in Table 3.5. The interaction ratios are close to the ones determined by using the AISC-LRFD and DAM-NL methods and their design results are identical.

Table 3.3 Sectional properties of the members of the two-story unbraced frame

Member	Section	A (in ²)	Z _x (in ³)	S _x (in ³)	P _y (kip)	M _n (in-kip)	M _y (in-kip)	M _n >1.2M _y
Column	W10×26	7.61	31.3	27.9	380.5	1565	1395	NO
Floor beam	W16×31	9.13	54.0	47.2	456.5	2700	2360	NO
Roof beam	W14×22	6.49	33.2	29.0	324.5	1660	1450	NO

Table 3.4 First-order analysis results and member stiffness reduction factors of the two-story unbraced frame

Member	Section	P (kips)	P/P _y	C	τ
AB	W10×26	68.4	0.18	1.0	1.0
BC	W10×26	27.9	0.07	-	-
DE	W10×26	29.7	0.08	-	-
EF	W10×26	75.6	0.20	1.0	1.0
BE	W16×31	5.2	0.01	-	-
CD	W14×22	16.2	0.05	-	-

Table 3.5 Adequacy check for the members of the two-story unbraced frame using DAM-MS method

Member	P_u (kips)	M_u (in-kip)	ΣI (DAM-MS)	ΣI (LRFD)	ΣI (DAM-MS)
AB	68.3	328.3	0.436	0.462	0.455
BC	27.9	965.8	0.732	0.741	0.724
DE	29.7	1234.7	0.926	0.928	0.941
EF	75.7	925.3	0.836	0.863	0.862
BE	5.2	2036.5	0.838	0.833	0.865
CD	16.2	1247.2	0.871	0.823	0.876

3.5 The Difficulties of Using Direct Analysis Method

3.5.1 Determination of the Directions of Notional Loads

In conjunction with external loads, the notional loads should be applied in adequate directions so as to cause the maximum destabilizing effect. If the directions of notional loads are not appropriate, the structural system will be strengthened instead of weakened. For the cantilever beam-column shown in Figure 3.1, the ultimate axial strength determined by DAM-NL is 297.2 kips if the notional load is applied at the top with the opposite direction of the external horizontal load. This value is higher than the one that the notional load is not applied and it is obviously incorrect.

It is straightforward to determine the directions of notional loads for a simple structural system. But, for a complex system, it may not be so obvious. One way to decide the directions of notional loads is to observe the deformed shape or the buckling mode of the structural system under the applied external loads. The notional loads should be applied with the design loads to cause further frame drift. However, an additional structural analysis of the system is needed.

3.5.2 Leaned Column Effects

In steel frame design, it is necessary to show special concern when considering leaned column frames that are quite common for some types of low-rise industrial structures. The effective lengths of leaned columns should be computed based on $K = 1$. In other words, leaned columns in a story sustain only gravity loads and contribute nothing to the sway stiffness of the story. The rigidly connected columns in the story support all the destabilizing $P-\Delta$ moment and brace the leaned columns at each floor level. Due to the destabilizing action of axial forces acting on the leaned columns, the effective length factors of beam-columns are enlarged. The modified effective length factor that considers story buckling is provided by AISC-LRFD Specification and expressed as equation (2.4). Therefore, the axial strengths of beam-columns in the lateral-resisting system involving leaned columns are greatly reduced. In the direct analysis method, the concept of effective length is waived and unsupported member length is used. Leaned column effects are not considered in its direct second-order analysis and the corresponding interaction requirements. It may lead to unconservative results. A leaned column frame example will be considered in Section 6.4.

3.6 Summary

The direct analysis method is a computer-based second-order elastic analysis method that can eliminate the determination of effective length factors. In the direct analysis method, the member compression strength in the plane of a frame is obtained by using unsupported member length. Initial geometric imperfections and member inelastic effects

must be taken into account in the analysis process instead of being implicitly involved in the beam-column interaction equations as the current AISC-LRFD method. Frame imperfections are accounted for by applying notional loads at floor levels, while the effects of member yielding are included by applying notional loads at floor levels or by modifying the flexural stiffness of the columns. The direct analysis method provides design results that are almost identical to the ones determined by AISC-LRFD method for general steel frame cases. However, difficulties exist in some particular cases. It is not straightforward to determine the adequate directions of notional loads for a complex system. In addition, since effective length factor is set to be equal to unity for all conditions, the direct analysis method cannot reflect the effects of different load patterns that are applied to a structural system. Therefore, limitations and modifications of this method will need to be addressed before this method can be used to practical analysis and design of steel frames. Although the direct analysis method reduces a lot of the work when compared with the AISC-LRFD method because the determination of effective length factors is waived, tedious individual member capacity checks are still needed. The only way to avoid the use of K-factors and to eliminate separate member capacity checks is by using second-order inelastic analysis. This will be considered in the next chapter.

CHAPTER 4

PRACTICAL ADVANCED ANALYSIS METHOD

4.1 Introduction

The key factors influencing steel frame behaviors are gradual yielding due to flexural and residual stresses, second-order effects, and initial geometric imperfections. In the current AISC-LRFD method, these effects are taken into account in the design equations. Advanced analysis refers to any steel design method that accurately captures the strength and stability of a structural system and its component members. Because it accounts for material and geometric nonlinearities in the analysis process directly instead of in the design equations [24], separate member capacity checks encompassing the determination of K factors are not required. By integrating analysis and design together coupled with the rapid development of computer hardware and software, it is expected that use of advanced analysis will significantly reduce the designer's effort. In addition, the advanced analysis method, which is the same as the conventional plastic design, can account for inelastic redistribution of internal forces after the strengths of certain members are reached. Moreover, it enables engineers to predict all possible failure modes of a structural system subjected to various load combinations.

In the first part of this chapter, the development of advanced analysis, from the first-order hinge-by-hinge analysis to the second-order elastic-plastic hinge analysis, is briefly reviewed. In the second part, the concept and formulation of second-order refined plastic

hinge analysis or advanced analysis are presented in details. A two-story unbraced frame is analyzed and designed using the advanced analysis method in the third part of this chapter.

4.2 First-Order Hinge-by-Hinge Analysis

In addition to providing the collapse load of a frame, the first-order elastic-plastic hinge analysis can be used to determine the sequence of formation of plastic hinges, the overstrength factor associated with the formation of each plastic hinge, and member force distributions in the frame between each plastic hinge formation. In a first-order hinge-by-hinge analysis, the structural members must be compact and adequately braced so that the plastic moment of each member can be reached. If local buckling or lateral torsional buckling governs the failure of the members, this analysis approach cannot be applied.

4.2.1 Assumptions

The assumptions used in the modeling of a beam or frame element in the plastic hinge analysis are:

1. *The member is initially straight and prismatic.*
2. *Plane section remains plane after deformation.*
3. *The member is compact and adequately braced so that its plastic capacity can be reached.*
4. *Member deformations are small, but large rigid-body displacements are allowed.*
5. *Spread of yielding and residual stresses are not considered.*

6. Member shear forces are small and the effects of shear deformations are neglected.
7. Axial shortening due to bowing effect is ignored.
8. The effects of axial force are not considered.

4.2.2 Analysis Procedures

The first-order hinge-by-hinge analysis is a series of elastic analyses. First, a linear elastic analysis is performed on the original structure. When the maximum moment in the structure reaches the plastic moment capacity of a member, a plastic hinge is formed at the location of maximum moment. The formation of the plastic hinge results in a reduction of one degree of indeterminacy from the structure. If the structure is determinate, it becomes unstable and then the ultimate load is obtained. If the structure is indeterminate, it is equivalent to a new and simpler structure in which a real hinge is used to replace the plastic hinge and a constant plastic moment is applied at the location. Next, another linear elastic analysis is performed on the new structure. The new plastic hinge can be located and a newer structure can be obtained. This process is performed until a sufficient number of plastic hinges are formed and the original structure is transformed into a failure mechanism.

In this process, the first-order elastic analysis is presented and second-order stability effects due to axial force are ignored. Without consideration of stability effects, the results of the first-order hinge-by-hinge analysis will overestimate the actual load-carrying capacity of the structural system.

4.2.3 Redistribution of Internal Forces

The plastic design has several benefits over the elastic analysis because one of the important properties of steel, ductility, is fully utilized. Plastification of steel is the process of yielding of steel fibers causing the change in stress distribution on a cross section as the bending moment increases. For a statically indeterminate beam or frame structure, a plastic hinge will be formed at the location of maximum moment. No additional moment can be sustained at this location and must be spread to other parts of the structure. This process is called moment redistribution. For indeterminate beams and frames, the plastic limit load will be higher than the initial yield load because of plastification of steel and moment redistribution of the system. In a first-order hinge-by-hinge analysis, we assume all the plastic rotations occur at the plastic hinges and the plastic hinge length is zero [25].

Figure 4.1a shows a fixed-end beam made of W8×31 section and the yield stress is 50 ksi. The plastic moment equals

$$M_p = Z_x F_y = (30.4)(50) = 1520 \text{ kip-in.}$$

By using a linear elastic analysis, the moment diagram of the original beam is determined and shown in the same figure. When the maximum moment located at point A reaches the plastic moment M_p , the first plastic hinge is formed at point A. It can be replaced by a real hinge with moment M_p , as shown in Figure 4.1b. The first hinge load P_1 is calculated as

$$12P_1 = 1520$$

$$P_1 = 126.67 \text{ kips}$$

By performing an elastic analysis to the new beam, the corresponding moment diagram can be obtained and shown in Figure 4.1b. Since the moment at point B is greater than the one at point C, the second plastic hinge will be formed at point B if loading keeps increasing. The second hinge load P_2 is

$$-760 + 14P_2 = 1520$$

$$P_2 = 162.86 \text{ kips}$$

The newer beam and its corresponding moment diagram are shown in Figures 4.1c. The third or final plastic hinge will form at point C. The third hinge load P_3 or plastic limit load P_p can be determined as

$$54P_3 - 7600 = 1520$$

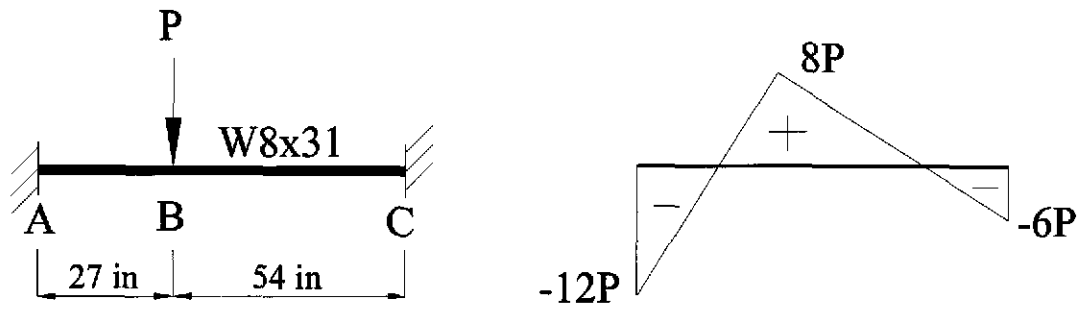
$$P_3 = P_p = 168.89 \text{ kips}$$

At $P = P_p$, a failure mechanism has formed and the beam collapses.

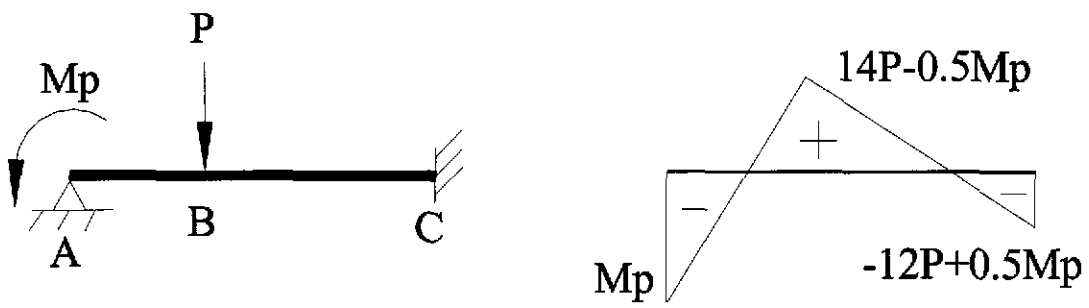
The percentage of plastic strength reserved in the beam beyond the elastic limit through moment redistribution is:

$$\frac{168.89 - 126.67}{126.67} = 33.33\%$$

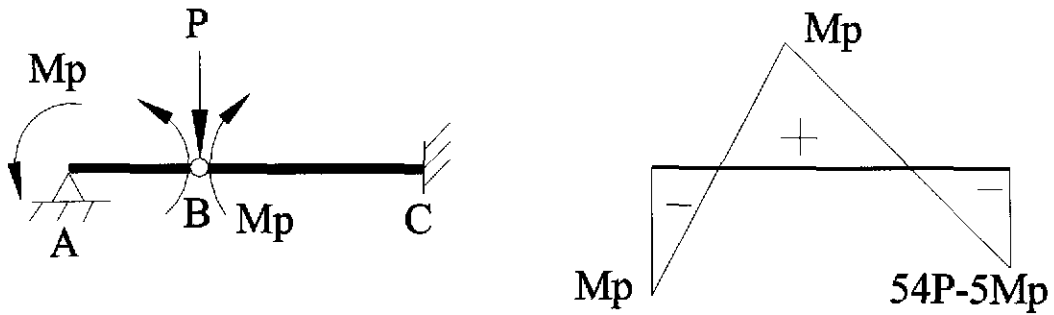
Although this percentage is overestimated because stability effects, residual stresses, and initial geometric imperfection are not considered, the plastic limit strength is still much higher than the initial yield strength.



(a) Elastic analysis



(b) Plastic hinge formed at end A



(c) Plastic hinges formed at ends A and B

Figure 4.1 Fixed-end beam

4.3 Second-Order Elastic-Plastic Hinge Model

In the first-order hinge-by-hinge analysis, the stability effects on structural members are neglected and the plastic limit strength is overestimated. To account for the secondary bending moments generated as the axial compressive force acts over the lateral displacement of the member, second-order analysis based on incremental load concept and stability functions are used to trace the behavior of a structure which allows the limit strength of the structure to be more accurately obtained. The assumptions used in this section are same as those in Section 4.2.1 excluding the eighth item.

4.3.1 Stability Functions

A beam-column member subjected to end moments M_A and M_B and axial compressive force P is shown in Figure 4.2a. By considering the equilibrium condition of the segment shown in Figure 4.2b and the boundary conditions $y(0) = 0$, $y(L) = 0$, the end rotations θ_A and θ_B can be determined and written in matrix form [20] as

$$\begin{Bmatrix} \theta_A \\ \theta_B \end{Bmatrix} = \frac{L}{EI} \begin{bmatrix} f_{11} & f_{12} \\ f_{21} & f_{22} \end{bmatrix} \begin{Bmatrix} M_A \\ M_B \end{Bmatrix} \quad (4.1)$$

where

$$f_{11} = f_{22} = \frac{\sin kL - kL \cos kL}{(kL)^2 \sin kL} \quad (4.2)$$

$$f_{12} = f_{21} = \frac{\sin kL - kL}{(kL)^2 \sin kL} \quad (4.3)$$

$$k^2 = \frac{P}{EI} \quad (4.4)$$

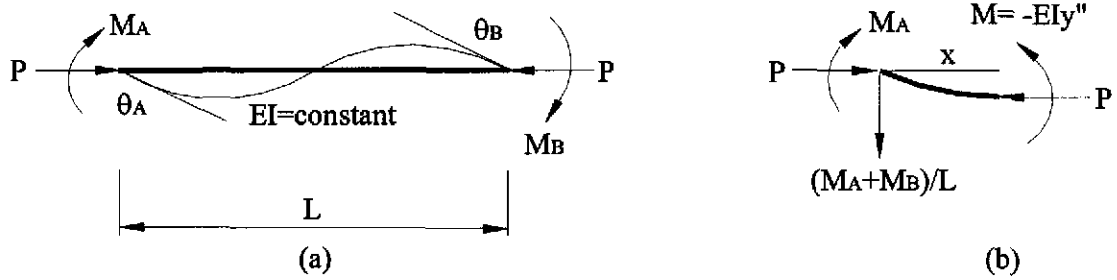


Figure 4.2 Beam-column subjected to end moments and axial force

From equation (4.1), the end moments M_A and M_B can be expressed by θ_A and θ_B

$$\begin{Bmatrix} M_A \\ M_B \end{Bmatrix} = \frac{EI}{L} \begin{bmatrix} f_{11} & f_{12} \\ f_{21} & f_{22} \end{bmatrix}^{-1} \begin{Bmatrix} \theta_A \\ \theta_B \end{Bmatrix} \quad (4.5)$$

or

$$\begin{Bmatrix} M_A \\ M_B \end{Bmatrix} = \frac{EI}{L} \begin{bmatrix} S_1 & S_2 \\ S_2 & S_1 \end{bmatrix} \begin{Bmatrix} \theta_A \\ \theta_B \end{Bmatrix} \quad (4.6)$$

where

$$S_1 = \frac{kL \sin kL - (kL)^2 \cos kL}{2 - 2 \cos kL - kL \sin kL} \quad (4.7)$$

$$S_2 = \frac{(kL)^2 - kL \sin kL}{2 - 2 \cos kL - kL \sin kL} \quad (4.8)$$

Equation (4.6) is the slope-deflection equation for a beam-column without transverse loadings and relative joint translation. Stability functions S_1 and S_2 account for the effects of out-of-straightness of the member subjected to axial force. It allows one element per member and maintains accuracy in the element stiffness terms for all ranges of axial loads.

Equations (4.7) and (4.8) are indeterminate when the axial force equals zero and the factor k becomes an imaginary number if the axial force is in tension. To avoid those difficulties, Lui and Chen [26] have proposed approximate expressions for S_1 and S_2 if $-2.0 \leq k \leq 2.0$.

$$S_1 = 4 + \frac{2\pi^2 \rho}{15} - \frac{(0.01\rho + 0.543)\rho^2}{4 + \rho} - \frac{(0.004\rho + 0.285)\rho^2}{8.183 + \rho} \quad (4.9)$$

$$S_2 = 2 - \frac{\pi^2 \rho}{30} + \frac{(0.01\rho + 0.543)\rho^2}{4 + \rho} - \frac{(0.004\rho + 0.285)\rho^2}{0.183 + \rho} \quad (4.10)$$

where

$$\rho = \frac{P}{P_e} = \frac{P}{\frac{\pi^2 EI}{L^2}} \quad (4.11)$$

4.3.2 Incremental Force-Displacement Relationship

In a second-order analysis, incremental load concept is applied to account for second-order effects. Without considering the bowing effects, the axial displacement of a member is

$$e = \frac{PL}{AE} \quad (4.12)$$

Combining equations (4.6) and (4.12), the incremental form of element force-displacement relationship may be expressed as

$$\begin{Bmatrix} \dot{M}_A \\ \dot{M}_B \\ \dot{P} \end{Bmatrix} = \frac{EI}{L} \begin{bmatrix} S_1 & S_2 & 0 \\ S_2 & S_1 & 0 \\ 0 & 0 & A/I \end{bmatrix} \begin{Bmatrix} \dot{\theta}_A \\ \dot{\theta}_B \\ \dot{e} \end{Bmatrix} \quad (4.13)$$

or

$$\dot{f}_c = k_c \dot{d}_c \quad (4.14)$$

where

$\dot{M}_A, \dot{M}_B, \dot{P}$ = incremental end moments and axial force

$\dot{\theta}_A, \dot{\theta}_B, \dot{e}$ = incremental end rotations and axial displacement

\dot{f}_c, \dot{d}_c = incremental element end force and displacement vectors

k_c = element tangent stiffness matrix

For a plane frame element, six degrees of freedom shown in Figure 4.3 are needed to describe the total displacement of the member. The incremental force-displacement relationship in the global coordinate system may be symbolically expressed as [13]

$$\dot{f}_g = k_g \dot{d}_g \quad (4.15)$$

where

\dot{d}_g = vector of incremental frame element end displacements in global coordinate system

$$= [d_{g1} \quad d_{g2} \quad d_{g3} \quad d_{g4} \quad d_{g5} \quad d_{g6}]^T$$

\dot{f}_g = vector of incremental frame element end forces corresponding to \dot{d}_g in global coordinate system

k_g = tangent stiffness matrix of a beam-column

$$= T_{cg}^T k_c T_{cg} + T_1 M_A + T_2 M_B + T_3 P \quad (4.16)$$

T_{cg} , T_1 , T_2 , and T_3 are transformation matrices.

$$T_{eg} = \begin{bmatrix} -s/L & c/L & 1 & s/L & -c/L & 0 \\ -s/L & c/L & 0 & s/L & -c/L & 1 \\ -c & -s & 0 & c & s & 0 \end{bmatrix} \quad (4.17)$$

$$T_1 = T_2 = \frac{1}{L^2} \begin{bmatrix} -2sc & c^2 - s^2 & 0 & 2sc & s^2 - c^2 & 0 \\ c^2 - s^2 & 2sc & 0 & s^2 - c^2 & -2sc & 0 \\ 0 & 0 & 0 & 0 & 0 & 0 \\ 2sc & s^2 - c^2 & 0 & -2sc & c^2 - s^2 & 0 \\ s^2 - c^2 & -2sc & 0 & c^2 - s^2 & 2sc & 0 \\ 0 & 0 & 0 & 0 & 0 & 0 \end{bmatrix} \quad (4.18)$$

$$T_3 = \frac{1}{L} \begin{bmatrix} s^2 & -sc & 0 & -s^2 & sc & 0 \\ -sc & c^2 & 0 & sc & -c^2 & 0 \\ 0 & 0 & 0 & 0 & 0 & 0 \\ -s^2 & sc & 0 & s^2 & -sc & 0 \\ sc & -c^2 & 0 & -sc & c^2 & 0 \\ 0 & 0 & 0 & 0 & 0 & 0 \end{bmatrix} \quad (4.19)$$

in which $s = \sin \theta$ and $c = \cos \theta$. θ is the inclination angle of the displaced element chord.



Figure 4.3 Degree of freedom numbering for the frame element

4.3.3 Modeling of Plastic Hinges

In elastic-plastic hinge analysis, the behavior of frame elements is assumed to be elastic until plastic hinges are formed at the ends of elements. It is assumed that the cross-section response is perfectly plastic with no strain hardening after the formation of plastic hinges. Once a plastic hinge is formed, the cross-sectional forces are assumed to move on the plastic strength curve only. Unloading is conservatively neglected so that the bending moment needs to be decreased if the axial force is increased on the cross section.

Although the formation of plastic hinges may occur between both ends of the element, it is not required to determine the exact location of the maximum moment and insert a plastic hinge for an accurate estimation of the maximum strength of the member [27].

4.3.3.1 Cross-Section Plastic Strength

To calibrate the design results of the AISC-LRFD method, the AISC-LRFD bilinear plastic strength curves are adopted for the bending about both strong and weak axes:

$$\frac{P}{\phi_c P_y} + \frac{8}{9} \frac{M}{\phi_b M_p} = 1.0 \quad \text{for } \frac{P}{\phi_c P_y} \geq 0.2 \quad (4.20a)$$

$$\frac{1}{2} \frac{P}{\phi_c P_y} + \frac{M}{\phi_b M_p} = 1.0 \quad \text{for } \frac{P}{\phi_c P_y} < 0.2 \quad (4.20b)$$

where

P_y = squash load

M_p = plastic bending moment

P, M = second-order axial force and bending moment on the cross-section considered,
 respectively

ϕ_c, ϕ_b = resistance factors

Figure 4.4 shows the plastic strength curves. To compare with the analytical solution [28], the resistance factors ϕ_c and ϕ_b are omitted in the figure. It can be seen that equation (4.20) gives a good fit to the strong-axis solution, but it is conservative for the weak-axis strength.

4.3.3.2 Modification of Element Stiffness for the Formation of Plastic Hinges

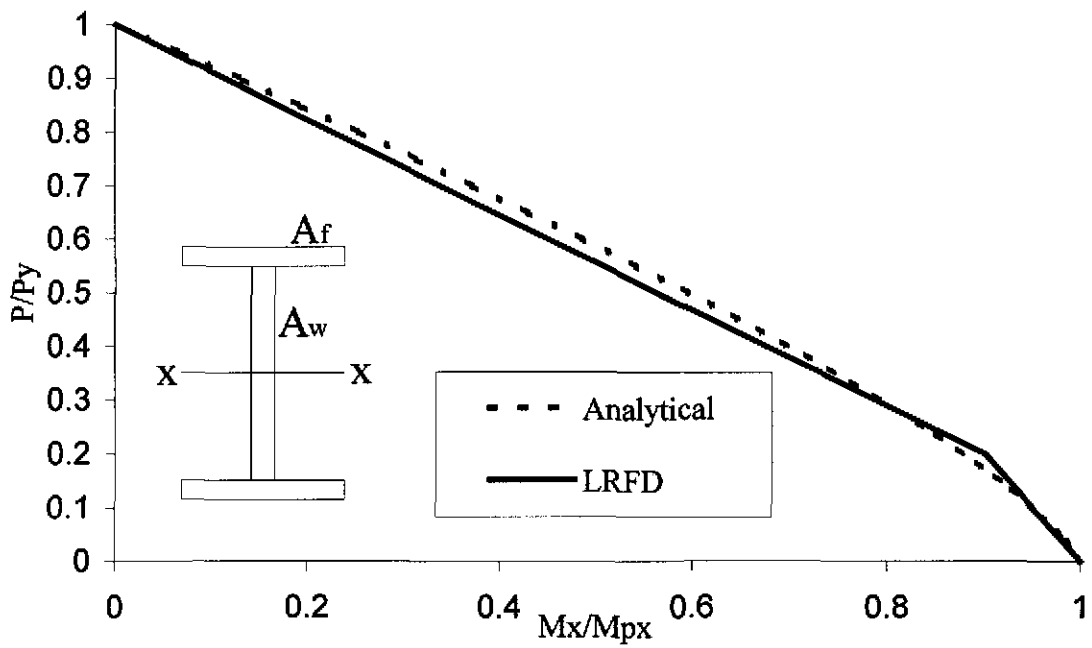
Equation (4.13) represents the elastic incremental force-displacement relationships of an element. It needs to be modified to account for the change in element behavior due to the formation of plastic hinges. For the element shown in Figure 4.2a, if a plastic hinge is formed at end A, equation (4.13) may be changed as follow:

$$\begin{Bmatrix} \Delta M_{pcA} \\ \dot{M}_B \\ \dot{P} \end{Bmatrix} = \frac{EI}{L} \begin{bmatrix} S_1 & S_2 & 0 \\ S_2 & S_1 & 0 \\ 0 & 0 & A/I \end{bmatrix} \begin{Bmatrix} \dot{\theta}_A \\ \dot{\theta}_B \\ \dot{e} \end{Bmatrix} \quad (4.21)$$

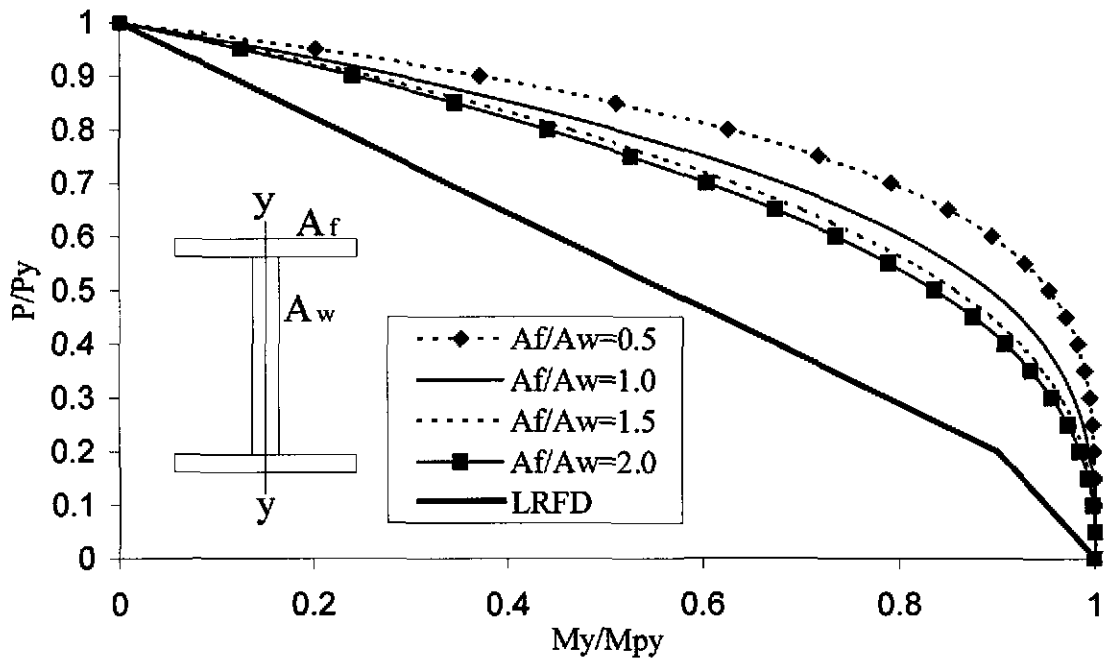
where ΔM_{pcA} is the change in plastic moment capacity at end A based on equation (4.20) as P changes.

From the first row of equation (4.21),

$$\dot{\theta}_A = \frac{L}{EI} \frac{\Delta M_{pcA}}{S_1} - \frac{S_2 \dot{\theta}_B}{S_1} \quad (4.22)$$



(a) Strong axis bending



(b) Weak axis bending

Figure 4.4 Strength interaction curves of wide flange sections

Substitute equation (4.22) into equation (4.13), the modified force-displacement relationships of the element is

$$\begin{Bmatrix} \dot{M}_A \\ \dot{M}_B \\ \dot{P} \end{Bmatrix} = \frac{EI}{L} \begin{bmatrix} S_1 & S_2 & 0 \\ S_2 & S_1 & 0 \\ 0 & 0 & A/I \end{bmatrix} \begin{Bmatrix} \frac{L}{EI} \frac{\Delta M_{pcA}}{S_1} - \frac{S_2 \dot{\theta}_B}{S_1} \\ \dot{\theta}_B \\ \dot{e} \end{Bmatrix} \quad (4.23)$$

Rearranged and the following is produced:

$$\begin{Bmatrix} \dot{M}_A \\ \dot{M}_B \\ \dot{P} \end{Bmatrix} = \frac{EI}{L} \begin{bmatrix} 0 & 0 & 0 \\ 0 & S_1 - S_2^2/S_1 & 0 \\ 0 & 0 & A/I \end{bmatrix} \begin{Bmatrix} \dot{\theta}_A \\ \dot{\theta}_B \\ \dot{e} \end{Bmatrix} + \begin{Bmatrix} 1 \\ S_2/S_1 \\ 0 \end{Bmatrix} \Delta M_{pcA} \quad (4.24)$$

Similarly, if a plastic hinge is formed at end B, equation (4.13) can be modified as:

$$\begin{Bmatrix} \dot{M}_A \\ \dot{M}_B \\ \dot{P} \end{Bmatrix} = \frac{EI}{L} \begin{bmatrix} S_1 - S_2^2/S_1 & 0 & 0 \\ 0 & 0 & 0 \\ 0 & 0 & A/I \end{bmatrix} \begin{Bmatrix} \dot{\theta}_A \\ \dot{\theta}_B \\ \dot{e} \end{Bmatrix} + \begin{Bmatrix} S_2/S_1 \\ 1 \\ 0 \end{Bmatrix} \Delta M_{pcB} \quad (4.25)$$

If plastic hinges are formed at both ends, then:

$$\begin{Bmatrix} \dot{M}_A \\ \dot{M}_B \\ \dot{P} \end{Bmatrix} = \frac{EI}{L} \begin{bmatrix} 0 & 0 & 0 \\ 0 & 0 & 0 \\ 0 & 0 & A/I \end{bmatrix} \begin{Bmatrix} \dot{\theta}_A \\ \dot{\theta}_B \\ \dot{e} \end{Bmatrix} + \begin{Bmatrix} \Delta M_{pcA} \\ \Delta M_{pcB} \\ 0 \end{Bmatrix} \quad (4.26)$$

For a plane frame element, the modified incremental force-displacement relationships in the global coordinate system can be symbolically written as [13]:

$$\dot{f}_g = K_{gh} \dot{d}_g + \dot{f}_{gp} \quad (4.27)$$

where

$$K_{gh} = T_{cg}^T k_{ch} T_{cg} + T_1 M_A + T_2 M_B + T_3 P \quad (4.28)$$

$$\dot{f}_{gp} = T_{cg}^T \dot{f}_{cp} \quad (4.29)$$

k_{ch} is the modified basic tangent stiffness matrix due to the presence of plastic hinges as shown in equation (4.24) through (4.26). \dot{f}_{cp} is the equilibrium force correction vector that comes from the change in moment capacity as P changes. \dot{f}_g , \dot{d}_g , T_{cg} , T_1 , T_2 and T_3 are defined in Section 4.3.2.

4.4 Second-Order Refined Plastic Hinge Method

In elastic-plastic hinge analysis, inelasticity in frame elements is assumed to concentrate at plastic hinges. However, for stocky members exhibiting significant yielding, the elastic-plastic hinge analysis over predicts the maximum strength of the structure [25] because of the assumptions that perfect plasticity and zero-length plastic hinges exist. Some refinements are needed to capture the effects of distributed yielding associated with plastification and residual stresses through the cross section. Residual stresses are a set of self-equilibrium stresses in the member cross section due to unavoidable error during the erection or fabrication process. Plastification means a gradual transition of the element stiffness from the onset of yielding to achievement of the full plastic moment. In the refined plastic hinge approach, the elastic modulus of the element is replaced by a tangent modulus to account for the gradual yielding due to residual stresses, while the two-surface stiffness degradation model is used to evaluate the effects of plastification.

4.4.1 Tangent Modulus Model Associated with Residual Stresses

Because of uneven cooling during manufacturing, initial residual stresses are induced in hot-rolled I-sections. Generally, compressive residual stresses occur at flange tips and mid-height of the web, while tensile residual stresses occur at the junctions of flanges and web. In accordance to the plastic theorem, the strength of a structure and its members is independent of residual stresses. However, the effects of residual stresses will reduce the member flexural stiffness and the structural stability [29]. Therefore, it is expected that there are more effects on slender frames than on stocky frames due to residual stresses. Although reduction of the elastic portion of the cross section causes degradation of the bending stiffness, elastic modulus E instead of moment of inertia I is reduced because it is easier to implement in the analysis.

Equation (2.8a) represents the column strength provided by AISC-LRFD Specification when the member material is still in the elastic range, while equation (2.8b) applies when part of the member material is yielded. The column tangent modulus, E_t , can be evaluated by dividing equation (2.8b) by equation (2.8a). Thus,

$$\frac{E_t}{E} = 1.0 \quad \text{for } P \leq 0.39P_y \quad (4.30a)$$

$$\frac{E_t}{E} = -2.7243 \frac{P}{P_y} \ln \left(\frac{P}{P_y} \right) \quad \text{for } P > 0.39P_y \quad (4.30b)$$

where

E = modulus of elasticity

P and P_y = axial force in the column member and squash load, respectively

It should be noted that this E_t model derived from the AISC-LRFD column strength formula implicitly involves the effects of residual stresses and geometric imperfections. However, for a member subjected to tensile axial force, only the effects of residual stresses should be considered in the stiffness degradation of the member. On the other hand, for a member subjected to compressive axial force, this model does not account for geometric imperfection effects when P is less than $0.39P_y$, because the AISC-LRFD tangent modulus is identical to the elastic modulus in this range. Therefore, the tangent modulus based on the CRC column strength formulae [22] that do not include geometric imperfections may be more appropriate for practical steel design. When CRC- E_t is employed, an incorporated model that considers geometric imperfections should be used in the analysis. The CRC- E_t can be presented as [23]:

$$\frac{E_t}{E} = 1.0 \quad \text{for } P \leq 0.5P_y \quad (4.31a)$$

$$\frac{E_t}{E} = 4 \frac{P}{P_y} \left(1 - \frac{P}{P_y} \right) \quad \text{for } P > 0.5P_y \quad (4.31b)$$

Equations (4.30) and (4.31) are plotted in Figure 4.5. The LRFD- E_t is reduced from the axial force P which equals $0.39P_y$, while the CRC- E_t is degraded when the value of P reaches $0.5P_y$. The normalized axial force-strain curves for these two models are plotted in Figure 4.6. It can be seen that the inelastic transition is a smooth curve instead of the two-straight line model that elastic-plastic hinge model adopts.

4.4.2 Two-Surface Stiffness Degradation Model Associated with Flexure

In the refined plastic hinge analysis, the parabolic model is assumed to simulate the degradation of element stiffness due to the plastification of the steel. The factor η representing a gradual stiffness reduction associated with flexure is proposed by Liew [30] and plotted in Figure 4.7.

$$\eta = 1 \quad \text{for } \alpha \leq 0.5 \quad (4.32a)$$

$$\eta = 4\alpha(1 - \alpha) \quad \text{for } \alpha > 0.5 \quad (4.32b)$$

In this model α is the force-state parameter obtained from the limit state surface corresponding to the member ends. The term α based on AISC-LRFD sectional strength curve is expressed as:

$$\alpha = \frac{P}{P_y} + \frac{8}{9} \frac{M}{M_p} \quad \text{for } \frac{P}{P_y} \geq \frac{2}{9} \frac{M}{M_p} \quad (4.33a)$$

$$\alpha = \frac{1}{2} \frac{P}{P_y} + \frac{M}{M_p} \quad \text{for } \frac{P}{P_y} < \frac{2}{9} \frac{M}{M_p} \quad (4.33b)$$

The smooth stiffness degradation curve for a work-hardening plastic hinge is plotted in Figure 4.8. Initial yielding is assumed to occur at $\alpha = 0.5$ and the yield surface function corresponding to $\alpha = 1.0$ represents the state of forces at which the cross section is fully yielded.

When these refined plastic hinges are presented at both ends of an element as shown in Figure 4.2a, the incremental force-displacement relationship as given in equation (4.13) can be modified as:

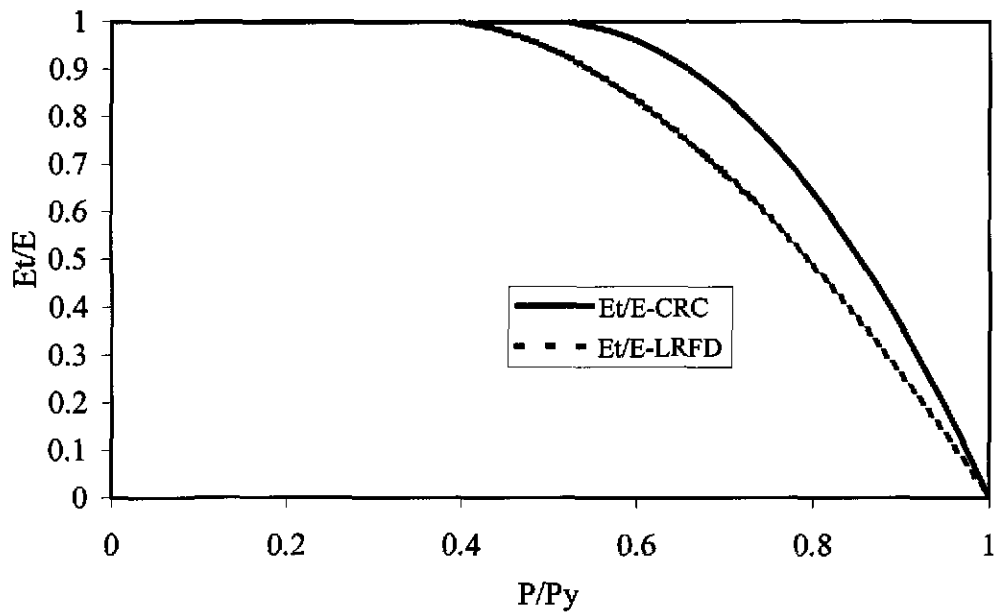


Figure 4.5 Member tangent stiffness degradation

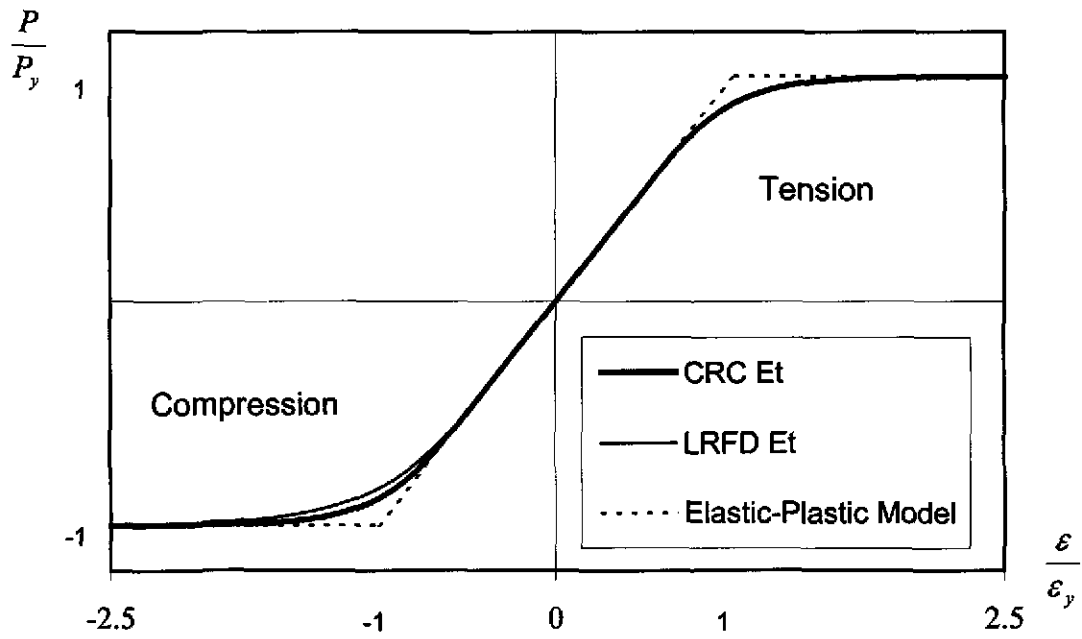


Figure 4.6 Normalized axial force-strain relationship

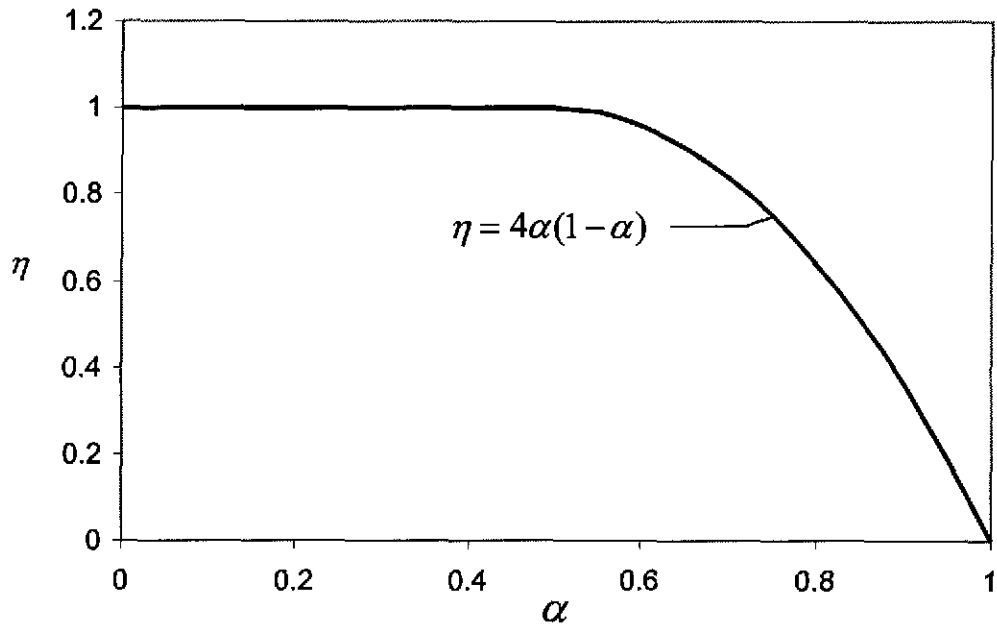


Figure 4.7 Parabolic plastic hinge stiffness degradation function

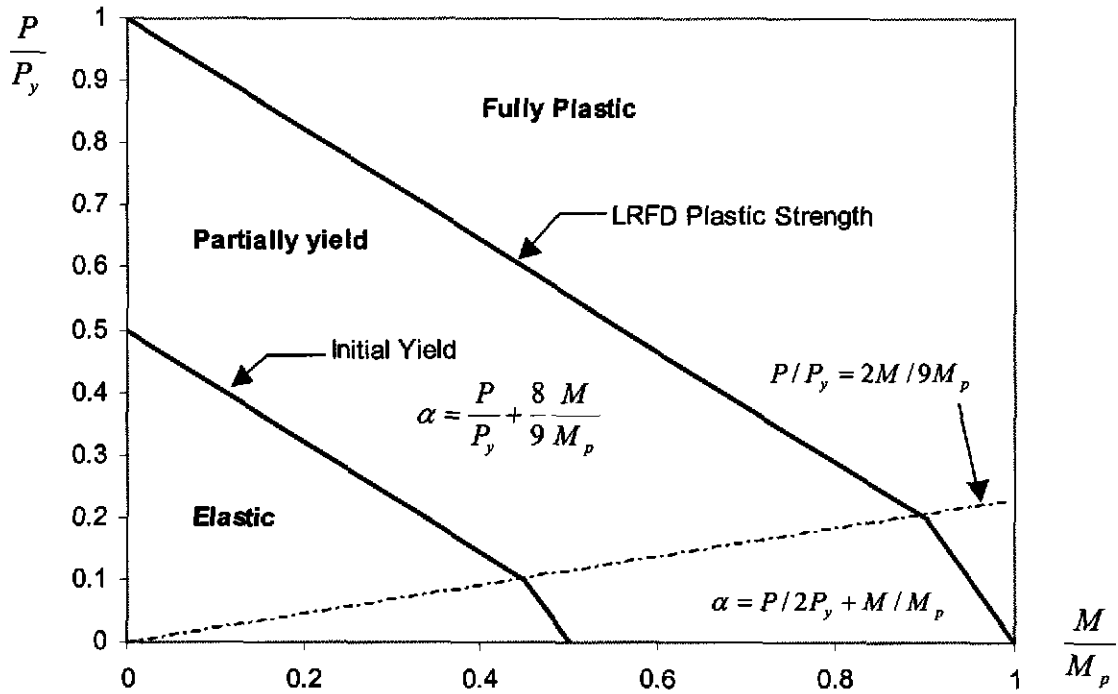


Figure 4.8 Stiffness degradation for a softening plastic hinge

$$\begin{Bmatrix} \dot{M}_A \\ \dot{M}_B \\ \dot{P} \end{Bmatrix} = \frac{E_t I}{L} \begin{bmatrix} \eta_A \left[S_1 - \frac{S_2^2}{S_1} (1 - \eta_B) \right] & \eta_A \eta_B S_2 & 0 \\ \eta_A \eta_B S_2 & \eta_B \left[S_1 - \frac{S_2^2}{S_1} (1 - \eta_A) \right] & 0 \\ 0 & 0 & A/I \end{bmatrix} \begin{Bmatrix} \dot{\theta}_A \\ \dot{\theta}_B \\ \dot{e} \end{Bmatrix} \quad (4.34)$$

where η_A and η_B are the stiffness reduction factors at ends A and B, respectively. Note that the modulus of elasticity E in equation (4.13) is replaced by the tangent modulus E_t to account for the effects of residual stresses.

4.4.3 Connection Nonlinearity

In conventional frame analysis, the behavior of beam-to-column connections is assumed to be either fully rigid or ideally pinned. However, most connections used in practice are semi-rigid types, which possess stiffness falling between the extreme cases of perfectly rigid and ideally pinned. The influence of semi-rigid connections on structural behavior would change not only the moment distribution in the beams and columns, but also increase the lateral drifts and the $P-\Delta$ effects of the structure. Therefore, it is necessary to involve the effects of semi-rigid connections in the analysis and design process if partially restrained connections are used.

In advanced analysis, the “three-parameter power model” proposed by Kishi and Chen [31] is adopted to model the behavior of semi-rigid connections. Figure 4.9 shows a beam-column element subjected to axial force and end moments with semi-rigid connections at both ends. If the effect of connection flexibility is considered in the

member stiffness, the incremental element force-displacement relationship of equation (4.27) should be modified as [13]:

$$\begin{Bmatrix} \dot{M}_A \\ \dot{M}_B \\ \dot{P} \end{Bmatrix} = \frac{E_t I}{L} \begin{bmatrix} S_{ii}^* & S_{ij}^* & 0 \\ S_{ij}^* & S_{jj}^* & 0 \\ 0 & 0 & A/I \end{bmatrix} \begin{Bmatrix} \dot{\theta}_A \\ \dot{\theta}_B \\ \dot{e} \end{Bmatrix} \quad (4.35)$$

where

$$S_{ii}^* = \left(S_{ii} + \frac{E_t I S_{ij} S_{jj}}{L R_{k_{tB}}} - \frac{E_t I S_{ij}^2}{L R_{k_{tB}}} \right) / R^* \quad (4.36)$$

$$S_{jj}^* = \left(S_{jj} + \frac{E_t I S_{ii} S_{jj}}{L R_{k_{tA}}} - \frac{E_t I S_{ij}^2}{L R_{k_{tA}}} \right) / R^* \quad (4.37)$$

$$S_{ij}^* = S_{ij} / R^* \quad (4.38)$$

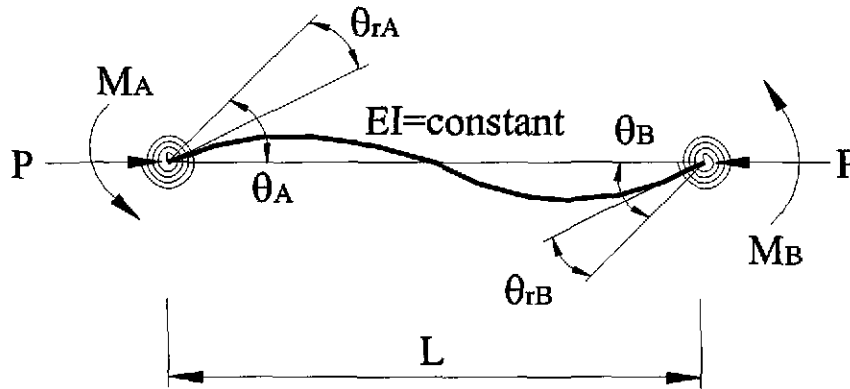


Figure 4.9 Frame element with end connections

where

$$S_{ii} = \eta_A \left[S_1 - \frac{S_2^2}{S_1} (1 - \eta_B) \right] \quad (4.39)$$

$$S_{jj} = \eta_B \left[S_1 - \frac{S_2^2}{S_1} (1 - \eta_A) \right] \quad (4.40)$$

$$S_{ij} = \eta_A \eta_B S_2 \quad (4.41)$$

$$R^* = \left(1 + \frac{E_t I S_{ii}}{L R_{kA}} \right) \left(1 + \frac{E_t I S_{jj}}{L R_{kB}} \right) - \left(\frac{E_t I}{L} \right)^2 \frac{S_{ij}^2}{R_{kA} R_{kB}} \quad (4.42)$$

R_{kA}, R_{kB} = tangent stiffness of connections A and B

4.4.4 Initial Geometric Imperfections

There are two types of initial geometric imperfections for steel members: out-of-straightness and out-of-plumbness. These imperfections cause additional moments in the column members and then the member bending stiffness is further reduced. Combined with the use of CRC- E_t , one of three geometric imperfection models is used in the advanced analysis method: the explicit imperfection modeling method, the equivalent notional load method, or the further reduced tangent modulus method.

4.4.4.1 Explicit Imperfection Modeling Method

According to the AISC Code of Standard Practice [1,3], the fabrication and erection tolerance for out-of-straightness is 1/1000 times the column length between braced points, and the maximum out-of-plumbness is limited to 1/500 times column length.

Although the out-of-straightness of a member should vary as a smooth curve, the imperfection shape is not known and many elements are needed in the analysis if the smooth shape is to be defined. In Figure 4.10a, two straight elements with a maximum initial deflection at the mid-height of the member are set to model the out-of-straightness of a braced member.

The explicit imperfection modeling of an unbraced frame member is shown in Figure 4.10b. To simplify the analysis, only the modeling of out-of-plumbness is considered for erection tolerance. Initial out-of-straightness of the column is ignored so that the same ultimate strength can be obtained for mathematically identical braced and unbraced members. The maximum out-of-plumbness for each frame story, $L_c/500$, is suitable for medium high (about 60 ft) or lower buildings. For taller buildings, this imperfection value is conservative because the accumulated geometric imperfections calculated by this value will be greater than the permitted erection tolerance of 2 inches that is specified in the building codes [1,3].

4.4.4.2 Equivalent Notional Load Method

Figure 4.11a shows a braced frame member with out-of-straightness of $L_c/1000$ at mid-height. The secondary moment at mid-point is $PL_c/1000$ leading to the lateral reactions of $P/500$ at two ends. To determine the equivalent notional load which is a fraction of the axial force of the member, a straight member braced at two ends shown in Figure 4.11b is considered. The member is subjected to an axial force P and an equivalent notional load nP is applied at its mid-height. In order to obtain the same out-

of-straightness $L_c/1000$ at mid-height of the member, it is assumed that Figures 4.11a and 4.11b are equivalent and the lateral reactions in Figure 4.11b must be equal to the ones in Figure 4.11a. Thus,

$$\frac{nP}{2} = \frac{P}{500}$$

or,

$$n = 0.004$$

Figure 4.12a shows an unbraced frame member with an out-of-plumbness of $L_c/500$. The out-of-plumb moment M_{IM} caused by the axial force P is $PL_c/500$ at the base. To determine the equivalent notional load accounting for the effects of initial geometric imperfection, consider a cantilever column shown in Figure 4.12b. The column is subjected to an axial force P and a lateral notional load nP at the top of the member. If the same out-of-plumbness of $L_c/500$ is assumed, Figures 4.12a and 4.12b must be equivalent and the base moment M_{NL} will be equal to M_{IM} . Thus,

$$(nP)(L_c) = \frac{PL_c}{500}$$

or,

$$n = 0.002$$

For a column member in a braced frame, the notional load of 0.004 times the axial force is applied at the mid-height of the member. For a sway frame, the notional load being equal to 0.002 times the total gravity loads applied on the considered story level is applied laterally at the top of each story.

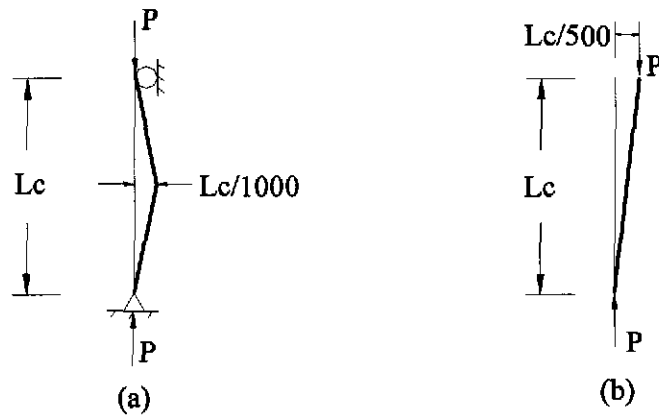


Figure 4.10 Explicit imperfection modeling

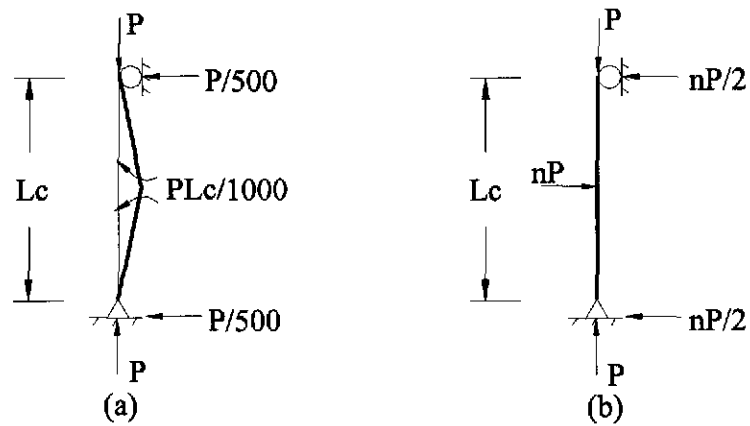


Figure 4.11 Equivalent notional load concept for modeling geometric imperfection of braced member

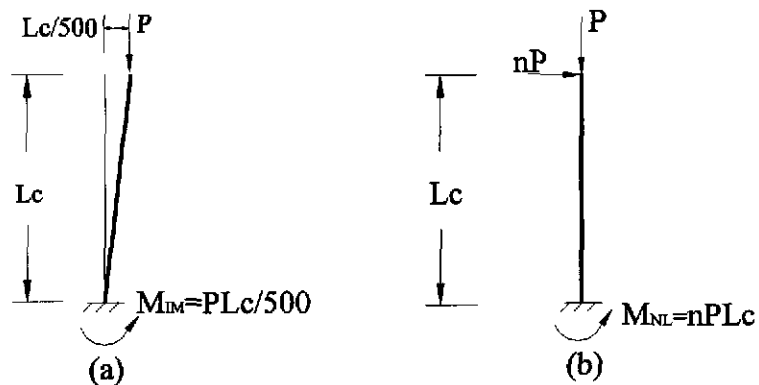


Figure 4.12 Equivalent notional load concept for modeling geometric imperfection of unbraced member

4.4.4.3 Further Reduced Tangent Modulus Method

Although the explicit imperfection modeling method and the equivalent notional load method can well account for the effects of initial geometric imperfection [13], tedious work still exists. For both methods, the directions of the imperfections or notional loads should coincide with the directions of the deflections caused by the bending moments. If the directions of setting the imperfections or notional loads are not adequate, they may not weaken the structural system, instead, the structure will be strengthened. Usually, a trial and error process is used to determine the directions of the imperfections or notional loads for complicated systems.

To eliminate this tedious work, the further reduced tangent modulus approach was proposed [13]. By including the effects of stiffness degradation due to geometric imperfection, the reduction factor of 0.85, which is determined by calibrating with the plastic-zone solutions, is used to further reduce the CRC- E_t as given in equation (4.31). The same reduction factor of 0.85 is used for both braced and unbraced structures. The further reduced tangent modulus curve is shown in Figure 4.13.

Although the reduction factor should be a function of the axial force in a column, a constant is used instead, because it allows for simplicity in the practical design process. Since the further reduced tangent modulus method can avoid the determination of the directions of the geometric imperfections and greatly reduce the input work that is necessary for the explicit imperfection modeling method and equivalent notional load method, it is recommended for practical steel frame design.

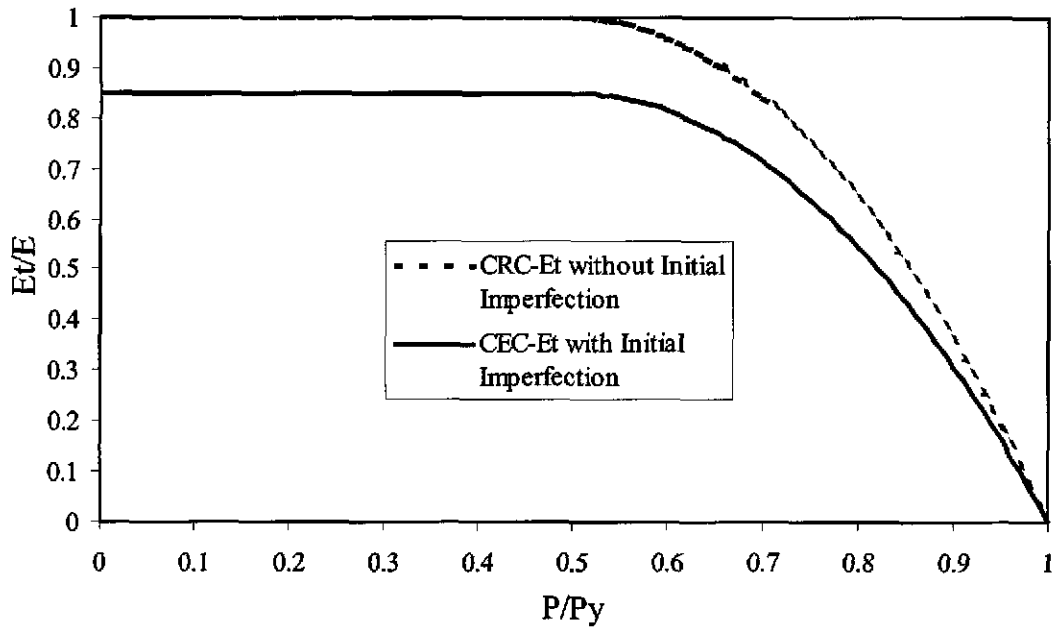


Figure 4.13 Further reduced tangent modulus

4.5 Advantages of Advanced Analysis in Steel Design

Advanced analysis is the state-of-the-art design method for structural engineering in the twenty-first century. Many advantages exist when it is compared to conventional steel analysis/design methods.

1. Advanced analysis method overcomes the difficulties of incompatibility between the elastic analysis of the structural system and limit state design of the structural members in the AISC-LRFD and direct analysis method.
2. Advanced analysis captures the limit state strength and stability of a structural system and its members directly. The tedious and time consuming individual member capacity checks involving the determination of K factors are not required.

3. Compared with the AISC-LRFD and direct analysis methods, the advanced analysis method provides more information such as the locations and sequences of formation of plastic hinges, failure mechanism, and overstrength factor of the structural system.
4. Inelastic redistribution of internal forces in the indeterminate frames can be considered by advanced analysis and a more economical design result could be obtained.
5. Since the advanced analysis method is developed by calibrating against the AISC-LRFD column curve and interaction equations, it meets the requirements of the AISC-LRFD method if the load-carrying capacity of the structure corresponding to the formation of the first plastic hinge is taken to signify failure.
6. Advanced analysis allows using one or two elements per member to accurately predict the strength of a structural system and its members. It leads to large savings in modeling and solution efforts.
7. Advanced analysis is user-friendly for a computer-based design process because the geometry and material nonlinearities are accounted for by using an iterative load-increment scheme.
8. It is easy for the advanced analysis method to optimize structural member sizes. To check the adequacy of the member design, it only needs to compare the applied loads with the load-carrying capacity determined by the advanced analysis program, whereas the LRFD and direct analysis methods require a repeat of separate member capacity checks for each optimization process.
9. Advanced analysis is a structural-based design approach which is consistent with the concepts of performance-based design.

4.6 Two-Story Unbraced Frame Example

In this section, the one-bay two-story unbraced steel shown in Figure 2.1 will be analyzed and designed by using the advanced analysis method. The FORTRAN-based program, PAAP, developed by Dr. S. E. Kim [13] is used. The results will be compared with the ones determined by using the AISC-LRFD and the direct analysis method.

4.6.1 Structural Modeling

Each column is modeled with one element and each beam is modeled with two. The node numbers and element numbers are shown in Figure 4.14. Uniform gravity loads are converted to equivalent concentrated loads applied at nodal points as shown in Figure 4.15. In the explicit imperfection modeling method, the initial out-of-plumbness equals $144/500=0.288$ in. and is set for the first and second stories. In the equivalent notional load method, horizontal notional loads of $0.002 \times (0.2 \times 288) = 0.1152$ kip and $0.002 \times (0.3 \times 288) = 0.1728$ kip are applied at the roof and floor levels, respectively. In the further reduced tangent modulus method, the program can account for the reduction of stiffness of column members intrinsically. The incremental loads are determined by dividing the total loads by a scaling factor of 20. The structural modeling schemes for the three methods are shown in Figures 4.16a through 4.16c. The input data based on the structural modeling are shown in Tables 4.1a through 4.1c.

4.6.2 Program Execution

The analysis results can be obtained after the execution of the PAAP program by simply entering the batch file, RUN.EXE. There are two output files: P.OUT1 is the echo of the information of the input data, while P.OUT2 shows the load-deflection behavior described by nodal forces, nodal displacements, and internal forces of all members at each incremental load step.

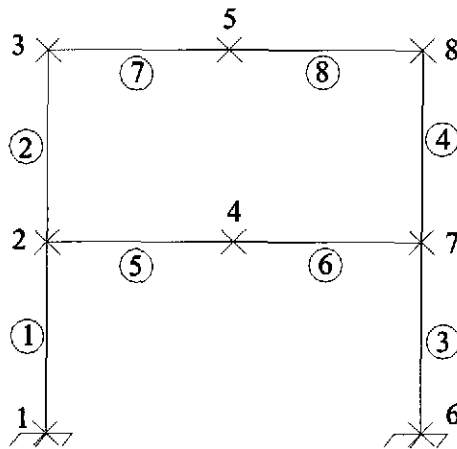


Figure 4.14 Structural modeling of the two-story unbraced frame

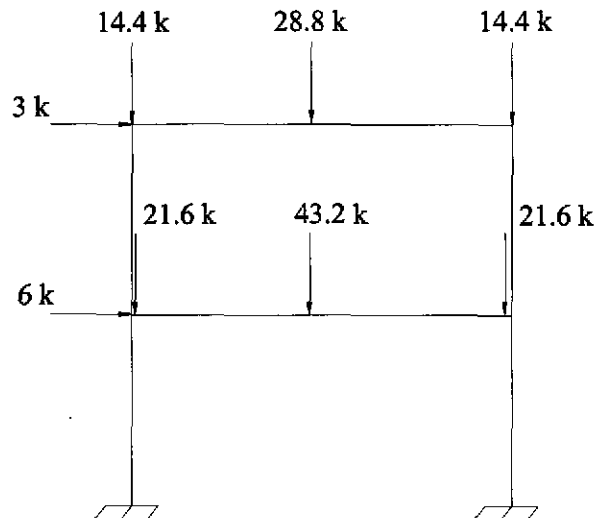


Figure 4.15 Equivalent loading condition of the two-story unbraced frame

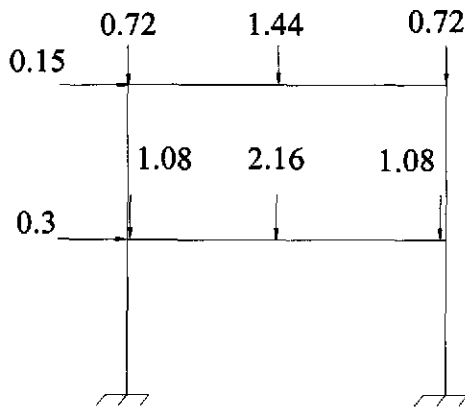
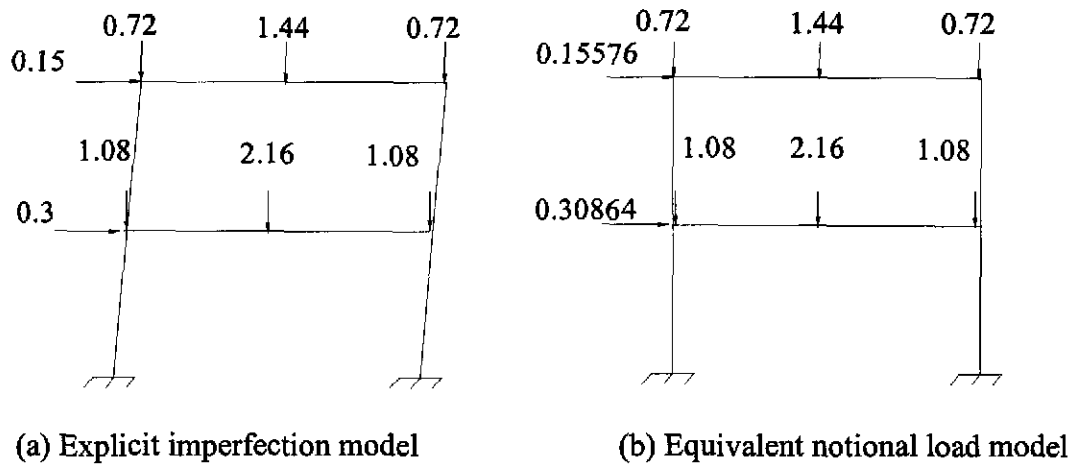


Figure 4.16 Three advanced analysis models for the two-story unbraced frame

3 (1.284) 1 (1.22) 2 (1.264)

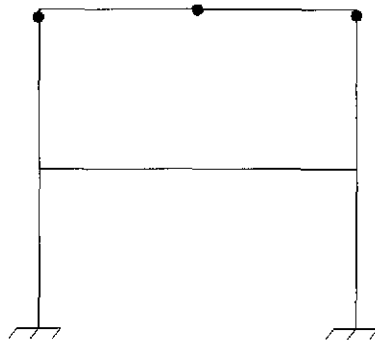


Figure 4.17 Locations and sequence of the formation of plastic hinges of the two-story unbraced frame

Table 4.1a Input data of the explicit imperfection modeling for the two-story unbraced frame

Two-story unbraced frame (AA-E.I.)

1	1						
8	2	100					
0	3	0					
0	8	0					
1		7.61	144.0	31.3	29000.0		50.0
2		9.13	375.0	54.0	29000.0		50.0
3		6.49	199.0	33.2	29000.0		50.0
1		0.288	144.0	1	1	2	2
3		0.288	144.0	1	6	7	2
5		144.0	0.0	2	2	4	
6		144.0	0.0	2	4	7	
7		144.0	0.0	3	3	5	
8		144.0	0.0	3	5	8	
1	1	1	1				
6	1	1	1				
2		0.12	-0.432				
3		0.06	-0.288				
4		0.0	-0.864				
5		0.0	-0.576				
7		0.0	-0.432				
8		0.0	-0.288				

Table 4.1b Input data of the equivalent notional load modeling for the two-story unbraced frame

Two-story unbraced frame (AA-N.L)

2	1						
8	2	100					
0	3	0					
0	8	0					
1		7.61	144.0	31.3	29000.0		50.0
2		9.13	375.0	54.0	29000.0		50.0
3		6.49	199.0	33.2	29000.0		50.0
1		0.0	144.0	1	1	2	2
3		0.0	144.0	1	6	7	2
5		144.0	0.0	2	2	4	
6		144.0	0.0	2	4	7	
7		144.0	0.0	3	3	5	
8		144.0	0.0	3	5	8	
1	1	1	1				
6	1	1	1				
2		0.123456	-0.432				
3		0.062304	-0.288				
4		0.0	-0.864				
5		0.0	-0.576				
7		0.0	-0.432				
8		0.0	-0.288				

Table 4.1c Input data of the further reduced tangent modulus modeling for the two-story unbraced frame

Two-story unbraced frame (AA-R. Et)

3	1						
8	2	100					
0	3	0					
0	8	0					
1		7.61	144.0	31.3	29000.0	50.0	1
2		9.13	375.0	54.0	29000.0	50.0	
3		6.49	199.0	33.2	29000.0	50.0	
1		0.0	144.0	1	1	2	2
3		0.0	144.0	1	6	7	2
5		144.0	0.0	2	2	4	
6		144.0	0.0	2	4	7	
7		144.0	0.0	3	3	5	
8		144.0	0.0	3	5	8	
1	1	1	1				
6	1	1	1				
2		0.12	-0.432				
3		0.06	-0.288				
4		0.0	-0.864				
5		0.0	-0.576				
7		0.0	-0.432				
8		0.0	-0.288				

4.6.3 Output Interpretation

Tables 4.2a through 4.2c show the final load step of the output file P.OUT2 for the three geometric imperfection methods. For the explicit imperfection modeling method, the collapse load at node 4 is 55.68 kips. Comparing with the applied external load of 43.2 kips at node 4 in Figure 4.15, the overstrength factor is $\lambda=55.68/43.2=1.289$. For the equivalent notional load method and the further reduced tangent modulus method, the collapse loads at node 4 are 55.65 kips and 55.48 kips and their corresponding overstrength factors are 1.288 and 1.284, respectively. Since the nominal strength of the frame is greater than the applied load, the member size design of the structure is adequate. The locations and sequence of the formation of plastic hinges are shown in

Figure 4.17. The corresponding overstrength factors are calculated from the analysis results based on the further reduced tangent modulus method. It can be seen that the steel frame fails because of the local collapse of roof beam.

Table 4.3 shows the overstrength factors of the one-bay two-story unbraced frame by using different analysis methods. In the AISC-LRFD method and the direct analysis method, the elastic limit is governed by the interaction requirement of roof beam, while the elastic limit of advanced analysis method occurs at the formation of the first plastic hinge. For all methods, the values of overstrength factors are close at this stage. Therefore, when the load-carrying capacity corresponding to the formation of the first plastic-hinge is taken as the design criterion, the advanced analysis and the AISC-LRFD method would predict the same design results. The overstrength factor at the collapse of the roof beam can be determined by the advanced analysis method. However, the AISC-LRFD and direct analysis methods are member-based design approaches and this value cannot be obtained through their use.

Two models of advanced analysis method are considered. One model is two elements per beam and the other one is ten elements per beam. Since the overstrength factors for the two models are almost identical, the use of two elements per beam is adequate for practical design.

4.6.4 Ductility Check

Adequate inelastic rotation capacity is required for members in order to develop their full plastic moment capacity. The column section of W10×26 is checked in this section.

Table 4.2a Final step of the output data of the explicit imperfection modeling for the two-story unbraced frame

 - LOAD STEP 81 -

LOAD SEQUENCE 1
 DETERMINANT OF STIFFNESS MATRIX = 0.668 TIMES 10 TO THE POWER 52
 TRACE OF STIFFNESS MATRIX = 0.653 TIMES 10 TO THE POWER 6

NODE	ITEM	X	Y	R
1	NODAL FORCE	0.0000D+00	0.0000D+00	0.0000D+00
	DISPLACEMENT	0.0000D+00	0.0000D+00	0.0000D+00
2	NODAL FORCE	0.7733D+01	-0.2784D+02	0.0000D+00
	DISPLACEMENT	0.8383D+00	-0.6155D-01	-0.1181D-01
3	NODAL FORCE	0.3867D+01	-0.1856D+02	0.0000D+00
	DISPLACEMENT	0.2614D+01	-0.9989D-01	-0.2890D-01
4	NODAL FORCE	0.0000D+00	-0.5568D+02	0.0000D+00
	DISPLACEMENT	0.8329D+00	-0.1623D+01	0.1206D-02
5	NODAL FORCE	0.0000D+00	-0.3712D+02	0.0000D+00
	DISPLACEMENT	0.2514D+01	-0.5199D+01	0.3412D-01
6	NODAL FORCE	0.0000D+00	0.0000D+00	0.0000D+00
	DISPLACEMENT	0.0000D+00	0.0000D+00	0.0000D+00
7	NODAL FORCE	0.0000D+00	-0.2784D+02	0.0000D+00
	DISPLACEMENT	0.8277D+00	-0.6756D-01	0.3050D-02
8	NODAL FORCE	0.0000D+00	-0.1856D+02	0.0000D+00
	DISPLACEMENT	0.2414D+01	-0.1032D+00	0.2859D-01

ELEMENT FORCES IN GLOBAL COORDINATE

FRAME ELEMENT :		ELEMENT FORCES		
ELEMENT NUMBER		Fx	Fy	Mz
1	i	0.8851395D+00	0.8807980D+02	0.3200701D+03
	j	-0.8851395D+00	-0.8807980D+02	-0.3482866D+03
2	i	0.1385626D+02	0.3719228D+02	-0.6161577D+03
	j	-0.1385626D+02	-0.3719228D+02	-0.1302186D+04
3	i	-0.1246926D+02	0.9747263D+02	0.8987446D+03
	j	0.1246926D+02	-0.9747263D+02	0.1005574D+04
4	i	-0.1776338D+02	0.3702122D+02	0.1298737D+04
	j	0.1776338D+02	-0.3702122D+02	0.1328398D+04
5	i	-0.5408321D+01	0.2318977D+02	0.9644444D+03
	j	0.5408321D+01	-0.2318977D+02	0.2366240D+04

Table 4.2a Final step of the output data of the explicit imperfection modeling for the two-story unbraced frame (cont.)

6	i	-0.5460853D+01	-0.3249527D+02	-0.2366240D+04
	j	0.5460853D+01	0.3249527D+02	-0.2304311D+04
7	i	0.1717479D+02	0.1851097D+02	0.1302197D+04
	j	-0.1717479D+02	-0.1851097D+02	0.1449291D+04
8	i	0.1713251D+02	-0.1869491D+02	-0.1449291D+04
	j	-0.1713251D+02	0.1869491D+02	-0.1328398D+04

>> SOLUTION DOES NOT CONVERGE, A LIMIT STATE MAY HAVE BEEN REACHED <<

=====

= SEQUENCE OF PLASTIC HINGE FORMATION =

=====

PLASTIC HINGE	LOCATION
1	B-TH END OF FRAME ELEMENT 7
2	B-TH END OF FRAME ELEMENT 4

Table 4.2b Final step of the output data of the equivalent notional load modeling for the two-story unbraced frame

- LOAD STEP 78 -

LOAD SEQUENCE 1

DETERMINANT OF STIFFNESS MATRIX = 0.243 TIMES 10 TO THE POWER 53

TRACE OF STIFFNESS MATRIX = 0.662 TIMES 10 TO THE POWER 6

NODE	ITEM	X	Y	R
1	NODAL FORCE	0.0000D+00	0.0000D+00	0.0000D+00
	DISPLACEMENT	0.0000D+00	0.0000D+00	0.0000D+00
2	NODAL FORCE	0.7955D+01	-0.2783D+02	0.0000D+00
	DISPLACEMENT	0.8303D+00	-0.5980D-01	-0.1168D-01
3	NODAL FORCE	0.4013D+01	-0.1855D+02	0.0000D+00
	DISPLACEMENT	0.2567D+01	-0.9406D-01	-0.2788D-01
4	NODAL FORCE	0.0000D+00	-0.5565D+02	0.0000D+00
	DISPLACEMENT	0.8251D+00	-0.1606D+01	0.1208D-02
5	NODAL FORCE	0.0000D+00	-0.3710D+02	0.0000D+00
	DISPLACEMENT	0.2473D+01	-0.5022D+01	0.4128D-01

Table 4.2b Final step of the output data of the equivalent notional load modeling for the two-story unbraced frame (cont.)

6	NODAL FORCE	0.0000D+00	0.0000D+00	0.0000D+00
	DISPLACEMENT	0.0000D+00	0.0000D+00	0.0000D+00
7	NODAL FORCE	0.0000D+00	-0.2783D+02	0.0000D+00
	DISPLACEMENT	0.8200D+00	-0.6585D-01	0.3035D-02
8	NODAL FORCE	0.0000D+00	-0.1855D+02	0.0000D+00
	DISPLACEMENT	0.2379D+01	-0.9808D-01	0.2740D-01

ELEMENT FORCES IN GLOBAL COORDINATE

FRAME ELEMENT :		ELEMENT FORCES		
ELEMENT NUMBER		Fx	Fy	Mz
1	i	0.6840448D+00	0.8803048D+02	0.3179037D+03
	j	-0.6840448D+00	-0.8803048D+02	-0.3432825D+03
2	i	0.1378018D+02	0.3714324D+02	-0.6248664D+03
	j	-0.1378018D+02	-0.3714324D+02	-0.1294836D+04
3	i	-0.1263548D+02	0.9742407D+02	0.8959230D+03
	j	0.1263548D+02	-0.9742407D+02	0.1003476D+04
4	i	-0.1783232D+02	0.3703065D+02	0.1297145D+04
	j	0.1783232D+02	-0.3703065D+02	0.1328292D+04
5	i	-0.5309825D+01	0.2320061D+02	0.9681488D+03
	j	0.5309825D+01	-0.2320061D+02	0.2364337D+04
6	i	-0.5361372D+01	-0.3245474D+02	-0.2364337D+04
	j	0.5361372D+01	0.3245474D+02	-0.2300622D+04
7	i	0.1726774D+02	0.1847411D+02	0.1294845D+04
	j	-0.1726774D+02	-0.1847411D+02	0.1448975D+04
8	i	0.1722584D+02	-0.1870842D+02	-0.1448975D+04
	j	-0.1722584D+02	0.1870842D+02	-0.1328292D+04

>> SOLUTION DOES NOT CONVERGE, A LIMIT STATE MAY HAVE BEEN REACHED <<

=====

= SEQUENCE OF PLASTIC HINGE FORMATION =

=====

PLASTIC HINGE	LOCATION
1	B-TH END OF FRAME ELEMENT 7
2	B-TH END OF FRAME ELEMENT 4

Table 4.2c Final step of the output data of the further reduced tangent modulus modeling for the two-story unbraced frame

 - LOAD STEP 79 -

LOAD SEQUENCE 1
 DETERMINANT OF STIFFNESS MATRIX = 0.725 TIMES 10 TO THE POWER 52
 TRACE OF STIFFNESS MATRIX = 0.631 TIMES 10 TO THE POWER 6

NODE	ITEM	X	Y	R
1	NODAL FORCE	0.0000D+00	0.0000D+00	.0000D+00
	DISPLACEMENT	0.0000D+00	0.0000D+00	0.0000D+00
2	NODAL FORCE	0.7705D+01	-0.2774D+02	0.0000D+00
	DISPLACEMENT	0.8710D+00	-0.6995D-01	-0.1228D-01
3	NODAL FORCE	0.3853D+01	-0.1849D+02	0.0000D+00
	DISPLACEMENT	0.2664D+01	-0.1090D+00	-0.3052D-01
4	NODAL FORCE	0.0000D+00	-0.5548D+02	0.0000D+00
	DISPLACEMENT	0.8652D+00	-0.1687D+01	0.1197D-02
5	NODAL FORCE	0.0000D+00	-0.3698D+02	0.0000D+00
	DISPLACEMENT	0.2558D+01	-0.5402D+01	0.1363D+00
6	NODAL FORCE	0.0000D+00	0.0000D+00	0.0000D+00
	DISPLACEMENT	0.0000D+00	0.0000D+00	0.0000D+00
7	NODAL FORCE	0.0000D+00	-0.2774D+02	0.0000D+00
	DISPLACEMENT	0.8595D+00	-0.7707D-01	0.4002D-02
8	NODAL FORCE	0.0000D+00	-0.1849D+02	0.0000D+00
	DISPLACEMENT	0.2452D+01	-0.1138D+00	0.2979D-01

ELEMENT FORCES IN GLOBAL COORDINATE

FRAME ELEMENT :		ELEMENT FORCES		
ELEMENT NUMBER		Fx	Fy	Mz
1	i	0.7106145D+00	0.8773909D+02	0.2812654D+03
	j	-0.7106145D+00	-0.8773909D+02	-0.3071326D+03
2	i	0.1387590D+02	0.3700486D+02	-0.6422287D+03
	j	-0.1387590D+02	-0.3700486D+02	-0.1289366D+04
3	i	-0.1225142D+02	0.9713773D+02	0.8596978D+03
	j	0.1225142D+02	-0.9713773D+02	0.9880103D+03
4	i	-0.1775348D+02	0.3694049D+02	0.1286692D+04
	j	0.1775348D+02	-0.3694049D+02	0.1328496D+04
5	i	-0.5636035D+01	0.2313891D+02	0.9493614D+03
	j	0.5636035D+01	-0.2313891D+02	0.2373318D+04

Table 4.2c Final step of the output data of the further reduced tangent modulus modeling for the two-story unbraced frame (cont.)

```

6   i   -0.5689089D+01  -0.3234352D+02  -0.2373318D+04
    j    0.5689089D+01   0.3234352D+02  -0.2274699D+04
7   i    0.1716431D+02   0.1840060D+02   0.1289370D+04
    j   -0.1716431D+02  -0.1840060D+02   0.1449378D+04
8   i    0.1711965D+02  -0.1867467D+02  -0.1449378D+04
    j   -0.1711965D+02   0.1867467D+02  -0.1328496D+04

```

>> SOLUTION DOES NOT CONVERGE, A LIMIT STATE MAY HAVE BEEN REACHED <<

=====
= SEQUENCE OF PLASTIC HINGE FORMATION =
=====

PLASTIC HINGE	LOCATION
1	B-TH END OF FRAME ELEMENT 7
2	B-TH END OF FRAME ELEMENT 4

Table 4.3 Overstrength factors of the two-story unbraced frame

Method		Elastic Limit	Collapse
AISC-LRFD		1.20	-
Direct Analysis	N. L.	1.18	-
	M. S.	1.18	-
Advanced Analysis (Two elements per beam)	E. I.	1.24	1.289
	N. L.	1.24	1.288
	R. E _t	1.22	1.284
Advanced Analysis (Ten elements per beam)	E. I.	1.22	1.292
	N. L.	1.22	1.289
	R. E _t	1.26	1.288

- Flanges

$$\left(\frac{b_f}{2t_f} = 6.56 \right) < \left(0.38 \sqrt{\frac{E}{F_{yf}}} = 9.152 \right) \quad \text{O.K.}$$

- Web

$$\frac{P_u}{\phi_b P_n} = \frac{76.55}{0.9 \times 380.5} = 0.224 > 0.125$$

$$\left(\frac{h}{t_w} = 34 \right) < \left(1.12 \sqrt{\frac{E}{F_y}} \left(2.33 - \frac{P_u}{\phi_b P_y} \right) = 56.818 \right) > \left(1.49 \sqrt{\frac{E}{F_y}} = 35.894 \right) \quad \text{O.K.}$$

4.7 Summary

The advanced analysis method is refined by modifying the conventional elastic analysis methods which treat stability and plasticity separately. Usually, these effects are considered through the use of member effective length factors and beam-column interaction equations. However, advanced analysis combines stability and theory of plasticity in the limit states design of steel frames. In advanced analysis, second-order effects can be taken into account by the stability functions and incremental load scheme. Gradual yielding due to residual stresses along the length of members under axial load can be accounted for by using the tangent modulus model. The effects of plastification due to flexure can be considered by applying the two-surface stiffness degradation model. Initial geometric imperfections of the members can be dealt with by one of the three methods: the explicit imperfection modeling method, the equivalent notional load method, and the further reduced tangent modulus method. Moment redistribution is

involved in the analysis after the strength of certain members is reached. By considering these material and geometric nonlinearities in analysis directly, individual member capacity checks involving the determination of effective length factors can be avoided. The example of a two-story unbraced frame in Section 4.6 shows the accuracy and simplicity of applying advanced analysis in steel frame design. Since advanced analysis is a structure-based design approach and the failure mechanism can be predicted, it is suitable for the state-of-the-art structural performance-based design.

CHAPTER 5

GUIDELINES FOR PRACTICAL STEEL FRAME DESIGN

USING ADVANCED ANALYSIS

5.1 Introduction

As illustrated in the preceding chapter, steel framed structures can be analyzed and designed in a direct manner by using the advanced analysis method. The FORTRAN-based program PAAP is the advanced analysis program based on the refined plastic hinge concept [30,32]. It is similar to in-house elastic analysis programs with simple modifications that deal with the geometric and material nonlinearities of structural systems. Since incremental loads and iteration process are implemented, it is necessary to use computers to determine the analysis results.

In Section 5.2, the design format of advanced analysis is introduced. The step-by-step analysis and design procedures of steel frames using the advanced analysis program, PAAP, developed by Kim and Chen [13] are proposed in Section 5.3. Design examples applying the proposed procedures will be considered in Chapter 6.

5.2 Design Format

To ensure that the factored load effects do not exceed the factored nominal resistance of the structural system, advanced analysis uses the same design format as that of the AISC-LRFD method. The design format can be expressed as [1]:

$$\phi R_n \geq \sum_{i=1}^m \gamma_i Q_i \quad (5.1)$$

where

R_n = nominal resistance

Q_i = load effect

ϕ = resistance factor

γ_i = load factor corresponding to Q_i

i = type of load

m = number of load types

In the advanced analysis, the above design format is used for the whole structural system, while the AISC-LRFD method uses it for the strength of individual members. The advanced analysis uses the same resistance and load factors as those in the AISC-LRFD method. The load-carrying capacity is obtained by applying incremental load until a structural system reaches its strength limit state such as yielding mechanism or buckling.

5.3 Analysis and Design Procedures

The flowchart shown in Figure 5.1 illustrates the step-by-step analysis and design procedure of steel frames using advanced analysis program, PAAP. The instructions for applying the procedure are described in this section.

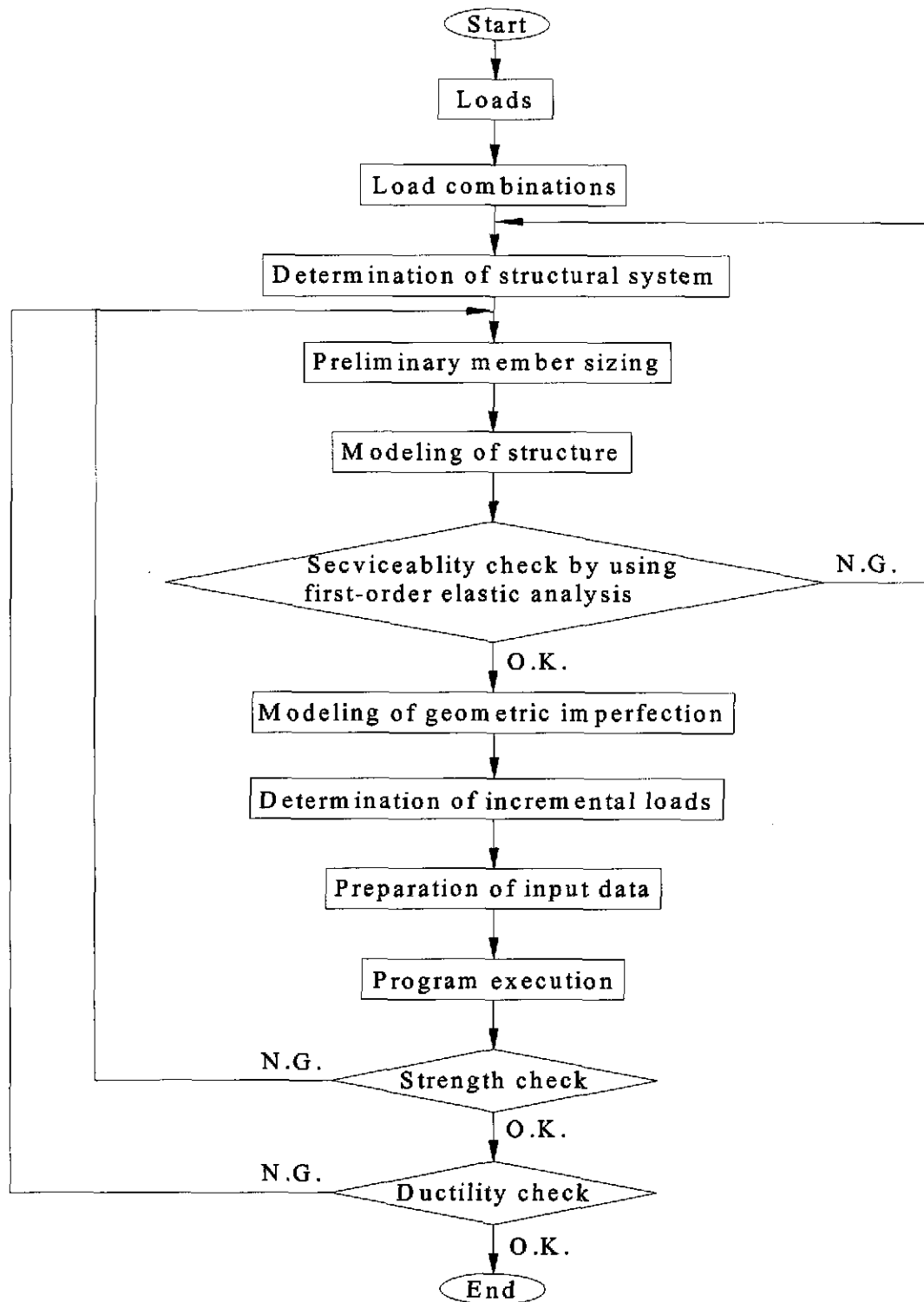


Figure 5.1 Analysis and design procedure for advanced analysis method

5.3.1 Load Combinations

The required strength of a structure and its member sizes are determined from an appropriate factored load combination. According to the AISC-LRFD Specification [1], the factored load combinations shall be those stipulated in ASCE 7 or applicable codes. Based on ASCE 7-98 [33], the design strength of a structure shall equal or exceed the effects of the factored loads in the following combinations:

$$1.4(D + F) \quad (5.2a)$$

$$1.2(D + F + T) + 1.6(L + H) + 0.5(L_r \text{ or } S \text{ or } R) \quad (5.2b)$$

$$1.2D + 1.6(L_r \text{ or } S \text{ or } R) + (0.5L \text{ or } 0.8W) \quad (5.2c)$$

$$1.2D + 1.6W + 0.5L + 0.5(L_r \text{ or } S \text{ or } R) \quad (5.2d)$$

$$1.2D + 1.0E + 0.5L + 0.2S \quad (5.2e)$$

$$0.9D + 1.6W + 1.6H \quad (5.2f)$$

$$0.9D + 1.0E + 1.6H \quad (5.2g)$$

where

D = dead load

E = earthquake load

L = live load

L_r = roof live load

R = rain load

T = self-straining force

W = wind load

F = load due to fluids

H = load due to lateral earth pressure, ground water pressure, or pressure of bulk materials

Except those limitations listed in the ASCE 7-98, live load could be reduced in the analysis of the structural system since it is unlikely that a considered area is uniformly and simultaneously supporting live loads. For members with $K_{LL} A_T$ greater than or equal to 400 ft², the reduced live load is:

$$L = L_0 \left(0.25 + \frac{4.57}{\sqrt{K_{LL} A_T}} \right) \geq \alpha L_0 \quad (5.3)$$

where

L = reduced design live load per square foot of area supported by the member

L_0 = unreduced design live load per square foot of area supported by the member

K_{LL} = live load element factors which are shown in Table 5.1

A_T = tributary area in square feet

α = 0.5 for members supporting one floor

= 0.4 for members supporting two or more floors

Table 5.1 Live load element factor, K_{LL} (from Table 4.2, ASCE 7-98)

Element	K_{LL}
Interior columns	4
Exterior columns without cantilever slabs	4
Edge columns with cantilever slabs	3
Corner columns with cantilever slabs	2
Edge beams without cantilever slabs	2
Interior beams	2
All other members not identified above	1

5.3.2 Preliminary Member Sizing

Since the structural displacements and the distribution of member forces are influenced by the stiffness of individual members in the structure, it is necessary to estimate the initial member sizes before beginning a structural analysis. Intrinsicly, the preliminary member sizing is dependent upon the engineers' experience or simplified analysis methods. To assist in creating a trial section, linear elastic analysis is usually performed to determine the approximate member forces. Several efficient tables and techniques have been proposed by many researchers [3,13,34,35].

5.3.3 Modeling of Elements

A sensitivity study based on the research of Kim and Chen [36] shows that only one or two elements per member is feasible to accurately predict the strength of both a structural system and its component members when the refined plastic-hinge analysis is used for steel frame design. For braced frames, two elements are used to model a column. A reason for this is because plastic hinges in braced frames may form between the two column ends. Another reason is that two elements with a maximum lateral deflection at the mid-height of a member are required to capture initial out-of-straightness effects. For columns in an unbraced frame, one element per column is adequate to consider the out-of-plumbness effects. For beams subjected to uniform loads, two elements are recommended and the loads need to be converted into equivalent concentrated loads. Nodal points should be set where concentrated loads are applied.

5.3.4 Serviceability Checks

In determining serviceability limit states such as deflection and lateral drift, the first-order elastic analysis with unfactored (service) loads should be used. The adequacy of a structural system and its members can be evaluated by comparing the determined displacements with the limiting values. The AISC-LRFD Specification does not provide specific serviceability criterion. Based on the studies by Ellingwood [37], the deflection limits for girder and story are:

- floor girder deflection under live load: $\frac{L}{360}$

- roof girder deflection: $\frac{L}{240}$

- overall lateral drift for wind load: $\frac{H}{400}$

- interstory drift for wind load: $\frac{h}{300}$

where

L = span length of the girder

H = building height

h = story height

5.3.5 Modeling of Initial Geometric Imperfection

In the PAAP program, one of three models can be chosen to account for the initial geometric imperfections. The explicit imperfection modeling method requires the user to input imperfections in the frame element data set. A geometric imperfection of $L_c / 1000$

at mid-height of the braced frame columns and $L_c / 500$ at the top of the unbraced frame columns are used. If the equivalent notional load modeling method is considered, notional loads must be combined with the external applied loads and inputted in the incremental load data set. For a braced frame column, the equivalent notional load equal to 0.004 times the axial force in the column is applied at the mid-height of the column. For an unbraced frame column, the notional load resulting from 0.002 times the story gravity load is added laterally at the top of each story. If further reduced tangent modulus is used, column members must be specified in the frame element property set and the imperfection effects will be taken into account automatically.

5.3.6 Determination of Incremental Loads

To trace nonlinear load-displacement behaviors, incremental loads instead of total factored loads should be input into the computer program. The incremental loads may be obtained by scaling down the total loads by using a scaling number. The advanced analysis program, PAAP, is a nonlinear analysis program that allows the load step sizes to vary automatically based on the curvature of the load-displacement curve. When a new plastic hinge is formed in the analysis process and changes in the element stiffness parameter exceed the defined tolerance, the scaling number will be automatically reduced to one fifth of the previous value. Therefore, the error associated with the unbalanced force residual can be minimized.

5.3.7 Preparation of Input Data

When the advanced analysis program PAAP is used to analyze a steel frame, the input data file P.DAT can be easily prepared according to the input data format in Table 5.2. It is similar to the data format of a linear elastic analysis with the consideration of initial geometric imperfections and incremental loads. PAAP can also be used for first- and second-order elastic analysis. If first-order elastic analysis is performed, the *number of load increments is equal to one and the total factored loads should be applied to suppress numerical iteration in the nonlinear analysis algorithm.* If the yield stress of steel is assumed to be an arbitrarily large number so that yielding of the material does not occur, PAAP becomes a second-order elastic analysis program.

In PAAP, there are no built-in units. All input data must have consistent units. The output data will conform to the same set of units.

5.3.8 Execution of the Analysis Program

The analysis results can be obtained by executing the batch file RUN.BAT. This batch file executes programs DATAGEN, INPUT, and PAAP in sequence. During these executions, four data files, INFILE, DATA0, DATA1, and DATA2, and two output files, P.OUT1 and P.OUT2, are produced. The operating procedures are shown in Figure 5.2.

Table5.2 Input data format for the program PAAP

Data Set	Column	Variable	Description	
1	Title	A70	-	Job title and general comments
2	Design control	1-5	IGEOIM	Geometric imperfection method 0: No geometric imperfection 1: Explicit imperfection modeling 2: Equivalent notional load modeling 3: Further reduced tangent modulus modeling
		6-10	ILRFD	Strength reduction factor 0: No reduction factors considered 1: Reduction factors considered
3	Job control	1-5	NNODE	Total number of nodal points of the structure
		6-10	NBOUND	Total number of supports
		11-15	NINCRE	Allowable number of load increments (default=100)
4	Total number of element type	1-5	NCTYPE	Number of connection types
		6-10	NFTYPE	Number of frame types
		11-15	NTTYPE	Number of truss types
5	Total number of element	1-5	NUMCNT	Number of connection elements
		6-10	NUMFRM	Number of frame elements
		11-15	NUMTRS	Number of truss elements
6	Connection property	1-5	ICTYPE	Connection type number
		6-15*	M_u	Ultimate moment capacity of connection
		16-25*	R_{ki}	Initial stiffness of connection
		26-35*	n	Shape parameter of connection
7	Frame element property	1-5	IFTYPE	Frame type number
		6-15*	A	Cross sectional area
		16-25*	I	Moment of inertia
		26-35*	Z	Plastic sectional modulus
		36-45*	E	Modulus of elasticity
		46-55*	FY	Yield stress
		55-60	IFCOL	Identification of column member, IFCOL=1 for column (default=0)
8	Truss element property	1-5	ITYPE	Truss type number
		6-15*	A	Cross sectional area
		16-25*	I	Moment of inertia
		26-35*	E	Modulus of elasticity
		36-45*	FY	Yield stress
		46-50	ITCOL	Identification of column member, ITCOL=1 for column (default=0)

Table5.2 Input data format for the program PAAP (cont.)

	Data Set	Column	Variable	Description
9	Connection element data	1-5	LCNT	Connection element number
		6-10	IFMCNT	Frame element number containing the connection
		11-15	IEND	Identification of element ends containing the connection 1: Connection attached at element end i 2: Connection attached at element end j
		16-20	JDCNT	Connection type number
		21-25	NOSMCN	Number of same elements for automatic generation (default=1)
		26-30	NELINC	Element number (IFMCNT) increment of automatically generated elements (default=1)
10	Frame element data	1-5	LFRM	Frame element number
		6-15*	FXO	Horizontal projected length; positive for i-j direction in global x-direction
		16-25*	FYO	Vertical projected length; positive for i-j direction in global y-direction
		26-30	JDFRM	Frame type number
		31-35	IFNODE	Number of node i
		36-40	JFNODE	Number of node j
		41-45	NOSMFE	Number of same elements for automatic generation (default=1)
		46-50	NODINC	Node number increment of automatically generated elements (default=1)
11	Truss element data	1-5	LTRS	Truss element number
		6-15*	TXO	Horizontal projected length; positive for i-j direction in global x-direction
		16-25*	TYO	Vertical projected length; positive for i-j direction in global y-direction
		26-30	JDTRS	Truss type number
		31-35	ITNODE	Number of node i
		36-40	JTNODE	Number of node j
		41-45	NOSMTE	Number of same elements for automatic generation (default=1)
		46-50	NODINC	Node number increment of automatically generated elements (default=1)

Table 5.2 Input data format for the program PAAP (cont.)

Data Set	Column	Variable	Description
12	Boundary condition	1-5	NODE Node number of support
		6-10	XFIX 1 for restrained in global x-direction
		11-15	YFIX 1 for restrained in global y-direction
		16-20	RFIX 1 for restrained in rotation
		21-25	NOSMBD Number of same boundary conditions for automatic generation (default=1)
		26-30	NODINC Node number increment of automatically generated supports (default=1)
10	Incremental loads	1-5	NODE Node number where a load applied
		6-15*	XLOAD Incremental load in global x-direction
		16-25*	YLOAD Incremental load in global y-direction
		26-35*	RLOAD Incremental moment in global θ -direction
		36-40	NOSMLD Number of same loads for automatic generation (default=1)
		41-45	NODINC Node number increment of automatically generated loads (default=1)

- The mark "*" indicates a real number ("F" format) to be input; otherwise an integer number ("I" format) is used.

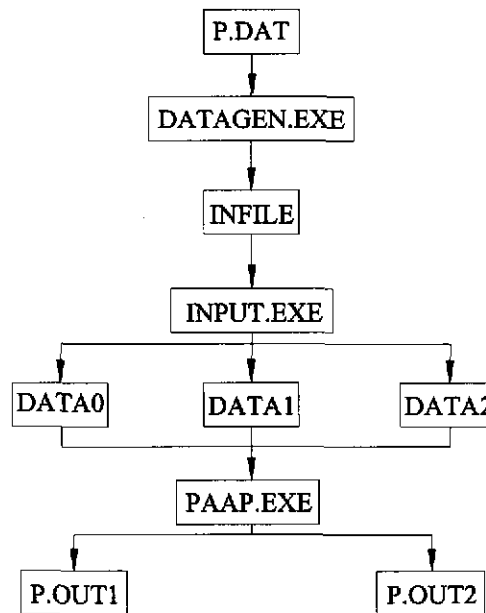


Figure 5.2 Operating procedures of the advanced analysis programs

5.3.9 Ultimate Load Carrying Capacity Checks

From the output file P.OUT2, the design load carrying capacity of a structure can be obtained. By comparing the load carrying capacity ϕR_n and the applied factored loads $\Sigma \gamma_i Q_i$ determined in Section 5.3.1, the adequacy of the member design of the structural system can be easily checked.

One benefit of advanced analysis is that inelastic moment redistribution of the structure can be considered and smaller member sizes may be allowed. For the cases in which load-carrying capacity is considered without moment redistribution, the advanced analysis method generally results in the same member sizes as the LRFD method. If the limit state of the structure, including the effects of moment redistribution, is considered, the ultimate load capacity can be obtained from the final load step provided by P.OUT2. If the moment redistribution is not desirable, the load capacity can be chosen from the load step when the first plastic hinge is formed.

5.3.10 Ductility Checks

In the advanced analysis method, a section is assumed to be able to sustain its plastic moment until instability or failure mechanism of the structure occurs. In order to develop the full plastic moment capacity, structural members should be adequately braced and their cross-sections should be compact so that the ductility requirements are achieved. Requirements for compact sections are defined in the AISC-LRFD Specification [1] as follow:

For flanges,

$$\frac{b_f}{2t_f} \leq 0.38 \sqrt{\frac{E}{F_{yf}}} \quad (5.4)$$

For webs,

$$\frac{h}{t_w} \leq 3.76 \sqrt{\frac{E}{F_{yw}}} \left[1 - \frac{2.75P_u}{\phi_b P_y} \right] \quad \text{for } \frac{P_u}{\phi_b P_y} \leq 0.125 \quad (5.5a)$$

$$\frac{h}{t_w} \leq 1.12 \sqrt{\frac{E}{F_{yw}}} \left[2.33 - \frac{P_u}{\phi_b P_y} \right] \geq 1.49 \sqrt{\frac{E}{F_{yw}}} \quad \text{for } \frac{P_u}{\phi_b P_y} > 0.125 \quad (5.5b)$$

where

b_f, t_f = width and thickness of flange, respectively

h = clear distance between flanges

t_w = thickness of web

F_{yf} = specified minimum yield stress of the flange material

F_{yw} = specified minimum yield stress of the web material

All ASTM A6 rolled wide flange shapes except W21×48, W14×99, W14×90, W12×65, W10×12, W8×31, W8×10, W6×15, W6×9, and W6×8.5 are compact at yield stress equal to or less than 50 ksi based on flange local buckling criteria.

5.3.11 Adjustment of Member Size

If design requirements cannot be satisfied, it is necessary to increase member sizes. On the contrary, if the applied factored load is significantly smaller than the load-carrying capacity of the structural system, members without plastic hinges could be replaced by

lighter sections. Adjustments can be made according to the sequence of plastic hinge formation that is shown in the file P.OUT2.

5.4 Summary

In this chapter, the step-by-step analysis and design procedures of using the advanced analysis program *PAAP* are summarized. The input data of *PAAP* consists of 13 data sets that are the same as those of a usual linear elastic analysis program with consideration of initial geometric imperfection and incremental loads. The global coordinate system is used for both input and output data. Units must be set consistently. The proposed procedures are available for conventional nonseismic design. The analysis and design procedure of using advanced analysis in seismic and fire resistance performance-based design is proposed in Chapter 7.

CHAPTER 6

NUMERICAL EXAMPLES

6.1 Introduction

The two-story unbraced frame example was considered using the AISC-LRFD method, the direct analysis method, and the advanced analysis method in the previous chapters. It is a general steel framed structure used to illustrate the analysis and design details of all three methods. It can be seen that the design results are close. However, the use of the current LRFD method requires a lot of effort in the analysis and design process. The advanced analysis, on the other hand, is the simplest and easiest to implement because it is highly dependent on the use of computers.

In this chapter, three additional examples are presented to discuss three important issues in the analysis and design of steel frames. Because the six-story frame is a highly redundant structure, it is chosen in Section 6.2 to show the effects of inelastic force redistribution. The AISC-LRFD method and the direct analysis method are both member-based design approaches that do not take into consideration the effects of inelastic force redistribution. On the other hand, the advanced analysis is a structure system-based analysis and design approach in which moment redistribution occurs before the failure mechanism of the structure forms. Thus, a more economical design can be achieved.

In Section 6.3, a braced frame is considered. Diagonal members of the structure are used to resist lateral forces and displacements. In the AISC-LRFD method, the effective length factors of braced columns can be conservatively chosen as one. The design results

will be compared with the ones using the direct analysis method and the advanced analysis method.

The leaned-column frame is discussed in Section 6.4. A leaning column is a pin-ended column which possesses no lateral stability. The lateral stability and resistance of the entire frame must be sustained by other parts of the structure. Therefore, the effective length factors for in-plane buckling of rigid columns will be enlarged to account for the destabilizing effects of the leaning column gravity loads. However, from this example, it will be seen that the direct analysis method sets $K = 1$ for rigid columns and leaned-column effects cannot be involved.

6.2 Six-Story Frame

The configuration and loading condition of a six-story steel frame are shown in Figure 6.1. All members are hot-rolled with properties listed in Table 6.1. The maximum compressive residual stress is $0.3F_y$. Yield stress of steel F_y is 23.5 kN/cm^2 and modulus of elasticity E equals 20500 kN/cm^2 . All beams are continuously braced about their weak axes and rigidly connected to the columns. Columns are bent about the strong axes.

6.2.1 AISC-LRFD Method

The six-story frame is divided into non-sway and sway components as shown in Figures 6.2a and 6.2b. The corresponding moment diagrams, determined by performing the first-order elastic analysis, are shown in Figures 6.3a and 6.3b, respectively. Member capacity checks are presented for the three bottom columns C11, C12, and C13 as follow:

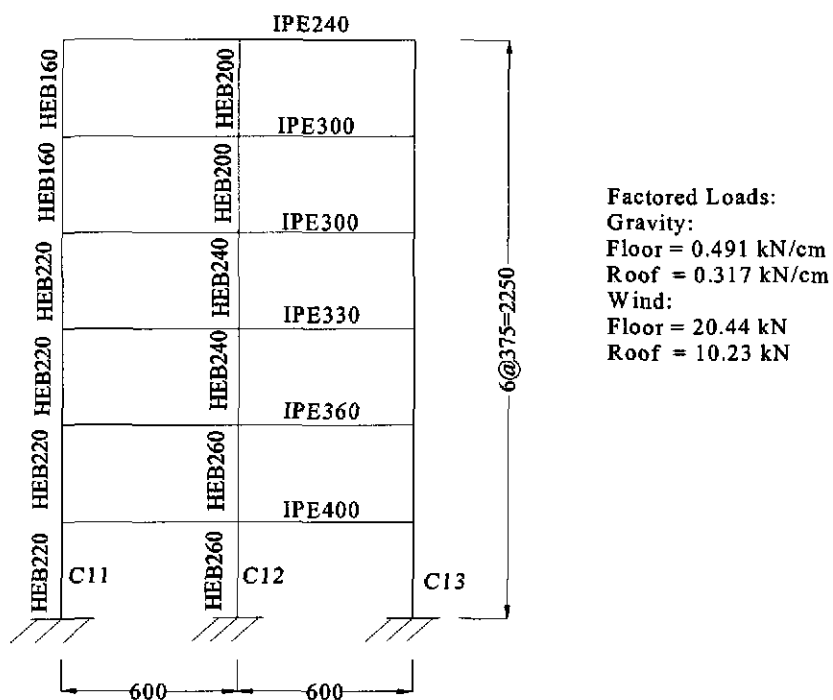
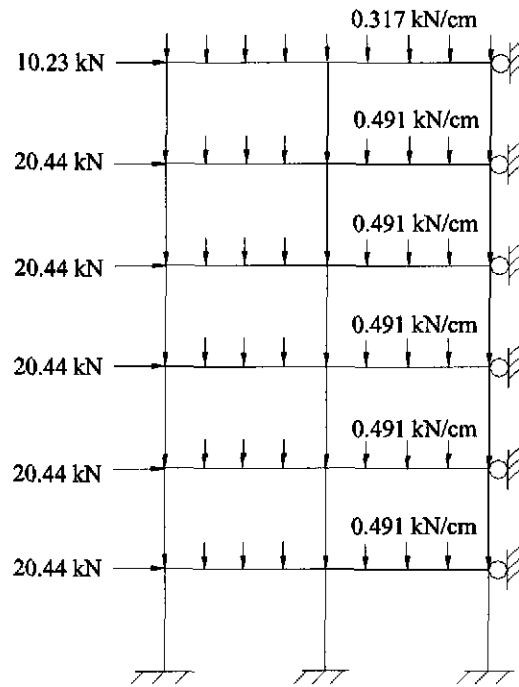


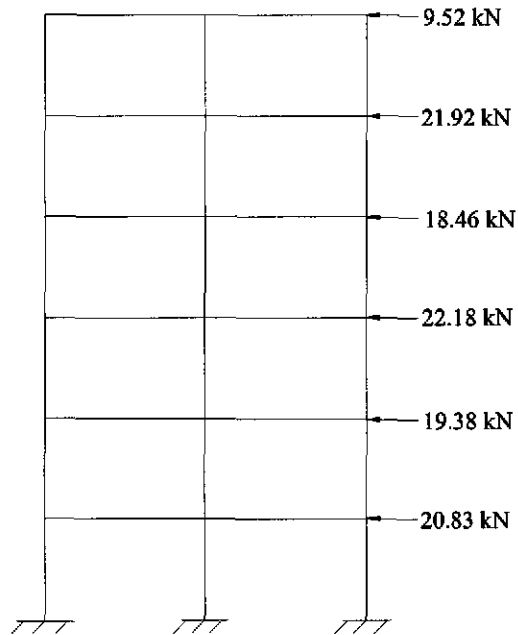
Figure 6.1 Configuration and load condition of the six-story frame (unit: cm)

Table 6.1 Sectional properties of the members of the six-story steel frame

Section	A (cm ²)	I _x (cm ⁴)	I _y (cm ⁴)	Z _x (cm ³)
IPE 240	39.1	3892	284	367
IPE 300	53.8	8356	604	628
IPE 330	62.6	11770	788	804
IPE 360	72.7	16270	1043	1019
IPE 400	84.5	23130	1318	1307
HEB 160	54.3	2492	889	354
HEB 200	78.1	5692	2003	643
HEB 220	91.0	8091	2843	827
HEB 240	106.0	11260	3923	1053
HEB 260	118.0	14920	5135	1283
HEB 300	149.0	25170	8563	1869
HEB 340	133.0	27690	7436	1850

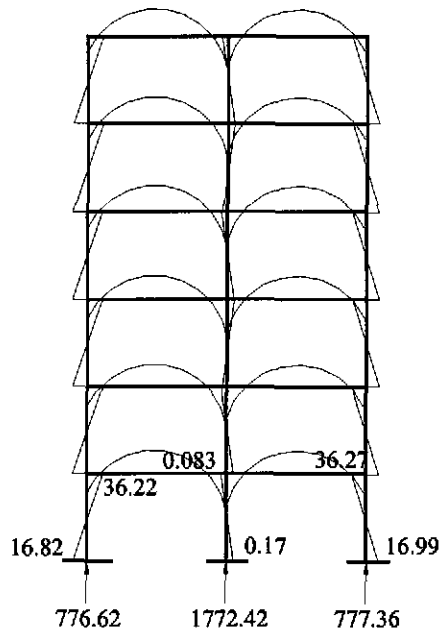


(a) Non-sway component

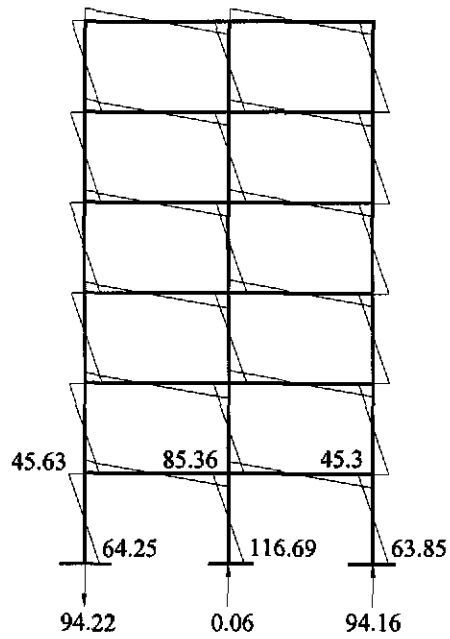


(b) Sway component

Figure 6.2 First-order analysis for the six-story frame



(a) Non-sway component



(b) Sway component

Figure 6.3 Member forces of the six-story frame determined by using a first-order analysis (unit: kN for force and kN-m for moment)

Member capacity check for Column C12:

(1) Determine $\phi_c P_n$

① Determine τ (Inelastic stiffness reduction factor)

$$P_u = 1772.42 + 0.6 = 1773.02 \text{ kN}$$

$$P_y = A_g F_y = (118)(23.5) = 2773 \text{ kN}$$

$$\frac{P_u}{P_y} = \frac{1773.02}{2773} = 0.6394 > \frac{1}{3}$$

$$\tau = -7.38 \left(\frac{P_u}{P_y} \right) \log \left(\frac{\frac{P_u}{P_y}}{0.85} \right) = 0.5834$$

For the column which is above Column C12,

$$\frac{P_u}{P_y} = \frac{1450.11}{2773} = 0.523 > \frac{1}{3}$$

$$\tau = -7.38(0.523) \log \left(\frac{0.523}{0.85} \right) = 0.814$$

② Determine L_g' (End-restrained correction factor)

$$L_{gr}' = L_{gr} \left(2 - \frac{M_{Fr}}{M_{Nl}} \right) = (600) \left(2 - \frac{9000.14}{8721.08} \right) = 580.8 \text{ cm}$$

$$L_{gl}' = L_{gl} \left(2 - \frac{M_{Fl}}{M_{Nl}} \right) = (600) \left(2 - \frac{9023.49}{8730.12} \right) = 579.84 \text{ cm}$$

③ Determine K_{12}

$$G_b = 1.0 \text{ (Fixed-end)}$$

$$G_t = \frac{\sum \left(\frac{\pi I_c}{L_c} \right)}{\sum \left(\frac{I_g}{L_g} \right)} = \frac{(0.5834 + 0.814) \left(\frac{14920}{375} \right)}{(23130) \left(\frac{1}{580.8} + \frac{1}{579.84} \right)} = 0.7$$

From the alignment chart of sidesway uninhibited,

$$K_{J2} = 1.28$$

④ Determine $\phi_c P_n$

$$\lambda_c = \frac{KL}{\pi} \sqrt{\frac{F_y}{E}} = \frac{(1.28)(375)}{(\pi)(11.245)} \sqrt{\frac{23.5}{20500}} = 0.46 < 1.5$$

$$P_n = (0.658^{\lambda_c}) P_y = 2537.94 \text{ kN}$$

$$\phi_c P_n = 2157.25 \text{ kN}$$

(2) Determine $\phi_b M_n$

① Determine L_b

$$\gamma_y = \sqrt{\frac{I_y}{A}} = \sqrt{\frac{5135}{118}} = 6.597 \text{ cm}$$

$$L_p = 1.76 \gamma_y \sqrt{\frac{E}{F_y}} = (1.76)(6.597) \sqrt{\frac{20500}{23.5}} = 342.93 \text{ cm}$$

$$X_1 \approx 2757.89 \text{ kN/cm}^2$$

$$X_2 \approx 1157.1 \times 10^{-6} \text{ cm}^4/\text{kN}^2$$

$$F_L = 23.5 - 6.9 = 16.6 \text{ kN/cm}^2$$

$$L_r = \frac{r_y X_1}{F_L} \sqrt{1 + \sqrt{1 + X_2 F_L^2}} = 1606.48 \text{ cm}$$

$$L_p < L_b = 375 \text{ cm} < L_r$$

② Determine C_b

From the moment diagram of sway component

$$M_{\max} = 116.69 \text{ kN}\cdot\text{m}, M_A = 66.18 \text{ kN}\cdot\text{m}, M_B = 15.67 \text{ kN}\cdot\text{m}, M_C = 34.85 \text{ kN}\cdot\text{m}$$

$$C_b = \frac{12.5M_{\max}}{2.5M_{\max} + 3M_A + 4M_B + 3M_C} = 2.218$$

③ Determine $\phi_b M_n$

$$M_p = Z_x F_y = (1283)(23.5) = 30150.5 \text{ kN}\cdot\text{cm} = 301.51 \text{ kN}\cdot\text{m}$$

$$M_r = S_x F_L = (1148)(16.6) = 19056.8 \text{ kN}\cdot\text{cm} = 190.57 \text{ kN}\cdot\text{m}$$

$$M_n = C_b \left[M_p - (M_p - M_r) \left(\frac{L_b - L_p}{L_r - L_p} \right) \right] = 662.5 \text{ kN}\cdot\text{m} > M_p$$

$$\text{Use } M_n = M_p = 301.51 \text{ kN}\cdot\text{m}$$

$$\phi_b M_n = 271.35 \text{ kN}\cdot\text{m}$$

(3) Determine P_u

$$P_u = 1773.02 \text{ kN}$$

(4) Determine M_u

① Determine B_1

$$C_m = 0.6 - 0.4 \left(\frac{M_1}{M_2} \right) = 0.6 - 0.4 \left(\frac{8.27}{17.11} \right) = 0.41$$

$$G_b = 1.0$$

$$G_t = \frac{2 \times \frac{14920}{375}}{2 \times \frac{23130}{600}} = 1.032$$

From the alignment chart of sidesway inhibited,

$$K = 0.774$$

$$P_{e1} = \frac{\pi^2 EI}{(KL)^2} = \frac{(\pi^2)(20500)(14920)}{(0.774 \times 375)^2} = 35832.57 \text{ kN}$$

$$B_1 = \frac{C_m}{1 - \frac{P_u}{P_{e1}}} = \frac{0.41}{1 - \frac{1773.02}{35832.57}} = 0.4313 < 1.0$$

Use $B_1 = 1.0$

② Determine B_2

$$\Sigma P_u = (0.491 \times 1200) + (0.317 \times 1200) \times 5 = 2491.2 \text{ kN}$$

For Column C12,

$$G_b = 1.0, G_t = 1.032$$

From the alignment chart of sidesway uninhibited,

$$K_{12} = 1.32$$

For Columns C11 and C13

$$G_b = 1.0, G_t = \frac{2 \times \frac{8091}{375}}{\frac{23130}{600}} = 1.12$$

$$K_{11} = K_{13} = 1.34$$

$$\Sigma P_{e2} = \Sigma \frac{\pi^2 EI}{(KL)^2} = \frac{(\pi^2)(20500)}{(375)^2} \left[2 \times \frac{8091}{(1.34)^2} + \frac{14920}{(1.32)^2} \right] = 25286.27 \text{ kN}$$

$$B_2 = \frac{1}{1 - \frac{\Sigma P_u}{\Sigma P_{e2}}} = \frac{1}{1 - \frac{2491.2}{25286.27}} = 1.11$$

③ Determine M_u

$$M_{u,top} = (1)(8.27) + (1.11)(8535.98) = 9483.21 \text{ kN-cm} = 94.83 \text{ kN-m}$$

$$M_{u,bottom} = (1)(17.11) + (1.11)(11669.32) = 12970.06 \text{ kN-cm} = 129.70 \text{ kN-m}$$

(5) Check interaction equation

$$\frac{P_u}{\phi_c P_n} = \frac{1773.02}{2157.25} = 0.82 > 0.2$$

$$\frac{P_u}{\phi_c P_n} + \frac{8}{9} \frac{M_u}{\phi_b M_n} = 0.82 + \frac{8}{9} \left(\frac{129.70}{271.35} \right) = 1.24 > 1.0 \quad \therefore \text{N.G.}$$

Member capacity check for Column C13

(1) Determine $\phi_c P_n$

① Determine τ

$$P_u = 777.36 + 94.16 = 871.52 \text{ kN}$$

$$P_y = (91)(23.5) = 2138.5 \text{ kN}$$

$$\frac{P_u}{P_y} = 0.408 > \frac{1}{3}$$

$$\tau = -7.38(0.408) \log\left(\frac{0.408}{0.85}\right) = 0.96$$

② Determine L'_g

$$L'_g = (600) \left(2 - \frac{8721.08}{9000.14} \right) = 618.6 \text{ cm}$$

③ Determine K_{I3}

$$K_{I3} = 1.34$$

④ Determine $\phi_c P_n$

$$\lambda_c = \frac{(1.34)(375)}{(\pi)(9.43)} \sqrt{\frac{23.5}{20500}} = 0.5743$$

$$P_n = (0.658^{(0.5743)^2}) (2138.5) = 1862.77 \text{ kN}$$

$$\phi_c P_n = (0.85)(1862.77) = 1583.35 \text{ kN}$$

(2) Determine $\phi_b M_n$

① Determine L_b

$$\gamma_y = \sqrt{\frac{2843}{91}} = 5.59 \text{ cm}$$

$$L_p = (1.76)(5.59)\sqrt{\frac{20500}{23.5}} = 290.58 \text{ cm}$$

$$X_1 \approx 3447.2 \text{ kN/cm}^2$$

$$X_2 \approx 504.9 \times 10^{-6} \text{ cm}^4/\text{kN}^2$$

$$L_r = \frac{r_y X_1}{F_L} \sqrt{1 + \sqrt{1 + X_2 F_L^2}} = 1669 \text{ cm}$$

$$L_p < L_b = 375 \text{ cm} < L_r$$

② Determine C_b

$$M_{\max} = 63.85 \text{ kN}\cdot\text{m}, M_A = 36.56 \text{ kN}\cdot\text{m}, M_B = 9.28 \text{ kN}\cdot\text{m}, M_C = 18.01 \text{ kN}\cdot\text{m}$$

$$C_b = \frac{12.5M_{\max}}{2.5M_{\max} + 3M_A + 4M_B + 3M_C} = 2.214$$

③ Determine $\phi_b M_n$

$$M_p = Z_x F_y = (827)(23.5) = 19434.5 \text{ kN}\cdot\text{cm} = 194.35 \text{ kN}\cdot\text{m}$$

$$M_r = S_x F_L = (735.5)(16.6) = 12209.3 \text{ kN}\cdot\text{cm} = 122.1 \text{ kN}\cdot\text{m}$$

$$M_n = C_b \left[M_p - (M_p - M_r) \left(\frac{L_b - L_p}{L_r - L_p} \right) \right] = 420.49 \text{ kN}\cdot\text{m} > M_p$$

$$\text{Use } M_n = M_p = 194.35 \text{ kN}\cdot\text{m}$$

$$\phi_b M_n = 174.92 \text{ kN}\cdot\text{m}$$

(3) Determine P_u

$$P_u = 871.52 \text{ kN}$$

(4) Determine M_u

① Determine B_1

$$C_m = 0.6 - 0.4 \left(\frac{1699.3}{3627.35} \right) = 0.413$$

$$G_b = 1.0, G_t = 1.12$$

From the alignment chart of sidesway inhibited,

$$K = 0.777$$

$$P_{e1} = \frac{\pi^2 EI}{(KL)^2} = \frac{(\pi^2)(20500)(8091)}{(0.777 \times 375)^2} = 19282 \text{ kN}$$

$$B_1 = \frac{C_m}{1 - \frac{P_u}{P_{e1}}} = \frac{0.413}{1 - \frac{871.52}{19282}} = 0.433 < 1.0$$

Use $B_1 = 1.0$

② Determine B_2

$$B_2 = 1.11$$

③ Determine M_u

$$M_{u,top} = (1)(36.27) + (1.11)(45.3) = 86.55 \text{ kN}\cdot\text{m}$$

$$M_{u,bottom} = (1)(16.99) + (1.11)(63.85) = 87.86 \text{ kN}\cdot\text{m}$$

(5) Check interaction equation

$$\frac{P_u}{\phi_c P_n} = \frac{871.52}{1583.35} = 0.55 > 0.2$$

$$\frac{P_u}{\phi_c P_n} + \frac{8}{9} \frac{M_u}{\phi_b M_n} = 0.55 + \frac{8}{9} \left(\frac{87.86}{174.92} \right) = 1.0 \quad \therefore \text{O.K.}$$

For Column C11, the nominal axial capacity and bending strength capacity are the same as for Column C13. Values of P_u and M_u can be calculated by using the same procedures above.

$$P_u = 682.4 \text{ kN}$$

$$M_u = 57.07 \text{ kN}\cdot\text{m}$$

Thus, the interaction ratio of Column C11 is

$$\frac{P_u}{\phi_c P_n} + \frac{8}{9} \frac{M_u}{\phi_b M_n} = \frac{682.4}{1583.35} + \frac{8}{9} \left(\frac{57.07}{174.92} \right) = 0.72 < 1.0 \quad \therefore \text{O.K.}$$

6.2.2 Direct Analysis Method

6.2.2.1 Notional Load Method

Since the initial geometric imperfection is assumed to be $L/450$ in this example, the notional loads dealing with the effects of initial out-of-plumbness and inelastic softening can be determined as follow:

$$NL = \frac{GL}{450} + 0.003GL$$

where GL is the gravity load at the considered story. At each floor, H_{floor} is the applied lateral load involving notional and wind loads.

$$GL = 0.491 \times 1200 = 589.2 \text{ kN}$$

$$H_{floor} = \frac{589.2}{450} + 0.003(589.2) + 20.44 = 23.517 \text{ kN}$$

At the roof, the notional load combined with wind load is H_{roof} .

$$GL = 0.317 \times 1200 = 380.4 \text{ kN}$$

$$H_{roof} = \frac{380.4}{450} + 0.003(380.4) + 10.23 = 12.217 \text{ kN}$$

Any second-order elastic analysis program can be used to analyze this six-story frame subjected to the combined notional and external factored loads. Here, the PAAP program with yield stress of steel F_y equaling an arbitrary large value is used. The modeling with load scaling number being 50 is shown in Figure 6.4. The determined axial forces and bending moments of the considered members are listed in Table 6.2.

Member capacity checks are performed for columns C11, C12, and C13:

Adequacy check for Column C11 and C13: (HEB 220)

$$\lambda_c = \frac{L}{\pi r} \sqrt{\frac{F_y}{E}} = \frac{375}{(\pi)(9.43)} \sqrt{\frac{23.5}{20500}} = 0.429 < 1.5$$

$$P_y = A_g F_y = (91)(23.5) = 2138.5 \text{ kN}$$

$$\phi_c P_n = (0.85)(0.658^2) P_y = 1683.22 \text{ kN}$$

$$M_p = Z_x F_y = (827)(23.5) = 19434.5 \text{ kN}\cdot\text{cm} = 194.35 \text{ kN}\cdot\text{m}$$

$$\phi_b M_n = \phi_b M_p = (0.9)(194.35) = 174.91 \text{ kN}\cdot\text{m}$$

For Column C11:

$$\frac{671.71}{1683.22} + \frac{8}{9} \left(\frac{65.69}{174.91} \right) = 0.73 < 1.0 \quad \therefore \text{O.K.}$$

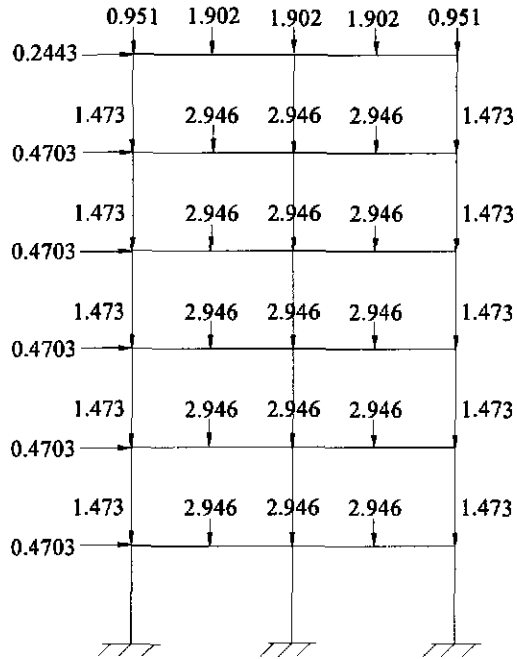


Figure 6.4 Analysis model of DAM-notional load method for the six-story frame by using PAAP program

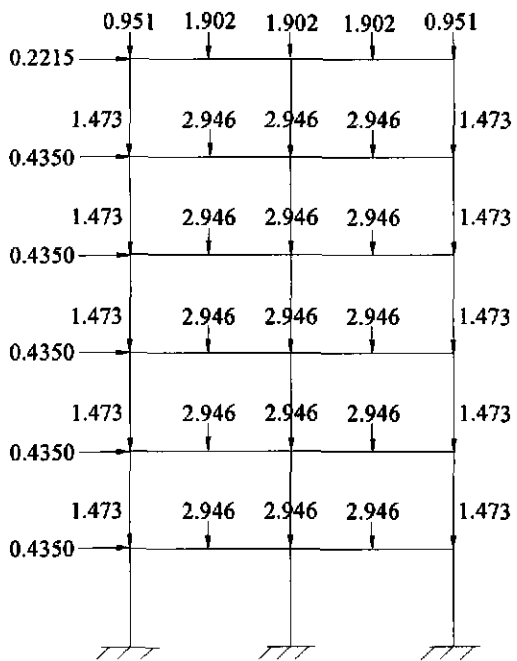


Figure 6.5 Analysis model of DAM-modified stiffness method for the six-story frame by using PAAP program

Table 6.2 Member forces of the six-story steel frame determined by using direct analysis method

Member		DAM-NL	DAM-MS (1 st analysis)	DAM-MS (2 nd analysis)
C11	P_u (kN)	671.71	681.35	682.27
	M_u (kN-m)	65.69	59.55	61.32
C12	P_u (kN)	1737.6	1737.6	1735.49
	M_u (kN-m)	148.45	137.05	132.72
C13	P_u (kN)	916.82	907.22	908.41
	M_u (kN-m)	93.44	87.36	89.48

For Column C13:

$$\frac{916.82}{1683.22} + \frac{8}{9} \left(\frac{93.44}{174.91} \right) = 1.02 \approx 1.0 \quad \therefore \text{O.K.}$$

Adequacy check for Column C12 (HEB 260)

$$\lambda_c = \frac{375}{(\pi)(11.22)} \sqrt{\frac{23.5}{20500}} = 0.36 < 1.5$$

$$P_y = (118)(23.5) = 2773 \text{ kN}$$

$$\phi_c P_n = (0.85) \left(0.658^{(0.36)^2} \right) (2773) = 2232.46 \text{ kN}$$

$$\phi_b M_n = \phi_b M_p = \frac{(0.9)(1283)(23.5)}{100} = 271.35 \text{ kN}\cdot\text{m}$$

$$\frac{1737.6}{2232.46} + \frac{8}{9} \left(\frac{148.45}{271.35} \right) = 1.26 > 1.0 \quad \therefore \text{N.G.}$$

The interaction requirement of Column C12 is violated and the member size must be increased.

6.2.2.2 Modified Stiffness Method

For the modified stiffness method, a two-step analysis is needed. In the first step, a first-order or second-order elastic analysis is performed to determine the axial forces in all members. If the ratio of the axial force to the squash load is greater than the specified value, the lateral stiffness of the member must be reduced to account for the effects of inelastic softening. In the second step, the framed structure with modified stiffness is analyzed by second-order elastic analysis to determine the internal forces of each member.

In the modified stiffness method, the notional loads account for the effects of initial out-of-plumbness only. They are determined by using the following expression in this example:

$$NL = \frac{GL}{450}$$

where GL is defined in Section 6.2.2.1. At each floor, H_{floor} is the lateral load involving notional load and wind load. Then,

$$H_{floor} = \frac{589.2}{450} + 20.44 = 21.75 \text{ kN}$$

At roof level, the notional load combined with wind load is H_{roof} .

$$H_{roof} = \frac{380.4}{450} + 10.23 = 11.075 \text{ kN}$$

Figure 6.5 shows the modeling with load scaling number being 50 if the PAAP program is used. Again, for an elastic analysis, the yield stress F_y is set to be an arbitrary large value. In the first analysis, the original modulus of elasticity which equals 20500 kN/cm² is used for all members. The determined axial forces and bending moments of columns C11, C12, and C13 are tabulated in Table 6.2. The ratio of axial force to the squash load for each of the three members can be determined as:

$$C11: \frac{P_u}{P_y} = \frac{681.35}{2138.5} = 0.32 < 0.5$$

$$C12: \frac{P_u}{P_y} = \frac{1737.6}{2773} = 0.627 > 0.5$$

$$C13: \frac{P_u}{P_y} = \frac{907.22}{2138.5} = 0.42 < 0.5$$

Since the ratio of P_u/P_y of column C12 is greater than 0.5, its lateral stiffness should be reduced.

$$\tau = 4 \left(\frac{P_u}{P_y} \right) \left(1 - \frac{P_u}{P_y} \right) = 0.936$$

For the section HEB 260,

$$M_p = Z_x F_y = 301.51 \text{ kN}\cdot\text{m}$$

$$M_y = S_x F_y = 269.78 \text{ kN}\cdot\text{m}$$

Since M_p is less than $1.2M_y$, the factor C equals one. Thus, the reduced modulus of elasticity of Column C12 is

$$E^* = C\tau E = (1.0)(0.936)(20500) = 19188 \text{ kN/cm}^2$$

The internal forces can be obtained after the second analysis and shown in Table 6.2.

Member capacity checks for the three columns are:

$$\text{For Column C11, } \frac{682.27}{1683.22} + \frac{8}{9} \left(\frac{61.32}{174.91} \right) = 0.72 < 1.0 \quad \therefore \text{O.K.}$$

$$\text{For Column C12, } \frac{1735.49}{2232.46} + \frac{8}{9} \left(\frac{132.72}{271.35} \right) = 1.21 > 1.0 \quad \therefore \text{N.G.}$$

$$\text{For Column C13, } \frac{908.41}{1683.22} + \frac{8}{9} \left(\frac{89.48}{174.91} \right) = 0.99 \approx 1.0 \quad \therefore \text{O.K.}$$

Again, the interaction requirement of Column C12 is not met and its member size must be increased.

6.2.3 Advanced Analysis Method

As shown in Figure 6.6, each column is modeled with one element and each beam is modeled with two. The uniform gravity loads applied on beams are converted to equivalent concentrated loads applied at the nodes. The incremental load is determined by dividing the total load by a scaling factor of 50. In the explicit imperfection model, the initial geometric imperfection of 0.8333 cm at each floor level is calculated by dividing the story height by 450. In the equivalent notional load model, a notional load of 0.845 kN at roof level and 1.3 kN at each floor level results from the total gravity load of 380.4 kN at roof level and 589.2 kN at floor level divided by 450, respectively. In the further reduced tangent modulus model, the program intrinsically accounts for the geometric imperfection of $L_c/500$. Therefore, additional geometric imperfection of $L_c/4500$ should

be applied to the structure. The three models of the advanced analysis method are shown in Figures 6.7a through 6.7c. The input data are shown in Table 6.3a through 6.3c.

After execution of the PAAP program, the load-carrying capacity of the structure can be checked from the output file P.OUT2. The explicit imperfection model and equivalent notional load model predict the same load-carrying capacity of 73.36 kN at the final stage with respect to the vertical load at node 2. The further reduced tangent modulus model predicts the load-carrying capacity of 74 kN. Since the vertical load-carrying capacities at node 2 determined by all three methods are almost equal to the applied load of 73.65 kN, the preliminary design of steel frame members is adequate.

6.2.4 Comparison of the Analysis/Design Results

The overstrength factors for plastic zone analysis and all three methods discussed in this study are listed in Table 6.4. When the AISC-LRFD or direct analysis method is used, Column C12 does not satisfy the interaction requirement under the specified loading. Interaction equations are used to check the strength of each member individually and no internal force redistribution can be considered. On the other hand, when the advanced analysis method is employed, additional forces transfer to other members after plastic hinges form and the whole structural system does not collapse until it loses its stability. Therefore, the design result obtained by using advanced analysis method is more economical than the one determined by using the AISC-LRFD or direct analysis method.

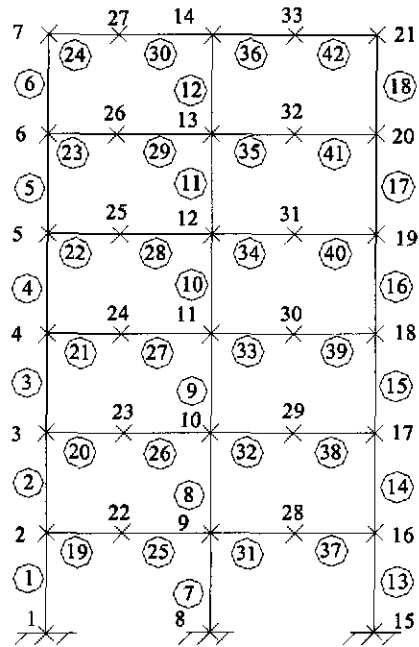
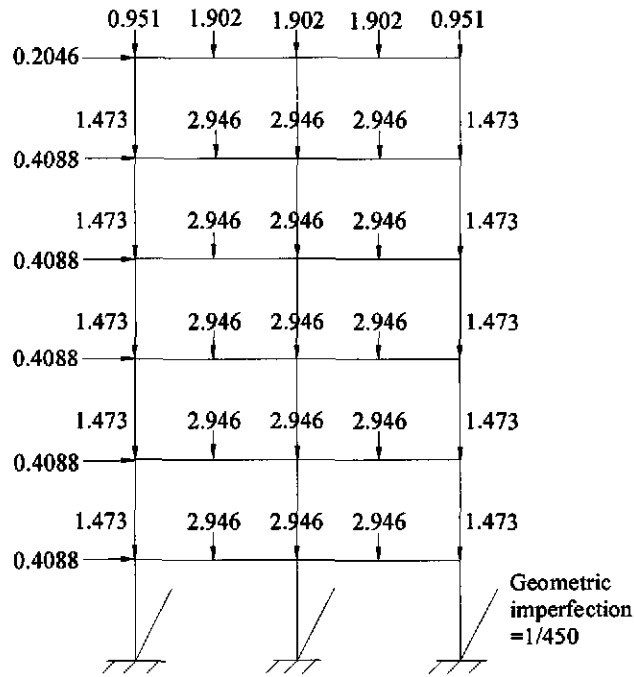
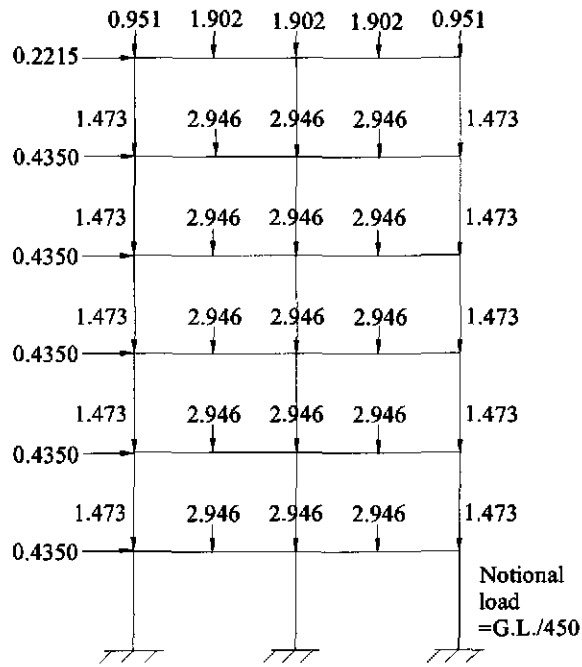


Figure 6.6 Structural modeling of the six-story frame

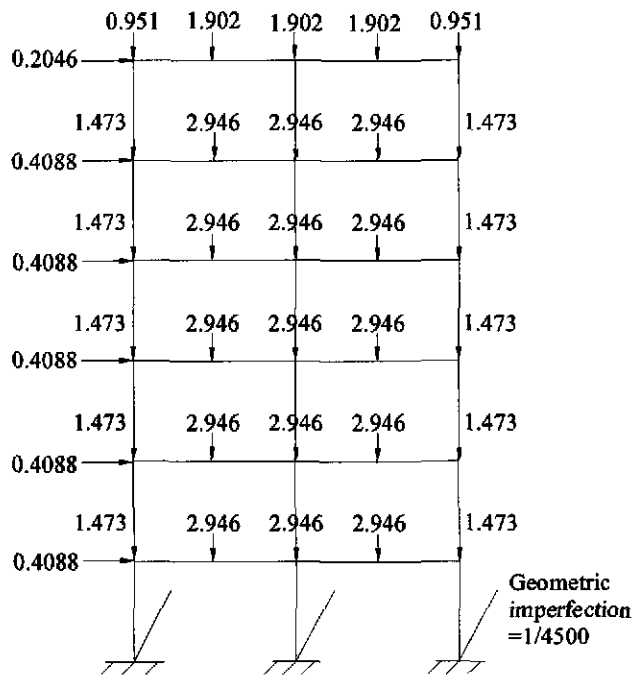


(a) Explicit imperfection model

Figure 6.7 Analysis models of advanced analysis method for the six-story frame



(b) Equivalent notional load model



(c) Further reduced tangent modulus model

Figure 6.7 Analysis models of advanced analysis method for the six-story frame (cont.)

Table 6.3a Input data of the explicit imperfection modeling for the six-story frame

Vogel Frame (AA-Explicit Imperfection Modeling)

1	1					
33	3	200				
0	10	0				
0	42	0				
1	39.1	3892.0	367.0	20500.0	23.5	
2	53.8	8356.0	628.0	20500.0	23.5	
3	62.6	11770.0	804.0	20500.0	23.5	
4	72.7	16270.0	1019.0	20500.0	23.5	
5	84.5	23130.0	1307.0	20500.0	23.5	
6	54.3	2492.0	354.0	20500.0	23.5	
7	78.1	5692.0	643.0	20500.0	23.5	
8	91.0	8091.0	827.0	20500.0	23.5	
9	106.0	11260.0	1053.0	20500.0	23.5	
10	118.0	14920.0	1283.0	20500.0	23.5	
1	0.8333	375.0	8	1	2	4
5	0.8333	375.0	6	5	6	2
7	0.8333	375.0	10	8	9	2
9	0.8333	375.0	9	10	11	2
11	0.8333	375.0	7	12	13	2
13	0.8333	375.0	8	15	16	4
17	0.8333	375.0	6	19	20	2
19	300.0	0.0	5	2	22	
20	300.0	0.0	4	3	23	
21	300.0	0.0	3	4	24	
22	300.0	0.0	2	5	25	
23	300.0	0.0	2	6	26	
24	300.0	0.0	1	7	27	
25	300.0	0.0	5	22	9	
26	300.0	0.0	4	23	10	
27	300.0	0.0	3	24	11	
28	300.0	0.0	2	25	12	
29	300.0	0.0	2	26	13	
30	300.0	0.0	1	27	14	
31	300.0	0.0	5	9	28	
32	300.0	0.0	4	10	29	
33	300.0	0.0	3	11	30	
34	300.0	0.0	2	12	31	
35	300.0	0.0	2	13	32	
36	300.0	0.0	1	14	33	
37	300.0	0.0	5	28	16	
38	300.0	0.0	4	29	17	
39	300.0	0.0	3	30	18	
40	300.0	0.0	2	31	19	
41	300.0	0.0	2	32	20	
42	300.0	0.0	1	33	21	
1	1	1				
8	1	1				
15	1	1				
2	0.4088	-1.473			5	
7	0.2046	-0.951				

Table 6.3a Input data of the explicit imperfection modeling for the six-story frame (cont.)

9	-2.946	5
14	-1.902	
16	-1.473	5
21	-0.951	
22	-2.946	5
27	-1.902	
28	-2.946	5
33	-1.902	

Table 6.3b Input data of the equivalent notional load modeling for the six-story frame

Vogel Frame (AA-Notional Load Method)

2	1					
33	3	200				
0	10	0				
0	42	0				
1	39.1	3892.0	367.0	20500.0	23.5	
2	53.8	8356.0	628.0	20500.0	23.5	
3	62.6	11770.0	804.0	20500.0	23.5	
4	72.7	16270.0	1019.0	20500.0	23.5	
5	84.5	23130.0	1307.0	20500.0	23.5	
6	54.3	2492.0	354.0	20500.0	23.5	
7	78.1	5692.0	643.0	20500.0	23.5	
8	91.0	8091.0	827.0	20500.0	23.5	
9	106.0	11260.0	1053.0	20500.0	23.5	
10	118.0	14920.0	1283.0	20500.0	23.5	
1	0.0	375.0	8	1	2	4
5	0.0	375.0	6	5	6	2
7	0.0	375.0	10	8	9	2
9	0.0	375.0	9	10	11	2
11	0.0	375.0	7	12	13	2
13	0.0	375.0	8	15	16	4
17	0.0	375.0	6	19	20	2
19	300.0	0.0	5	2	22	
20	300.0	0.0	4	3	23	
21	300.0	0.0	3	4	24	
22	300.0	0.0	2	5	25	
23	300.0	0.0	2	6	26	
24	300.0	0.0	1	7	27	
25	300.0	0.0	5	22	9	
26	300.0	0.0	4	23	10	
27	300.0	0.0	3	24	11	
28	300.0	0.0	2	25	12	
29	300.0	0.0	2	26	13	
30	300.0	0.0	1	27	14	
31	300.0	0.0	5	9	28	
32	300.0	0.0	4	10	29	
33	300.0	0.0	3	11	30	
34	300.0	0.0	2	12	31	
35	300.0	0.0	2	13	32	

Table 6.3b Input data of the equivalent notional load modeling for the six-story frame (cont.)

36	300.0	0.0	1	14	33
37	300.0	0.0	5	28	16
38	300.0	0.0	4	29	17
39	300.0	0.0	3	30	18
40	300.0	0.0	2	31	19
41	300.0	0.0	2	32	20
42	300.0	0.0	1	33	21
1	1	1	1		
8	1	1	1		
15	1	1	1		
2	0.4350	-1.473			5
7	0.2215	-0.951			
9		-2.946			5
14		-1.902			
16		-1.473			5
21		-0.951			
22		-2.946			5
27		-1.902			
28		-2.946			5
33		-1.902			

Table 6.3c Input data of the further reduced tangent modulus modeling for the six-story frame

Vogel Frame (AA-Fur. Red. Et)

3	1						
33	3	200					
0	10	0					
0	42	0					
1	39.1	3892.0	367.0	20500.0	23.5		
2	53.8	8356.0	628.0	20500.0	23.5		
3	62.6	11770.0	804.0	20500.0	23.5		
4	72.7	16270.0	1019.0	20500.0	23.5		
5	84.5	23130.0	1307.0	20500.0	23.5		
6	54.3	2492.0	354.0	20500.0	23.5	1	
7	78.1	5692.0	643.0	20500.0	23.5	1	
8	91.0	8091.0	827.0	20500.0	23.5	1	
9	106.0	11260.0	1053.0	20500.0	23.5	1	
10	118.0	14920.0	1283.0	20500.0	23.5	1	
1	0.0833	375.0	8	1	2	4	
5	0.0833	375.0	6	5	6	2	
7	0.0833	375.0	10	8	9	2	
9	0.0833	375.0	9	10	11	2	
11	0.0833	375.0	7	12	13	2	
13	0.0833	375.0	8	15	16	4	
17	0.0833	375.0	6	19	20	2	
19	300.0	0.0	5	2	22		
20	300.0	0.0	4	3	23		

Table 6.3c Input data of the further reduced tangent modulus modeling for the six-story frame (cont.)

21	300.0	0.0	3	4	24
22	300.0	0.0	2	5	25
23	300.0	0.0	2	6	26
24	300.0	0.0	1	7	27
25	300.0	0.0	5	22	9
26	300.0	0.0	4	23	10
27	300.0	0.0	3	24	11
28	300.0	0.0	2	25	12
29	300.0	0.0	2	26	13
30	300.0	0.0	1	27	14
31	300.0	0.0	5	9	28
32	300.0	0.0	4	10	29
33	300.0	0.0	3	11	30
34	300.0	0.0	2	12	31
35	300.0	0.0	2	13	32
36	300.0	0.0	1	14	33
37	300.0	0.0	5	28	16
38	300.0	0.0	4	29	17
39	300.0	0.0	3	30	18
40	300.0	0.0	2	31	19
41	300.0	0.0	2	32	20
42	300.0	0.0	1	33	21
1	1	1			
8	1	1			
15	1	1			
2	0.4088	-1.473			5
7	0.2046	-0.951			
9		-2.946			5
14		-1.902			
16		-1.473			5
21		-0.951			
22		-2.946			5
27		-1.902			
28		-2.946			5
33		-1.902			

Table 6.4 Member strength and overstrength factors for six-story frame

Method		C11			C12			C13			Overstrength Factor
		P_u	M_u	ΣI	P_u	M_u	ΣI	P_u	M_u	ΣI	
Plastic Zone		683	67	-	1720	115.0	-	921	99.0	-	-
A A	E.I	682	112.0	-	1704	84.6	-	926	94.7	-	1.0
	N.L.	682	112.1	-	1704	84.7	-	926	94.6	-	1.0
	R.E _t	692	109.2	-	1721	82.4	-	928	93.0	-	1.0
D A M	N.L.	672	65.7	0.73	1737	148.5	1.26	917	93.4	1.02	0.8
	M.S.	682	61.3	0.72	1735	132.7	1.21	908	89.5	0.99	0.84
LRFD		688	55.0	0.71	1738	128.6	1.23	900	82.9	0.99	0.82

* Unit: kN, m

6.3 Braced Frame

Figure 6.8 shows the dimensions and loading condition for a one-bay, eight-story, braced steel frame. Consideration of live load reduction is induced in the factored loads shown in this figure. It is assumed that the columns are braced to prevent out-of-plane displacements and the beams and diagonal braces are pin-connected to the columns. The preliminary sizes of members are W14×61 for columns, W16×31 for beams, and L4×4×7/16 for braces. Yield stress of steel is 50 ksi.

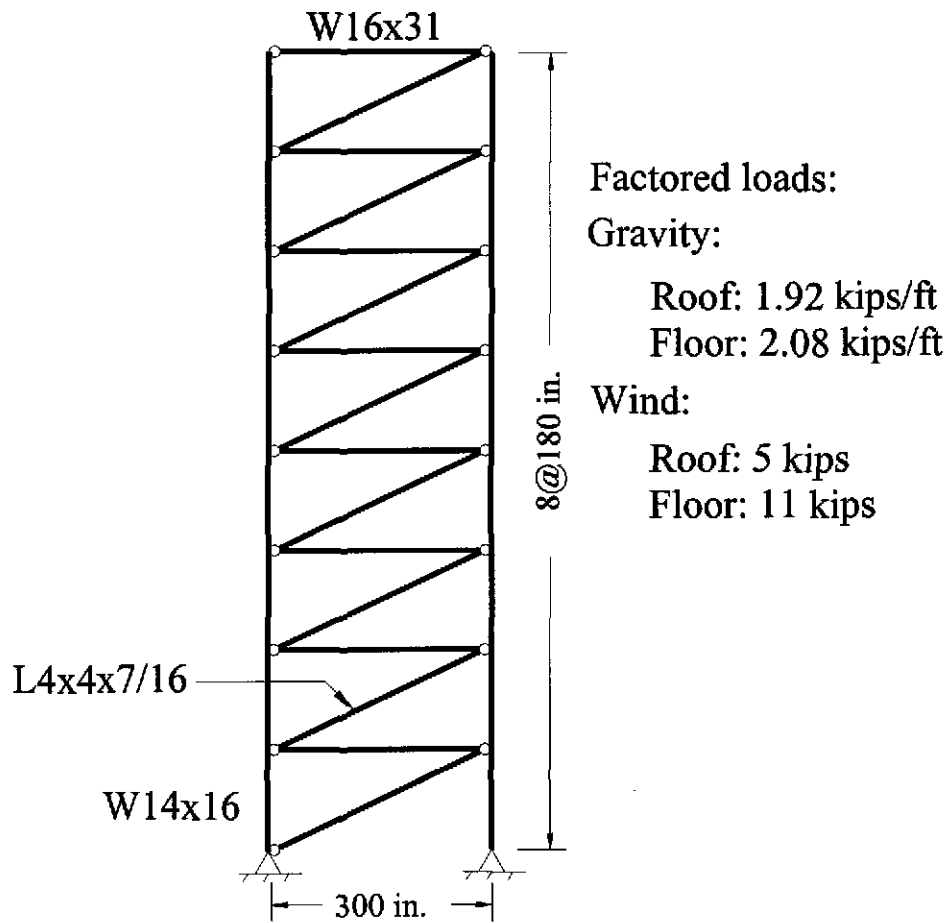


Figure 6.8 Configuration and load condition of the braced steel frame

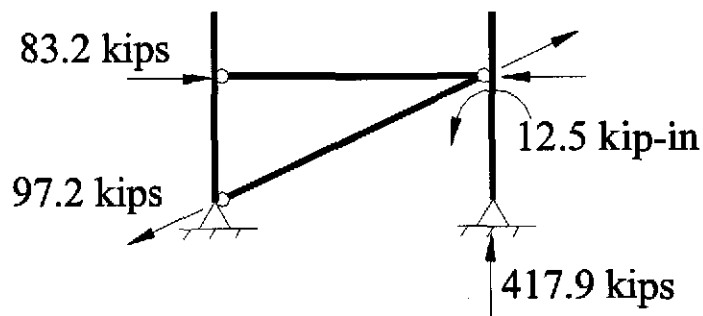


Figure 6.9 Member forces of the braced steel frame determined by using a second-order elastic analysis

6.3.1 AISC-LRFD Method

A second-order elastic analysis is implemented to the braced steel frame directly. The member forces obtained from the analysis are shown in Figure 6.9. Member capacity checks are carried out as follows:

Member capacity check for columns: (W14×61: $A = 17.9$, $I_y = 107.0$, $Z_y = 32.8$, $\gamma_y = 2.45$)

The right column at the first floor is the most critical member. It is used to check for the safety requirements. The moments in columns are small and can be ignored.

(1) Determine $\phi_c P_n$

$$P_y = A_g F_y = (17.9)(50) = 895 \text{ kips}$$

According to the AISC-LRFD Manual of Steel Construction [1], $K = 1$ is conservatively chosen because a small relative movement of the brace points is anticipated.

$$\lambda_c = \frac{KL}{\pi \gamma_x} \sqrt{\frac{F_y}{E}} = \frac{(1.0)(180)}{(\pi)(2.45)} \sqrt{\frac{50}{29000}} = 0.971 < 1.5$$

$$\phi_c P_n = \phi_c (0.658^{2\lambda_c}) P_y = (0.85)(0.658^{(0.971)^2})(895) = 512.67 \text{ kips}$$

(2) Determine the axial force in the column

$$P_u = 417.9 \text{ kips}$$

(3) Check interaction equation

$$\frac{P_u}{\phi_c P_n} + \frac{8 M_u}{9 \phi_b M_n} \approx \frac{417.9}{512.67} = 0.815 < 1.0 \quad \therefore \text{O.K.}$$

Member capacity check for beams: (W16×31: $A = 9.13$, $I_x = 375$, $Z_x = 54$, $\gamma_x = 6.41$)

Since the beam is laterally braced, P_n is controlled by the strong-axis buckling.

(1) Determine $\phi_c P_n$

$$P_y = A_g F_y = (9.13)(50) = 456.5 \text{ kips}$$

$$\lambda_{cx} = \frac{(1.0)(300)}{(\pi)(6.41)} \sqrt{\frac{50}{29000}} = 0.6186 < 1.5$$

$$\phi_c P_n = (0.85) \left[0.658^{(0.6186)^2} \right] (456.5) = 330.6 \text{ kips}$$

(2) Determine $\phi_b M_n$

$$\phi_b M_n = \phi_b M_p = (0.9)(54 \times 50) = 2430 \text{ kip-in}$$

(3) Determine ultimate member forces

$$P_u = 83.2 \text{ kips}$$

$$M_u = \frac{1}{8} \left(\frac{2.08}{12} \right) (300)^2 = 1950 \text{ kip-in}$$

(4) Check interaction equation

$$\frac{P_u}{\phi_c P_n} = \frac{83.2}{330.6} = 0.252 > 0.2$$

$$\frac{P_u}{\phi_c P_n} + \frac{8}{9} \frac{M_u}{\phi_b M_n} = 0.252 + \frac{8}{9} \frac{1950}{2430} = 0.97 < 1.0 \quad \therefore \text{O.K.}$$

Member capacity check for braces: (L4×4×7/16: A = 3.31)

(1) Determine $\phi_c P_n$

$$\phi_c P_n = (0.9)(3.31 \times 50) = 148.95 \text{ kips}$$

(2) Check interaction equation

$$P_u = 97.2 \text{ kips}$$

$$\frac{P_u}{\phi_c P_n} = \frac{97.2}{148.95} = 0.65 < 1.0 \quad \therefore \text{O.K.}$$

6.3.2 Direct Analysis Method

For the braced frame, the notional load of $0.002GL = 0.002 \times (1.92 \times 25) = 0.096$ kip is laterally added to the top of the building, while the notional load of $0.002GL = 0.002 \times (2.08 \times 25) = 0.104$ kip is laterally applied to each floor level. The axial force in the considered column can be obtained by an execution of a second-order elastic analysis.

Adequacy check for column:

(1) $P_u = 420.17$ kips

(2) Determine $\phi_c P_n$

The value of $\phi_c P_n$ is identical to the one of AISC-LRFD in this example because the unsupported column length is used in the direct analysis method. Thus, $\phi_c P_n = 512.67$ kips.

(3) Check interaction equation

$$\frac{P_u}{\phi_c P_n} + \frac{8}{9} \frac{M_u}{\phi_b M_n} \approx \frac{420.17}{512.67} = 0.82 < 1.0 \quad \therefore \text{O.K.}$$

Adequacy check for beams:

The calculation of nominal axial and bending strength of beam members is identical to the AISC-LRFD method. The ultimate axial force and bending moment of the first floor beam are $P_u = 84$ kips and $M_u = 1950$ kip-in. Thus,

$$\frac{P_u}{\phi_c P_n} + \frac{8}{9} \frac{M_u}{\phi_b M_n} = \frac{84}{330.6} + \frac{8}{9} \frac{1950}{2430} = 0.967 < 1.0 \quad \therefore \text{O.K.}$$

Adequacy check for braces:

The determined ultimate axial force in the critical diagonal brace is $P_u = 98.13$ kips.

$$\frac{P_u}{\phi_c P_n} = \frac{98.13}{148.95} = 0.66 < 1.0 \quad \therefore \text{O.K.}$$

6.3.3 Advanced Analysis Method

Because of the redundancy of this structure, the column size can be reduced to W14×53 from the preliminary member size W14×61. Figure 6.10 shows the structural modeling of the braced steel structure. Each column is modeled with two elements and each brace is modeled as one truss member. The incremental load is determined by dividing the total loads by a scaling factor of 50. The three models of advanced analysis method are shown in Figures 6.11a through 6.11c and the input data are shown in Table 6.5a through 6.5c.

Results of the analysis are tabulated in Table 6.6. In this table, V_3 represents the load-carrying capacity of the structure at the final stage with respect to the vertical load at node 3, while γ is the overstrength factor. Since the values of overstrength factor for all

three methods are almost equal to one, the preliminary design is adequate under this loading condition.

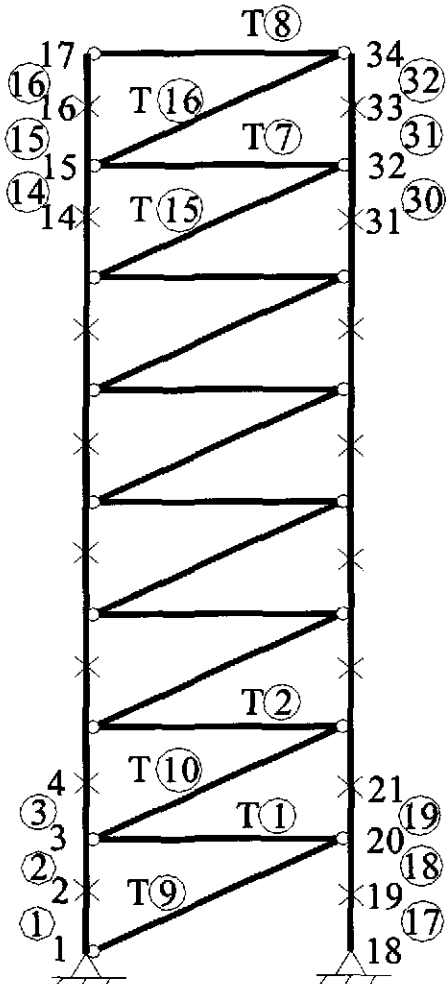
6.3.4 Comparison of the Analysis/Design Results

It can be seen that the results of analysis by using the AISC-LRFD and direct analysis method are almost identical. In the direct analysis method, the notional load that accounts for the effects of initial out-of-plumbness does not reduce the strength of the structure. This is because the lateral displacement is small for braced frames. For both the AISC-LRFD and direct analysis method, determination of the effective length factors for braced structures is not required. Therefore, use of the direct analysis method is more complicated than use of the AISC-LRFD method and, it is not recommended for the analysis and design for braced structures.

The same member size beams and diagonal braces are determined by all three methods. A smaller column size is predicted by the advanced analysis method. This is caused by the effective length of the first floor column being less than one due to the restraint from the upper columns. The AISC-LRFD and direct analysis method simply assume $K = 1$ and the nominal axial strength of the column is underestimated.

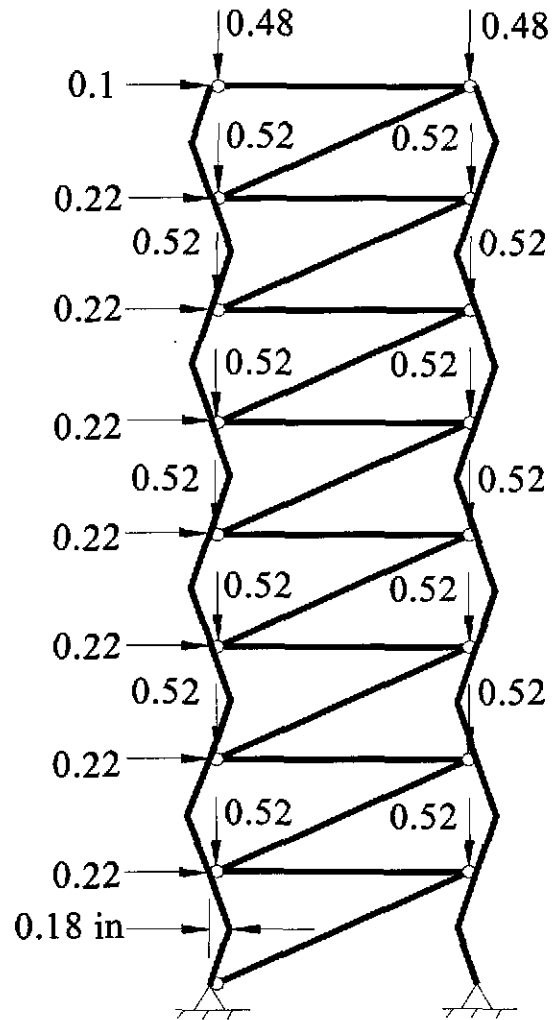
When the equivalent notional load model of the advanced analysis method is implemented, additional analysis is needed to determine the axial forces in the columns and the notional loads. The smallest structural capacity could be obtained based on the directions of initial geometric imperfections and notional loads shown in Figures 6.11a and 6.11b, respectively. Because determination of these directions needs a trial and error

process, the further reduced tangent modulus model will be convenient and recommended for use.



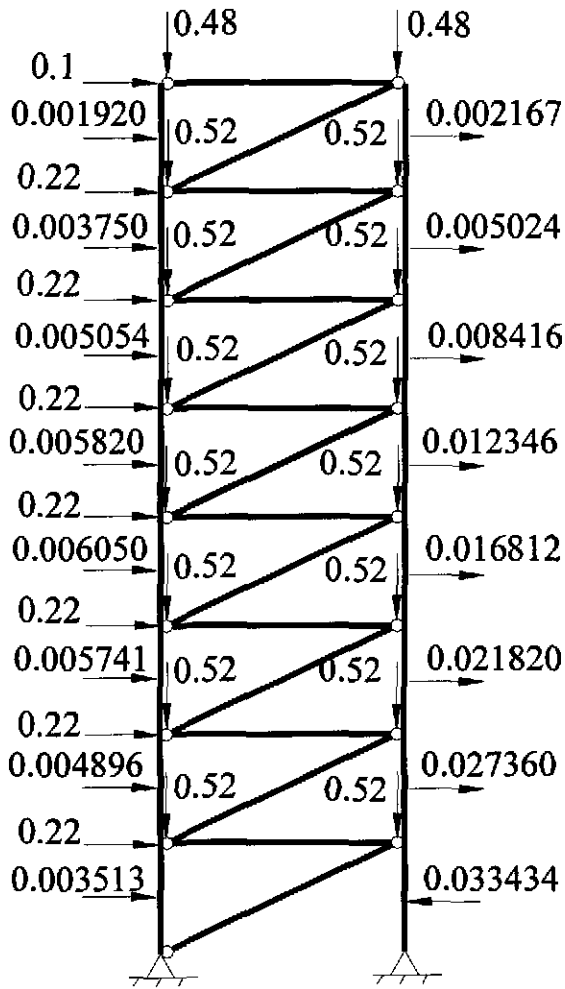
Frame member: ○
 Truss member: T○

Figure 6.10 Structural modeling of the braced steel frame

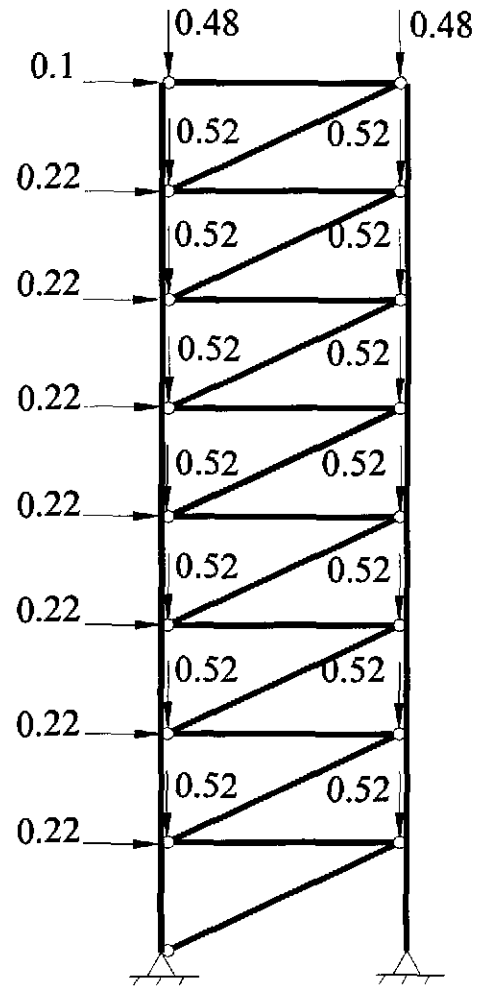


(a) Explicit imperfection model

Figure 6.11 Analysis models of advanced analysis method for the braced steel frame (unit: kip)



(b) Equivalent notional load model



(c) Further reduced tangent modulus model

Figure 6.11 Analysis models of advanced analysis method for the braced steel frame (cont.) (unit: kip)

Table 6.5a Input data of the explicit imperfection modeling for the braced frame

Braced Eight-Story Frame (AA-Explicit Imperfection)

1	1						
34	2	100					
0	1	2					
0	32	16					
1		15.6	57.7	22.0	29000.0		50.0
1		9.13	375.0	29000.0		50.0	
2		3.3	4.97	29000.0		50.0	
1		0.18	90.0	1	1	2	
2		-0.18	90.0	1	2	3	
3		-0.18	90.0	1	3	4	
4		0.18	90.0	1	4	5	
5		0.18	90.0	1	5	6	
6		-0.18	90.0	1	6	7	
7		-0.18	90.0	1	7	8	
8		0.18	90.0	1	8	9	
9		0.18	90.0	1	9	10	
10		-0.18	90.0	1	10	11	
11		-0.18	90.0	1	11	12	
12		0.18	90.0	1	12	13	
13		0.18	90.0	1	13	14	
14		-0.18	90.0	1	14	15	
15		-0.18	90.0	1	15	16	
16		0.18	90.0	1	16	17	
17		-0.18	90.0	1	18	19	
18		0.18	90.0	1	19	20	
19		0.18	90.0	1	20	21	
20		-0.18	90.0	1	21	22	
21		-0.18	90.0	1	22	23	
22		0.18	90.0	1	23	24	
23		0.18	90.0	1	24	25	
24		-0.18	90.0	1	25	26	
25		-0.18	90.0	1	26	27	
26		0.18	90.0	1	27	28	
27		0.18	90.0	1	28	29	
28		-0.18	90.0	1	29	30	
29		-0.18	90.0	1	30	31	
30		0.18	90.0	1	31	32	
31		0.18	90.0	1	32	33	
32		-0.18	90.0	1	33	34	
1		300.0	0.0	1	3	20	8 2
9		300.0	180.0	2	1	20	8 2
1	1	1					
18	1	1					
3		0.22	-0.52			7	2
17		0.1	-0.48				
20			-0.52			7	2
34			-0.48				

Table 6.5b Input data of the equivalent notional load modeling for the braced frame

Braced eight-Story Frame (AA-Equivalent notional Load)

2	1							
34	2	100						
0	1	2						
0	32	16						
1		15.6	57.7		22.0	29000.0		50.0
1		9.13	375.0		29000.0		50.0	
2		3.3	4.97		29000.0		50.0	
1		0.0	90.0	1	1	2	16	
17		0.0	90.0	1	18	19	16	
1		300.0	0.0	1	3	20	8	2
9		300.0	180.0	2	1	20	8	2
1	1	1						
18	1	1						
2		0.003513						
3		0.22	-0.52			7	2	
4		0.004896						
6		0.005741						
8		0.006050						
10		0.005820						
12		0.005054						
14		0.003750						
16		0.001920						
17		0.1	-0.48					
19		-0.033434						
20			-0.52			7	2	
21		0.027360						
23		0.021820						
25		0.016812						
27		0.012346						
29		0.008416						
31		0.005024						
33		0.002167						
34			-0.48					

Table 6.5c Input data of the further reduced tangent modulus modeling for the braced frame

Braced Eight-Story Frame (AA-Further Reduced tangent Modulus)

3	1							
34	2	100						
0	1	2						
0	32	16						
1		15.6	57.7	22.0	29000.0	50.0	1	
1		9.13	375.0	29000.0	50.0			
2		3.3	4.97	29000.0	50.0			
1		0.0	90.0	1	1	2	16	
17		0.0	90.0	1	18	19	16	
1		300.0	0.0	1	3	20	8	2
9		300.0	180.0	2	1	20	8	2
1	1	1						
18	1	1						
3		0.22	-0.52			7	2	
17		0.1	-0.48					
20			-0.52			7	2	
34			-0.48					

Table 6.6 Analysis results of the braced frame using advanced analysis method

Method	V ₃ (kips)	γ
Explicit Imperfection	25.97	1.0
Equivalent Notional Load	25.61	0.99
Further Reduced Tangent Modulus	27.59	1.06

6.4 Leaned Column Frame

Leaned column frame structures are usually used for low-rise industrial buildings. Figure 6.12 shows the dimensions and loading condition of an auto plant. Sections W24×76 and W10×49 are preliminarily chosen for beams and columns, respectively. Out-of-plane displacements are prevented. Yield stress of steel is 50 ksi.

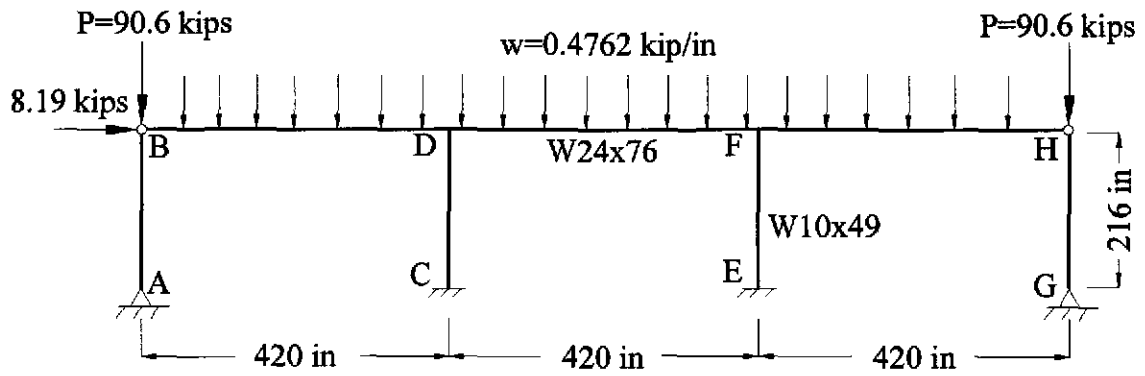


Figure 6.12 Configuration and load condition of the leaned column frame

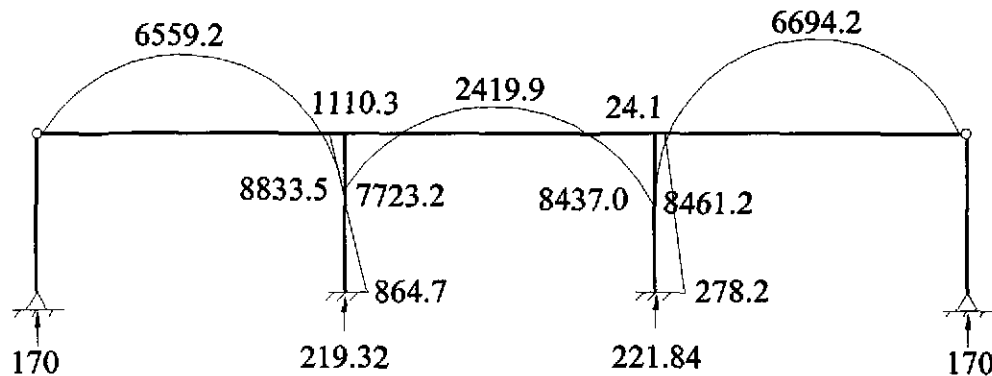


Figure 6.13 Member forces of the leaned column frame determined by using a second-order elastic analysis (unit: kip for force and kip-in for moment)

6.4.1 AISC-LRFD Method

In the AISC-LRFD method, second-order elastic analysis could be used directly. The determined member forces are shown in Figure 6.13. When determining the axial capacities of rigid columns, the effective length factors must be amplified by equation (2.4) to account for the leaned column effects.

Member capacity check for column CD:

(1) Determine $\phi_c P_n$

① Determine τ

$$P_y = A_g F_y = (14.4)(50) = 720 \text{ kips}$$

$$\frac{P_u}{P_y} = \frac{219.3}{720} = 0.3 < \frac{1}{3}$$

$$\tau = 1.0$$

② Determine L_g'

$$L_{gt}' = 2 \times L_g = 2 \times 420 = 840 \text{ in.}$$

$$L_{gr}' = L_{gr} \left(2 - \frac{M_{Fr}}{M_{Nr}} \right) = (420) \left(2 - \frac{8437.0}{7723.2} \right) = 381.2 \text{ in.}$$

③ Determine K

$$G_c = 1.0$$

$$G_D = \frac{\sum \left(\tau \frac{I_c}{L_c} \right)}{\sum \left(\frac{I_g}{L_g} \right)} = \frac{\frac{272}{216}}{\frac{2100}{840} + \frac{2100}{381.2}} = 0.157$$

From the alignment chart of *sidesway uninhibited*,

$$K_x = 1.18$$

Since the exterior pinned-ended columns lean on the column considered, the K value must be adjusted.

$$K = \sqrt{\frac{\sum P_u I_i}{P_{ui} \sum \left(\frac{I_i}{K_i^2} \right)}} = \sqrt{\frac{781.2 \cdot 272}{219.3 \cdot \frac{272}{1.18^2} \times 2}} = 1.57$$

④ Determine $\phi_c P_n$

$$\lambda_c = \frac{KL}{\pi r} \sqrt{\frac{F_y}{E}} = \frac{(1.57)(216)}{(\pi)(4.35)} \sqrt{\frac{50}{29000}} = 1.03 < 1.5$$

$$\phi_c P_n = \phi_c \left[0.658^{\lambda_c^2} \right] P_y = (0.85) \left[0.658^{(1.03)^2} \right] (720) = 392.4 \text{ kips}$$

(2) Determine $\phi_b M_n$

$$\phi_b M_n = \phi_b M_p = (0.9)(60.4 \times 50) = 2718 \text{ kip-in}$$

(3) Check adequacy of Column CD

$$\frac{P_u}{\phi_c P_n} = \frac{219.3}{392.4} = 0.56 > 0.2$$

$$\frac{P_u}{\phi_c P_n} + \frac{8 M_u}{9 \phi_b M_n} = 0.56 + \frac{8 \cdot 1110.3}{9 \cdot 2718} = 0.92 < 1.0 \quad \therefore \text{O.K.}$$

Member capacity check for beams:

$$\phi_b M_n = \phi_b M_p = (0.9)(200 \times 50) = 9000 \text{ kip-in}$$

$$\frac{M_u}{\phi_b M_n} = \frac{8833.5}{9000} = 0.982 < 1.0 \quad \therefore \text{O.K.}$$

Member capacity check for leaned columns:

$$K_x = 1.0$$

$$\lambda_c = \frac{(1.0)(216)}{(\pi)(4.35)} \sqrt{\frac{50}{29000}} = 0.656 < 1.5$$

$$\phi_c P_n = (0.85) \left[0.658^{(0.656)^2} \right] (720) = 511 \text{ kips}$$

$$\frac{P_u}{\phi_c P_n} = \frac{170}{511} = 0.33 < 1.0 \quad \therefore \text{O.K.}$$

6.4.2 Direct Analysis Method

6.4.2.1 Notional Load Method

Combined with the applied lateral load, the notional load of 3.906 kips is added to the top of the frame. By performing a second-order elastic analysis, the member forces are determined and shown in Figure 6.14.

Adequacy check for Column CD:

The nominal axial strength of Column CD is identical to the one of leaned columns determined by using the AISC-LRFD method. Thus, $\phi_c P_n = 511$ kips.

$$\frac{P_u}{\phi_c P_n} = \frac{218.7}{511} = 0.428 > 0.2$$

$$\frac{P_u}{\phi_c P_n} + \frac{8}{9} \frac{M_u}{\phi_b M_n} = 0.428 + \frac{8}{9} \frac{1370.1}{2718} = 0.876 < 1.0 \quad \therefore \text{O.K.}$$

Adequacy check for beams:

$$\frac{M_u}{\phi_b M_n} = \frac{8923.8}{9000} \approx 1.0 \quad \therefore \text{O.K.}$$

Adequacy check for leaned columns:

$$\frac{P_u}{\phi_c P_n} = \frac{171}{511} = 0.335 < 1.0 \quad \therefore \text{O.K.}$$

6.4.2.2 Modified Stiffness Method

The results of a second-order elastic analysis are shown in Figure 6.15. Since the ratios of P_u/P_y and $M_p/1.2M_y$ for all members are respectively less than 0.5 and 1.0, no lateral stiffness reduction is required. The safety check is calculated as follow:

Adequacy check for Column CD:

$$\frac{P_u}{\phi_c P_n} + \frac{8}{9} \frac{M_u}{\phi_b M_n} = \frac{219.1}{511} + \frac{8}{9} \frac{1214.1}{2718} = 0.83 < 1.0 \quad \therefore \text{O.K.}$$

Adequacy check for beams:

$$\frac{M_u}{\phi_b M_n} = \frac{8869.6}{9000} = 0.99 < 1.0 \quad \therefore \text{O.K.}$$

Adequacy check for leaned column:

$$\frac{P_u}{\phi_c P_n} = \frac{171}{511} = 0.335 < 1.0 \quad \therefore \text{O.K.}$$

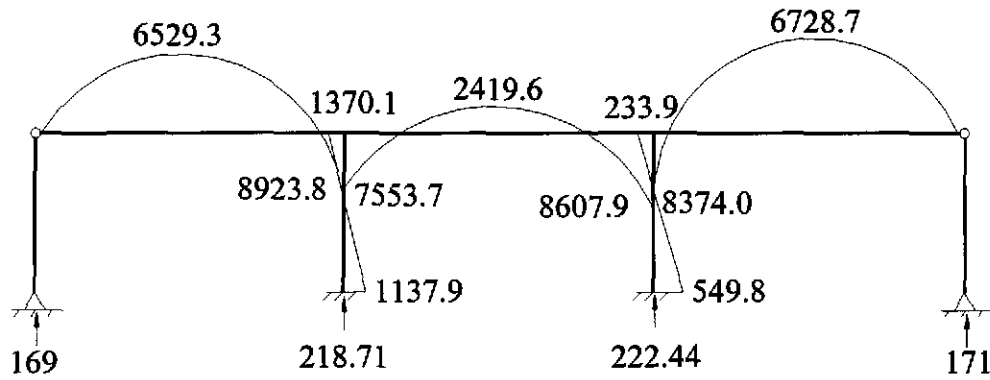


Figure 6.14 Member forces of the leaned column frame determined by using the DAM-NL method (unit: kip for force and kip-in for moment)

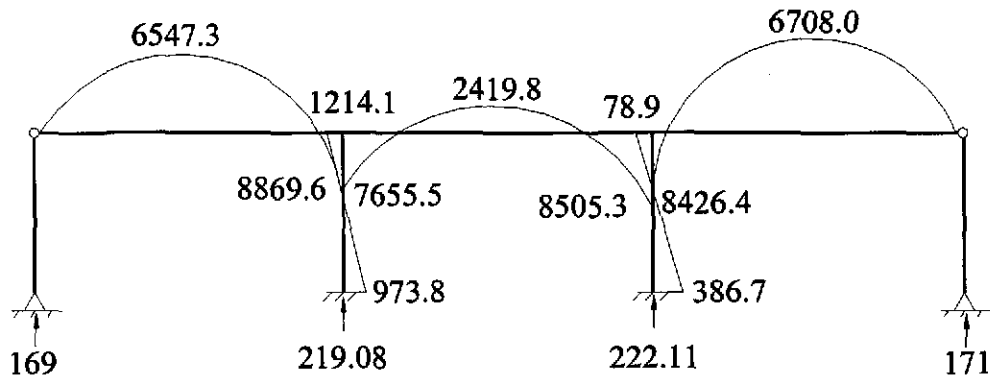


Figure 6.15 Member forces of the leaned column frame determined by using the DAM-MS method (unit: kip for force and kip-in for moment)

6.4.3 Advanced Analysis Method

The structural modeling of the low-rise industrial frame is shown in Figure 6.16. To accurately calculate the bending moments, each beam is modeled with ten elements. Both columns CD and EF are modeled as one frame element, while columns AB and GH are modeled as one truss element. In the explicit imperfection model, the initial geometric imperfection of 0.432 in. at the top of the structure is calculated by $L_c/500$. In the

equivalent notional load model, the notional load of 1.5624 kips results from 0.2% times the total gravity load of 781.2 kips and is combined with the lateral load. The PAAP program can automatically account for the effects of initial geometric imperfection if further reduced tangent modulus model is chosen. The incremental load is determined based on the scaling number of 50. All three models are shown in Figures 6.17a through 6.17c. The corresponding input data are shown in Table 6.7a through 6.7c.

The adequacy of the design can be checked from the analysis results shown in the output file P.OUT2. Both the explicit imperfection and further reduced tangent modulus model predict the same load-carrying capacity of 122.9 kips at the final stage with respect to the vertical load at node 1, while the equivalent notional load model predicts the load-carrying capacity of 122.8 kips. Since the applied vertical load at node 1 is 100.6 kips, preliminary design of the structural members is adequate.

6.4.4 Comparison of the Analysis/Design Results

For both the AISC-LRFD and direct analysis method, the interaction ratios at D of Beam BD are almost equal to unity. For the advanced analysis method, the overstrength factor corresponding to the formation of the first plastic hinge occurring at D of Beam BD equals 1.04. Therefore, all three methods predict the same design results if the load-carrying capacity at the first plastic hinge formed is chosen for the advanced analysis method. Because of redundancy of the structure, the column size may be reduced for the advanced analysis method if the load-carrying capacity at the ultimate state is adopted.

From the safety check of Column CD, the difference of the interaction ratios between the AISC-LRFD and direct analysis method is evident. This is because the direct analysis method does not consider the leaned column effects and the column axial capacity is overestimated.

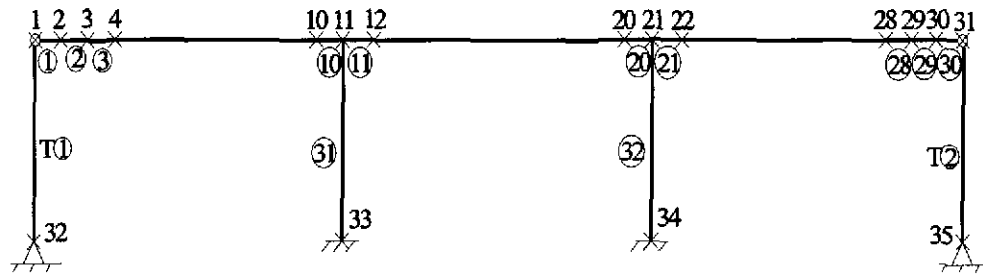
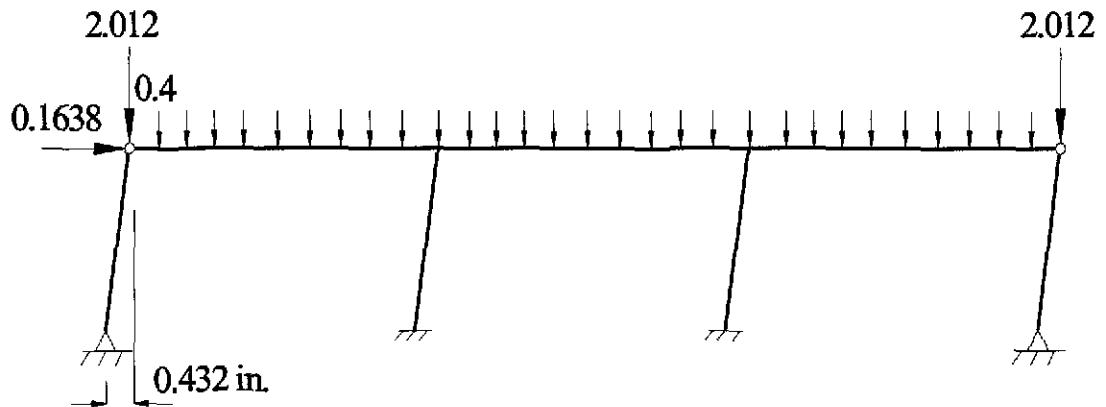
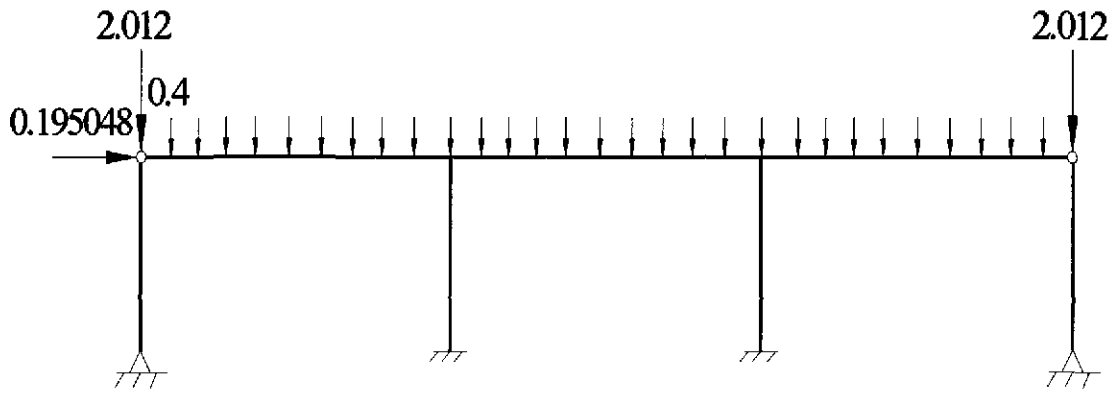


Figure 6.16 Structural modeling of the leaned column frame

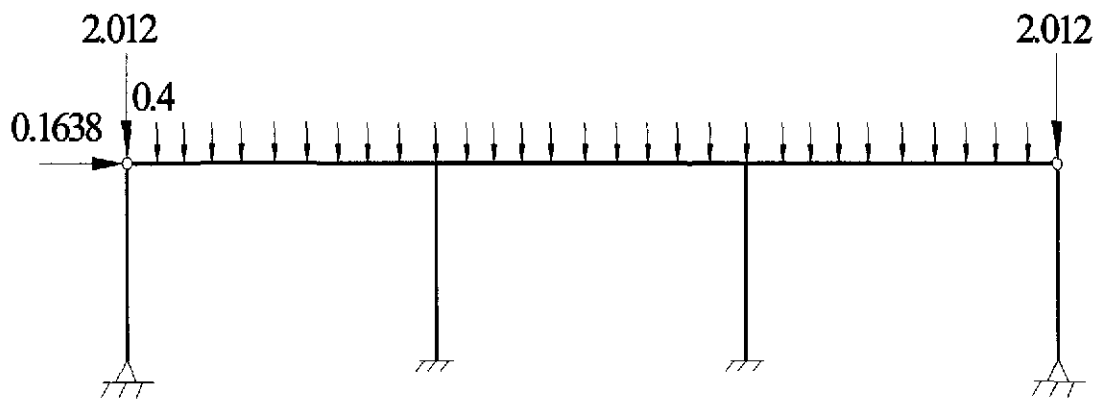


(a) Explicit imperfection model (unit: kip)

Figure 6.17 Analysis models of advanced analysis method for the leaned column frame



(b) Equivalent notional load model (unit: kip)



(c) Further reduced tangent modulus model (unit: kip)

Figure 6.17 Analysis models of advanced analysis method for the leaned column frame (cont.)

Table 6.7a Input data of the explicit imperfection modeling for the leaned column frame

Leaned column frame(AA-Explicit Imperfection)

1	1					
35	4	200				
0	2	1				
0	32	2				
1		22.4	2100.0	200.0	29000.0	50.0
2		14.4	272.0	60.4	29000.0	50.0
1		14.4	272.0	29000.0	50.0	
1		42.0	0.0	1	1	2 30
31		0.432	216.0	2	33	11
32		0.432	216.0	2	34	21
1		0.432	216.0	1	32	1
2		0.432	216.0	1	35	31
32	1	1	1			
33	1	1	1			
34	1	1	1			
35	1	1	1			
1		0.1638	-2.012			
2			-0.4		29	
31			-2.012			

Table 6.7b Input data of the equivalent notional load modeling for the leaned column frame

Leaned column frame(AA-Equivalent Notional Load)

2	1					
35	4	200				
0	2	1				
0	32	2				
1		22.4	2100.0	200.0	29000.0	50.0
2		14.4	272.0	60.4	29000.0	50.0
1		14.4	272.0	29000.0	50.0	
1		42.0	0.0	1	1	2 30
31		0.0	216.0	2	33	11
32		0.0	216.0	2	34	21
1		0.0	216.0	1	32	1
2		0.0	216.0	1	35	31
32	1	1	1			
33	1	1	1			
34	1	1	1			
35	1	1	1			
1		0.195048	-2.012			
2			-0.4		29	
31			-2.012			

Table 6.7c Input data of the further reduced tangent modulus modeling for the leaned column frame

Leaned column frame (AA-Further Reduced Tangent Modulus)

3	1						
35	4	200					
0	2	1					
0	32	2					
1		22.4	2100.0	200.0	29000.0	50.0	
2		14.4	272.0	60.4	29000.0	50.0	1
1		14.4	272.0	29000.0	50.0	1	
1		42.0	0.0	1	1	2	30
31		0.0	216.0	2	33	11	
32		0.0	216.0	2	34	21	
1		0.0	216.0	1	32	1	
2		0.0	216.0	1	35	31	
32	1	1	1				
33	1	1	1				
34	1	1	1				
35	1	1	1				
1		0.1638	-2.012				
2			-0.4		29		
31			-2.012				

6.5 Summary

Three special examples are presented in this chapter. In Section 6.2, the six-story frame example indicates that higher structural resistance could be obtained for highly redundant structures due to the benefits of the inelastic moment redistribution. From the analysis and design of the braced steel frame in Section 6.3, it shows that the use of the direct analysis method is more complex than that of the conventional AISC-LRFD method. For the advanced analysis method, the further reduced tangent modulus model is more convenient than the other two because of the difficulties of determining the directions of initial geometric imperfections and notional loads. From the example in Section 6.4, it is evident that great care is needed when determining the axial capacities

of rigid columns in a leaned column frame for both AISC-LRFD and direct analysis methods.

From all three examples in this chapter, implementation of the advanced analysis method is much more simple than the others. Determination of the effective length factors and individual member capacity checks can be eliminated. Using the load-carrying capacity corresponding to the formation of the first plastic hinge results in the same member sizes as the AISC-LRFD method, while using the load-carrying capacity corresponding to the ultimate state leads to more economical design results.

CHAPTER 7

PERFORMANCE-BASED DESIGN

7.1 Introduction

The service operational and ultimate strength limit states are usually adopted in conventional steel design approaches, while the performance-based design is a multi-level design approach. Performance-based design refers to the design method in which a set of performance objectives is used to express the structural design criteria. Performance objectives are statements describing the expected performance of a structure. The performance can be measured by using analytical results such as drift ratios or strength and ductility demand on individual elements. When subjected to fire or earthquake, structures could be designed by performance-based design involving the benefits of more opportunities for innovation, better levels of safety, and greater cost effectiveness in construction.

Performance-based fire resistance and seismic design cases are considered in this chapter. In Section 7.2, the analysis procedures for determining the duration that the structure could last under elevated temperature are proposed. Although the advanced analysis program was not originally developed for fire resistance design, the desired purpose can be achieved by a trial and error process. The failure mode of the steel frame under fire can also be determined by advanced analysis. It will be shown that the failure

modes of a steel frame with or without the effects of fire are quite different. A multi-story steel frame which is similar to the six-story frame is used as an example in this section.

In Section 7.3, performance-based seismic design using advanced analysis is considered. Although earthquake force is dynamic, ASCE 7-98 equivalent static force procedures are followed. The Federal Emergency Management Agency FEMA 273 document [38] defines a set of performance levels and objectives and proposes drift limits for lateral load resisting steel structures at different performance levels. These criteria will be adopted in this study. A one-bay two-story steel frame is chosen as an example for simplicity. Performance curves of the frame can be easily obtained by an iteration process when advanced analysis is used. The roof drift of the building can be determined and the corresponding performance level can also be identified if a particular magnitude of earthquake is specified.

7.2 Fire Resistance Design

After the event at the World Trade Center in New York on September 11, 2001, the performance-based fire resistance design has attracted many structural engineers. The twin towers remained standing for a considerable length of time after the initial impact, in one case for as much as an hour and a half, despite massive explosions and a raging fire in which the temperature was likely to have reached upwards of 2500 °F. The structure's *inherent strength and resilience created an interval between impact and collapse that provided many occupants the chance to escape.* However, there are many occupants who did not escape in time and more than two hundred firemen lost their lives in this event.

Therefore, it is an important issue for performance-based design to confirm the period of structural safety for a steel building under fire. In this section, the advanced analysis method is used to predict the length of time between a structure's initial introduction to fire and collapse.

7.2.1 Overview

Fire resistance refers to the ability of a structure assembly to withstand the effects of fire. Mechanical material properties including the modulus of elasticity, yield strength, and tensile strength are temperature dependent. For structural steel, the variation in these material properties under fire are given by the AISC-LRFD manual [1] and shown in Figures 7.1a to 7.1c. Based on the research of Talamona *et al.* [39], the most important factor that affects the structural behavior under fire is the effective value of yield stress. In general, structural steel will lose part of its strength and stiffness at elevated temperature. As a result, the structure under high temperature may collapse or lose its stability at the same load level that the structure would be safe if no fire was introduced.

Conventionally, fire resistance design of steel structures is typically conducted by testing its critical member heated in a standard fire, which is provided by fire design codes such as ASTM E119. The standard fire curve defined in the ASTM E119 [40] is shown in Figure 7.2. The time-temperature curve is achieved by controlling the rate of fuel supply or fire loading. However, it has been found that a steel member in a structural system subjected to a natural or real fire performs much better than if subjected to a standard fire [41]. The intensity and duration of a natural fire in a building compartment

are governed by many factors such as the amount of combustible materials, the area of windows and doors, and the thermal characteristics of the structural members. Moreover, it is recognized that the use of sprinkler systems will reduce the intensity of fire and a reduction factor should be applied to the time-temperature relations of a natural fire.

The effect of ventilation and rate of fuel supply on temperature severity in a natural fire is shown in Figure 7.3 for a typical office with a ventilation area of 50 percent of one wall [42]. While the standard fire is based on a continuous supply of fuel, the fuel supply of a natural fire is exhaustible. Hence, instead of the temperature continuously increasing such as in a standard fire, it can be seen that the natural fire has three phases of combustion: the growth phase, the fully developed phase, and the cooling phase. In addition, the temperature of the natural fire is lower and the duration is shorter for this well-ventilated case. Although the natural fire curve represents the real time-temperature relations of a structure under fire, it varies greatly for different fire events and structures. Therefore, it is difficult to derive the appropriate natural fire curves in practical fire resistance design of steel structures.

A number of full-scale fire tests were conducted by the Building Research Establishment, U.K. in 1995 and 1996. The results of these tests show that the design of steel frame under fire based on single element behavior does not give a realistic frame behavior [43]. The tested steel frames were subjected to compartment fires. Because some members are heated, while the others remain cool, force redistribution occurred due to the change of strength and stiffness of those heated members. Heat transmission will also affect temperatures in unexposed members of a structure and their structural

behavior. In general, the fire resistance design of a steel frame based on current fire codes is quite conservative.

In the performance-based design for fire resistance, it is an important issue to predict the time that the steel frame would not collapse under severe fire. The delay of the collapse of the building, especially for high-rise buildings, means more occupants and firefighters would have a better chance to escape. Since the advanced analysis is a structure-based approach, it can predict the failure modes corresponding to possible loading conditions including fire. If time-temperature relation is specified, the temperature and time that is needed for the collapse of the building can be predicted. The predictions should be made for the performance-based design of a tall building. It could also be made for existing buildings and stored in fire department computers for firemen to make strategic decisions while fire fighting.

7.2.2 Basic Assumptions

The main focus of Section 7.2 is on application of the advanced analysis described in Chapter 5 for the prediction of the duration that a steel frame subjected to an elevated temperature would lose its stability. The following assumptions are employed for this application.

1. Uniform heating along the members and across the sections is assumed.
2. Steel members are adequately restrained to prevent out-of-plane deformation.
3. Plastic hinges occur at element ends only.
4. Connections are considered as rigid.

5. When a section is at an elevated temperature, the residual stress would be gradually relieved. The residual stress is a function of temperature [44] and its pattern may change due to thermal effects [45]. In this section, the ratio of the tangent modulus, which accounts for the effects of residual stresses, to the effective modulus of elasticity at elevated temperatures is assumed to follow equations (4.24a) and (4.24b).
6. The study assumes that the heating rate and history will not affect the structural behavior. In other words, the behavior of a steel frame at a temperature is considered as independent of the one at other temperature. This assumption can be illustrated in *Figure 7.4*.
7. Fireproofing and sprinkler system are not considered.
8. Since natural fire may not cause the collapse of the building, standard fire provided by ASTM E119 is used.

7.2.3 Verification

The numerical results of simply supported beams and steel frames determined by the advanced analysis method proposed in chapter five are verified by comparing with the experimental results reported by Rubert and Schaumann [46]. Conducted by Chan and Chan [47], the numerical results of the same structures determined by using the modified non-linear finite element program, GMNAF, are also compared with the results of the present method.

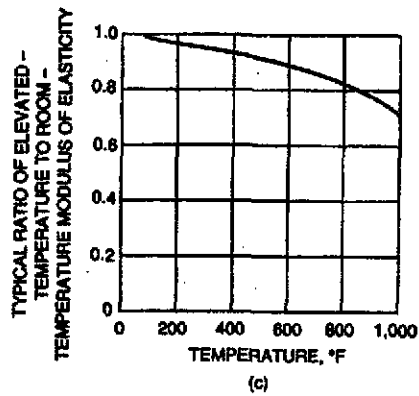
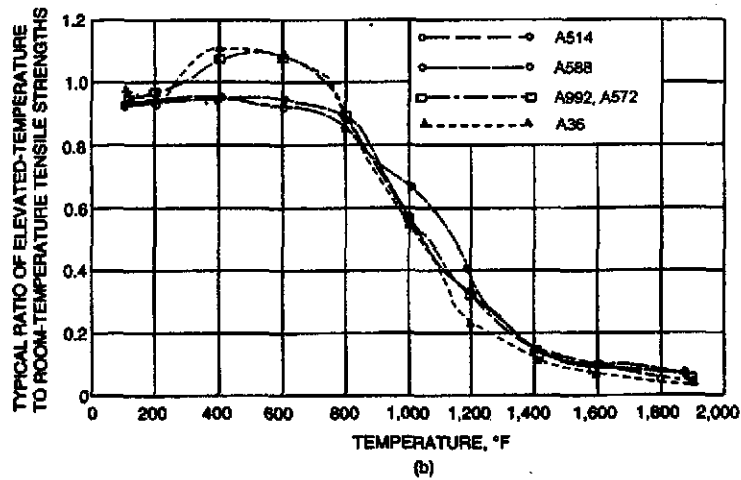
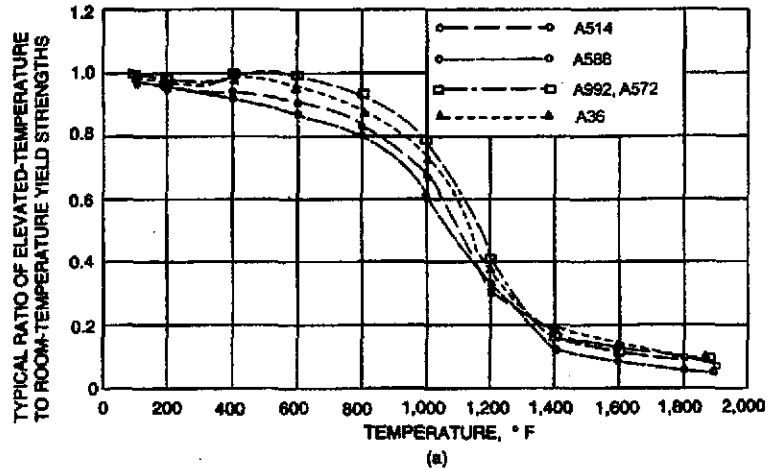


Figure 7.1 Effect of temperature on yield strength, tensile strength, and modulus of elasticity of structural steel (from Fig.2-8, AISC-LRFD, 1999)

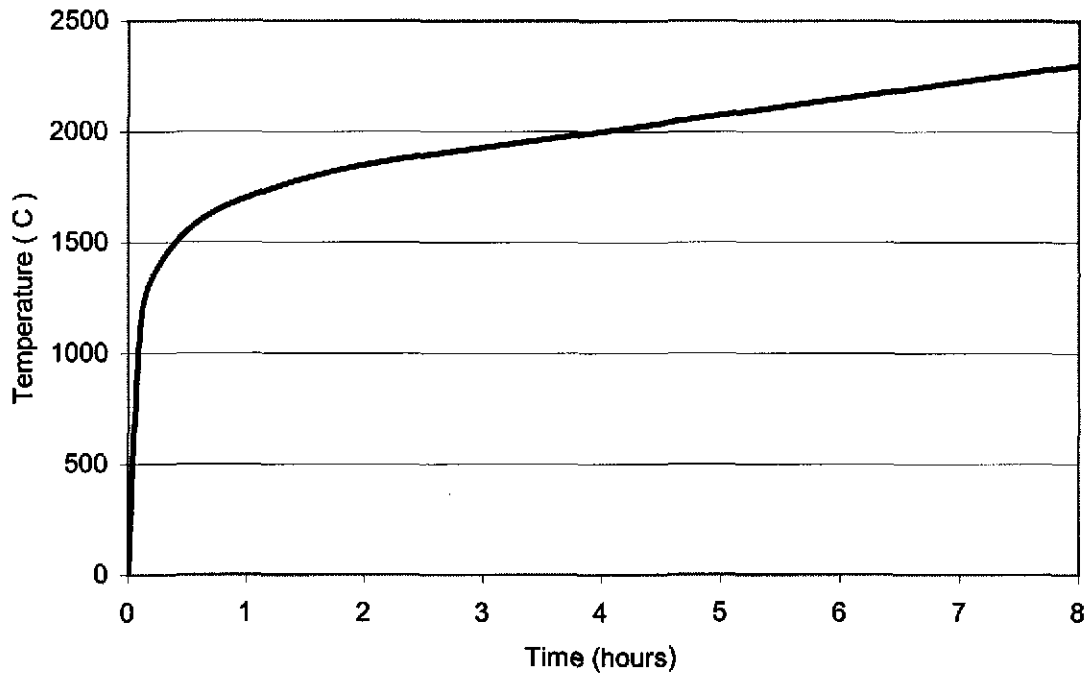


Figure 7.2 Time-temperature curve of standard fire

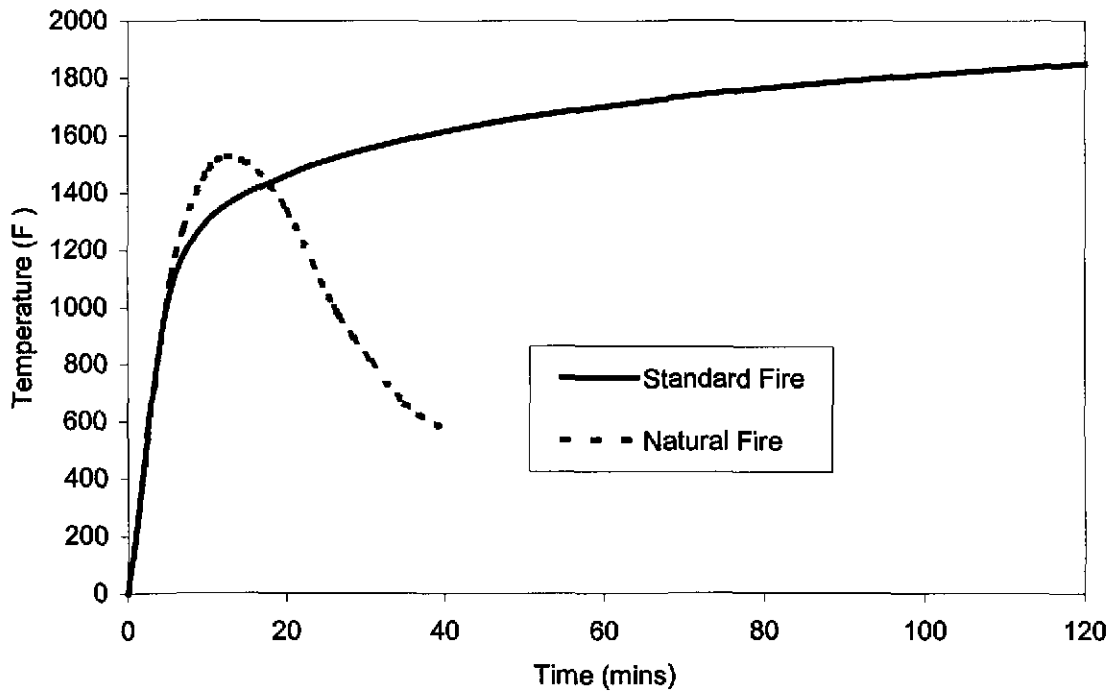


Figure 7.3 Influence of natural ventilation on fire severity

Due to the degradation of mechanical properties at elevated temperature, the sectional strength and stiffness of members are reduced. The temperature-dependent mechanical properties, the effective yield stress, $F_{y\theta}$, and the effective modulus of elasticity, E_θ , used in the research of Chan and Chan are tabulated in Table 7.1 and plotted in Figure 7.5. [47]. In Table 7.1, θ is the considered temperature. F_{y20} and E_{20} are respectively the values of yield stress and modulus of elasticity at the temperature of 20°C.

7.2.3.1 Simply Supported Beams

The configuration of the tested simply supported beams is shown in Figure 7.6. In these tests, the beams are subjected to a concentrated load at mid-span and heated uniformly along the entire length of the member. The temperature at which beams fail for four different ratios of F_c/F_u , in which F_c and F_u are respectively the applied and ultimate concentrated loads, are evaluated. The modulus of elasticity, E_{20} , is selected as 210×10^3 N/mm² and the yield stress F_{y20} are selected corresponding to different F_c/F_u ratios. The area A , moment of inertia about strong axis I_x , and plastic modulus about strong axis Z_x of the beam section IPE 80 are 764 mm², 801400 mm⁴, and 23220 mm³, respectively. The numerical results determined by using advanced analysis are tabulated in Table 7.2. It can be seen that the results compare very well with the experimental results reported by Rubert and Schaumann [46] and the numerical results determined by Chan and Chan [47].

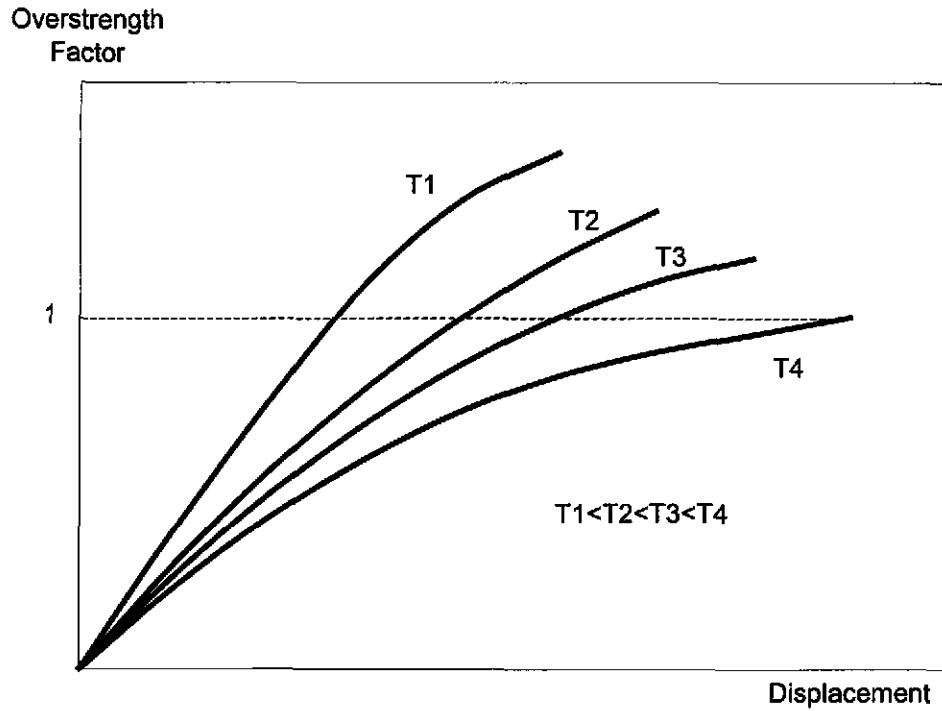


Figure 7.4 Strategy of the advanced analysis method for fire resistance design

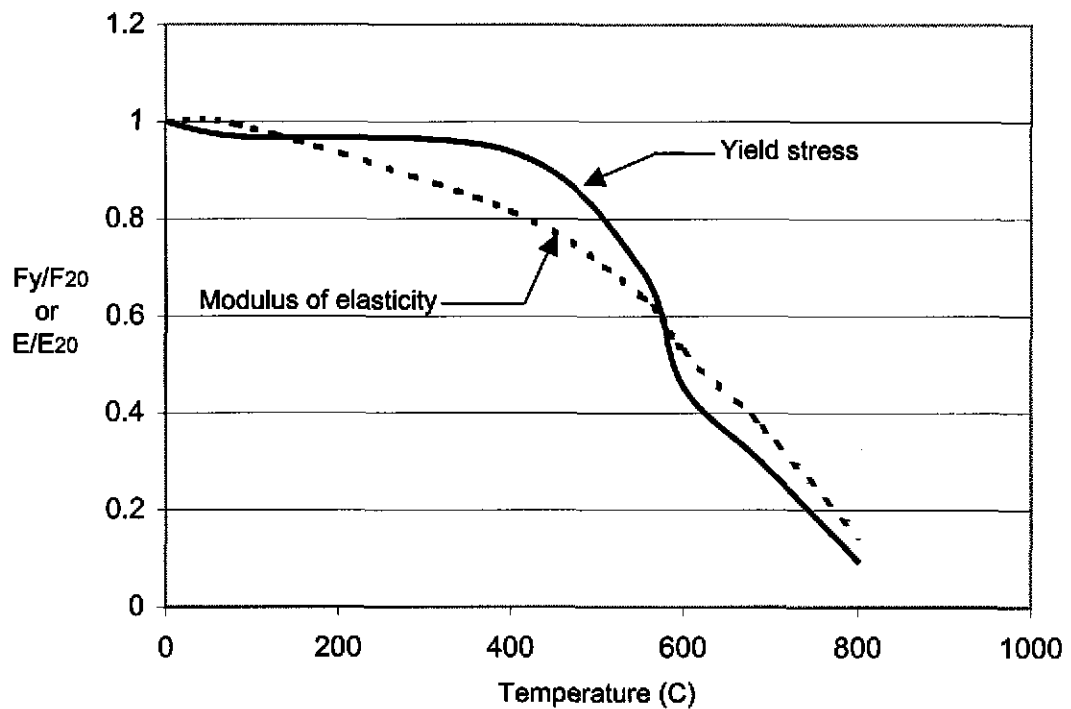


Figure 7.5 Effective yield stress and modulus of elasticity under elevated temperature

Table 7.1 Mathematical expressions of yield stress and modulus of elasticity at elevated temperature

Temperature range (°C)	Yield stress $f_{y\theta}$	Modulus of elasticity E_{θ}
$80 < \theta \leq 400$	$f_{y20} \left(0.978 - 0.034 \frac{\theta}{350} \right)$	$E_{20} \left[1 - 2.8 \left(\frac{\theta - 20}{1485} \right)^2 \right]$
$400 < \theta \leq 550$	$f_{y20} \left(1.553 - 0.155 \frac{\theta}{100} \right)$	$E_{20} \left[1 - 2.8 \left(\frac{\theta - 20}{1485} \right)^2 \right]$
$550 < \theta \leq 600$	$f_{y20} \left(2.34 - 0.22 \frac{\theta}{70} \right)$	$E_{20} \left[1 - 3.0 \left(\frac{\theta - 20}{1463} \right)^2 \right]$
$600 < \theta \leq 690$	$f_{y20} \left(1.374 - 0.078 \frac{\theta}{50} \right)$	$E_{20} \left[1 - 3.0 \left(\frac{\theta - 20}{1463} \right)^2 \right]$
$690 < \theta \leq 800$	$f_{y20} \left(1.12 - 0.128 \frac{\theta}{100} \right)$	$E_{20} \left[1 - 3.0 \left(\frac{\theta - 20}{1463} \right)^2 \right]$

7.2.3.2 Steel Frames

Figures 7.7a to 7.7c show the tested steel frames, which involve three types of geometry. Systems EHR are inverted L-shaped frames and systems EGR are single-bay portal frames. These two types of frames are completely and uniformly heated except that the beams of systems EGR7 and EGR8 remain at room temperature during the fire tests. The double-bay portal frames ZSR are heated on their left bays only. The geometrical properties and measured yield stresses of these frames are shown in Table 7.3. All sections are IPE80 I-shape. The modulus of elasticity at ambient temperature is 210×10^6 N/mm². Out-of-plane deformation is prohibited. Since the measured initial geometric imperfections of frame columns are small [46], they are waived in the analysis procedures.

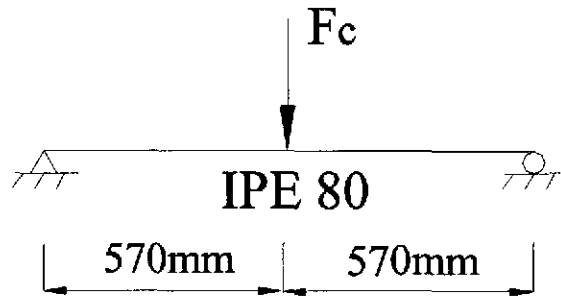
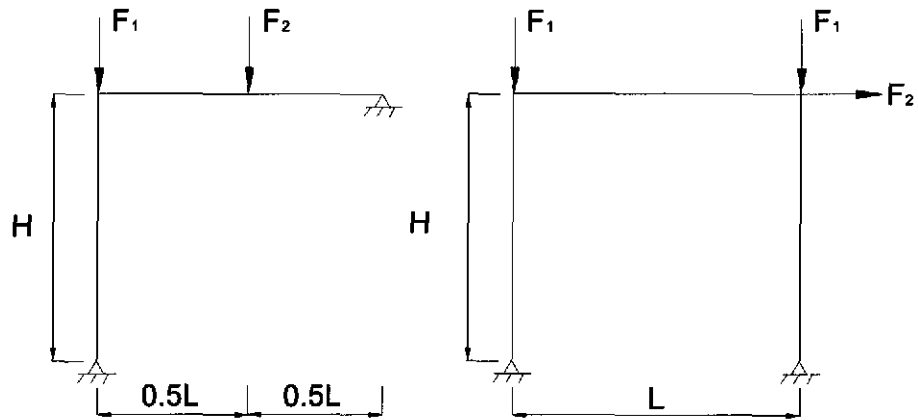
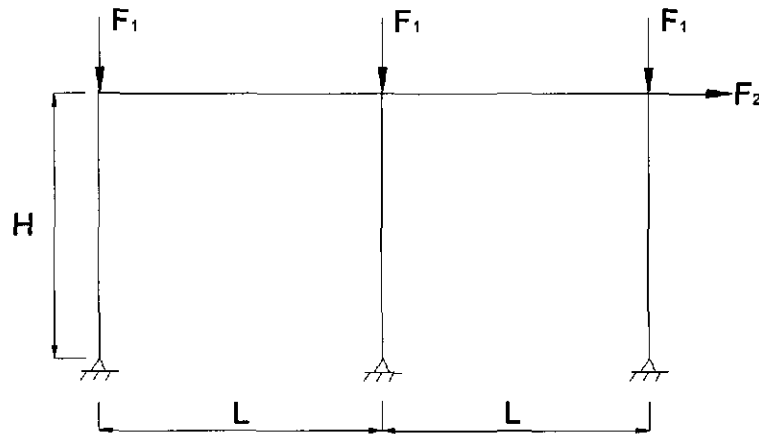


Figure 7.6 Configuration of the simply supported beam for fire tests



(a) EHR

(b) EGR



(c) ZSR

Figure 7.7 Configuration of the steel frames for fire tests

Table 7.2 Critical temperatures of the simply supported beam in fire

System	Test (°C)	SL Chan (°C)	A.A (°C)	Diff1=SL/Test	Diff2=AA/Test
Fc=0.20Fu	740	710	721	0.9595	0.9743
Fc=0.50Fu	605	585	587	0.9669	0.9702
Fc=0.70Fu	545	545	550	1.0000	1.0090
Fc=0.85Fu	520	455	453	0.8750	0.8712

Table 7.3 Test data of the steel frames

System	L (cm)	H (cm)	f_{y20} (N/mm ²)	F1 (kN)	F2 (kN)	Remark
EHR1	119	117	395	56	14	• Systems EHR1 to EHR3 are fully heated and bent about strong axis.
EHR2	124	117	395	84	21	
EHR3	124	117	382	112	28	
EHR4	125	150	389	20	5	• Systems EHR4 to EHR6 are fully heated and bent about weak axis.
EHR5	125	150	389	24	6	
EHR6	125	150	389	27	6.7	
EGR1b	122	117	382	65	2.5	• Systems EGR1 to EGR6 are fully heated and bent about strong axis.
EGR1c	122	117	382	65	2.5	
EGR2	122	117	385	40	1.6	
EGR3	122	117	385	77	3	• Systems EGR7 and EGR8 are partly heated on columns and bent about strong axis; Beams remain at ambient temperature.
EGR4	122	117	412	77	3	
EGR5	122	117	412	88	3.4	
EGR6	122	117	412	88	3.4	
EGR7	122	117	320	68.5	2.6	
EGR8	122	117	385	77	3	
ZSR1	120	118	355	74	2.85	• All three systems are partly heated on left bay and bent about strong axis.
ZSR2	120	118	380	84.5	3.25	
ZSR3	120	118	432	68.5	2.64	

Table 7.4 Critical temperatures of the tested frames in fire

System	Test (°C)	SL Chan (°C)	Diff1=SL/Test	A.A (°C)	Diff2=AA/Test
EHR1	600	626	1.0433	643	1.0717
EHR2	530	559	1.0547	562	1.0604
EHR3	475	475	1.0000	490	1.0316
EHR4	562	529	0.9413	589	1.0480
EHR5	460	450	0.9783	555	1.2065
EHR6	523	374	0.7151	550	1.0516
EGR1b	533	476	0.8931	538	1.0094
EGR1c	515	476	0.9243	538	1.0447
EGR2	612	580	0.9477	653	1.0670
EGR3	388	425	1.0954	465	1.1985
EGR4	424	435	1.0259	480	1.1321
EGR5	335	400	1.1940	395	1.1791
EGR6	350	400	1.1429	395	1.1286
EGR7	454	466	1.0264	505	1.1123
EGR8	464	455	0.9806	490	1.0560
ZSR1	547	504	0.9214	560	1.0238
ZSR2	479	469	0.9791	550	1.1482
ZSR3	574	577	1.0052	619	1.0784

* Results predicted by Chan and Chan using eight elements per beam and column

The temperatures at the time collapse of the tested frames are predicted by using advanced analysis method and are summarized in Table 7.4. For comparison, the experimental results reported by Rubert and Schaumann [46] and the numerical results determined by Chan and Chan [47] are also listed in the same table. Except systems

EGR3 and EGR5, the critical temperatures of all other systems can be predicted well by using the advanced analysis method.

7.2.4 Analysis Procedures

In the analysis, the behavior of a structure subjected to fire should be based on the deformed configuration of the structure under service loads. Although the loading on the structure may vary during fire because of variables, such as escaping occupants and other factors, the specified ultimate loads are used in the analysis. The procedures predicting the critical temperature using the advanced analysis method are summarized in the flow chart shown in Figure 7.8 and outlined as follows:

1. Perform an elastic analysis for the structure under service loads and determine the deformed configuration.
2. Estimate the critical temperature and determine the effective yield stress and modulus of elasticity corresponding to the estimated temperature.
3. Implement the advanced analysis to the deformed structure under factored loads. Effective yield stress and modulus of elasticity should be applied to those members exposed to fire.
4. Determine the overstrength factor from the results of the advanced analysis method.
5. If the overstrength factor is greater than one, reduce the estimated temperature. On the other hand, if the overstrength factor is less than one, increase the estimated temperature.

6. Repeat steps 2 to 5 until the overstrength factor equals one. Then the temperature that leads the structure to collapse is obtained.
7. The collapse time corresponding to the critical temperature can be identified from the specified time-temperature curve.

7.2.5 Multi-Story Frame Example

Because of its high redundancy, the multi-story steel frame shown in Figure 7.9 is chosen as an example for predicting the duration of the building under fire. It will be seen clearly that the structural behavior is changed due to where the fire is burning in the structure. Those members subjected to elevated temperatures in the multi-story steel frame are marked and shown in Figure 7.9. The sectional properties of the members of the frame are listed in Table 7.5. The lateral service wind loads are 10.22 kN at each floor level and 5.115 kN at the roof level, while the gravity roof service dead and live loads are respectively 0.16 kN/cm and 0.1232 kN/cm and the gravity service dead and live loads on each floor are 0.16 kN/cm and 0.4016 kN/cm, respectively.

Before considering the effects of the fire on specified members, the deformed shape of the steel frame due to the application of external service loads must be determined. To do this, a first-order elastic analysis is implemented and the results are shown in Figure 7.10. In Figure 7.10, there are two numbers for each element. For each column, the first number represents the relative displacement of its two ends in horizontal direction, while the second number shows the magnitude of shortening (negative) of the column. For each beam element, the first number represents the magnitude of shortening (negative) or

elongation (positive) of the element and the second number is the relative displacement of its two ends in the vertical direction. Note that the relative displacements are positive when their projections in the global x - y coordinate are positive and vice versa.

In the advanced analysis method, the further reduced tangent modulus approach is used in this example. Each column is modeled with one element and each beam is modeled with two. The deformed structure is obtained by changing the horizontal and vertical projected length for each element in the input data file shown in Table 7.6. The yield stress and modulus of elasticity of those elements subjected to fire are varied based on the temperature-yield stress and temperature-modulus of elasticity relation shown in Figures 7.1a and 7.1c, respectively. After executing the advanced analysis program and several trial and error processes, the yield stress and modulus of elasticity of those members subjected to fire corresponding to the overstrength factor being equal to one can be determined as 3.5955 kN/cm^2 and 7175 kN/cm^2 , respectively, and the critical temperature is 1570°F . The period before the collapse of the frame structure is about 34 minutes if the elevated time-temperature relation shown in Figure 7.2 is applied.

Figure 7.11 shows the failure mode of the steel frame under fire, while the failure mode of the structure without the effects of fire is shown in Figure 7.12. It can be seen that the order of formation of plastic hinges and their locations are different because those specified members subjected to fire become weaker.

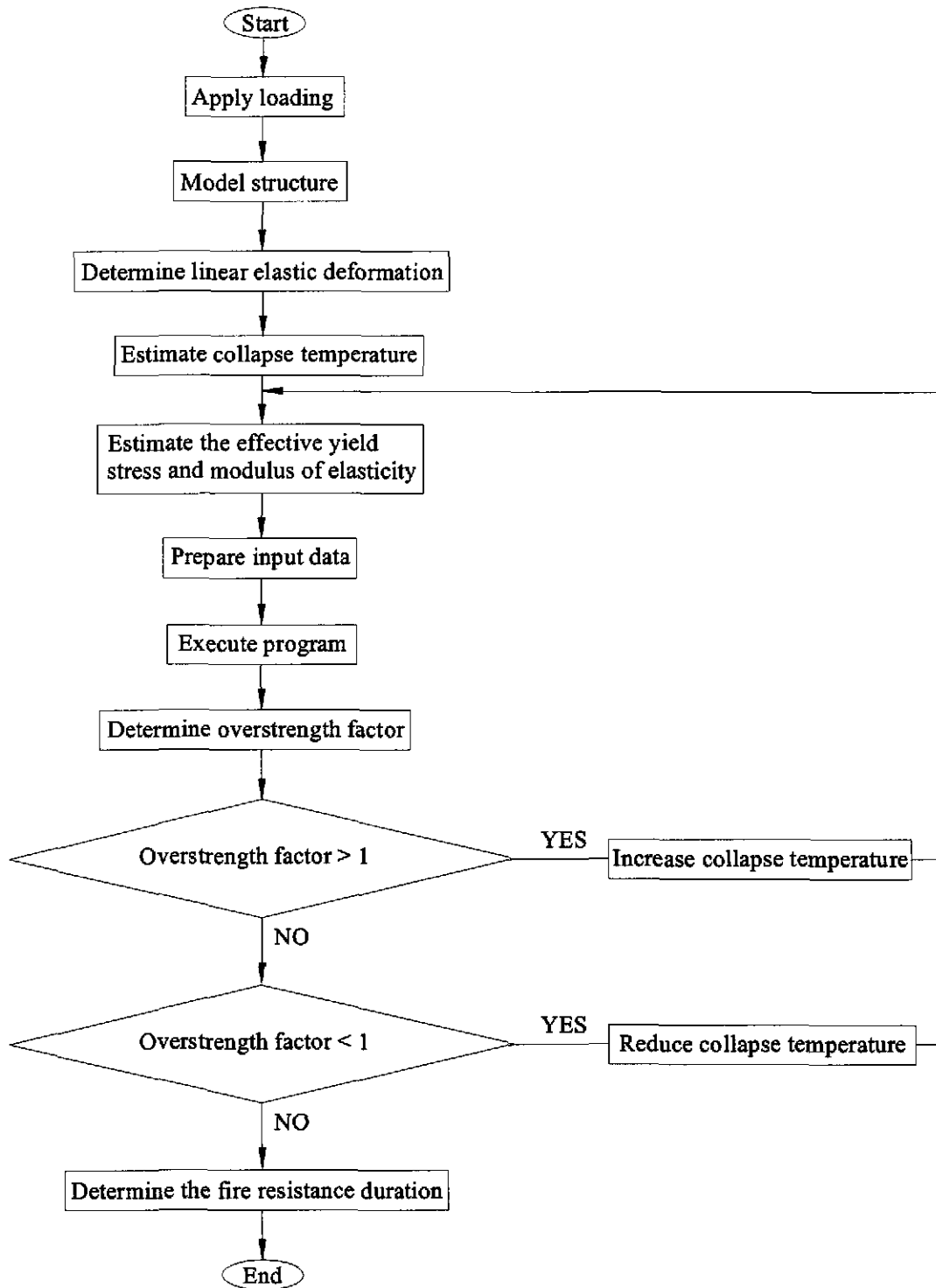
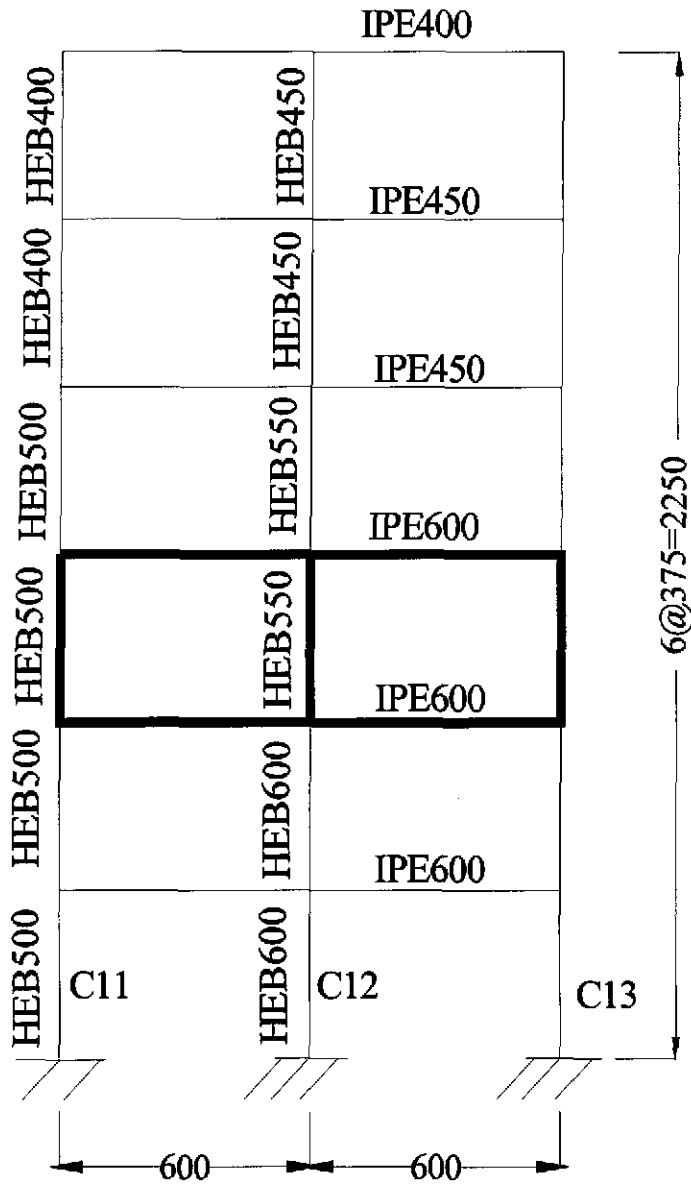


Figure 7.8 Analysis procedure for the determination of fire resistance duration of steel structures



Service Loading:
 Wind:
 Floor Levels: 10.22 kN
 Roof Level: 5.115 kN
 Gravity:
 Floor Levels:
 Dead: 0.16 kN/cm
 Live: 0.4016 kN/cm
 Roof Level:
 Dead: 0.16kN/cm
 Live: 0.1232 kN/cm
 $F_y = 23.5 \text{ kN/cm}^2$
 $E = 20500 \text{ kN/cm}^2$

Figure 7.9 Configuration and load condition of the multi-story frame under fire

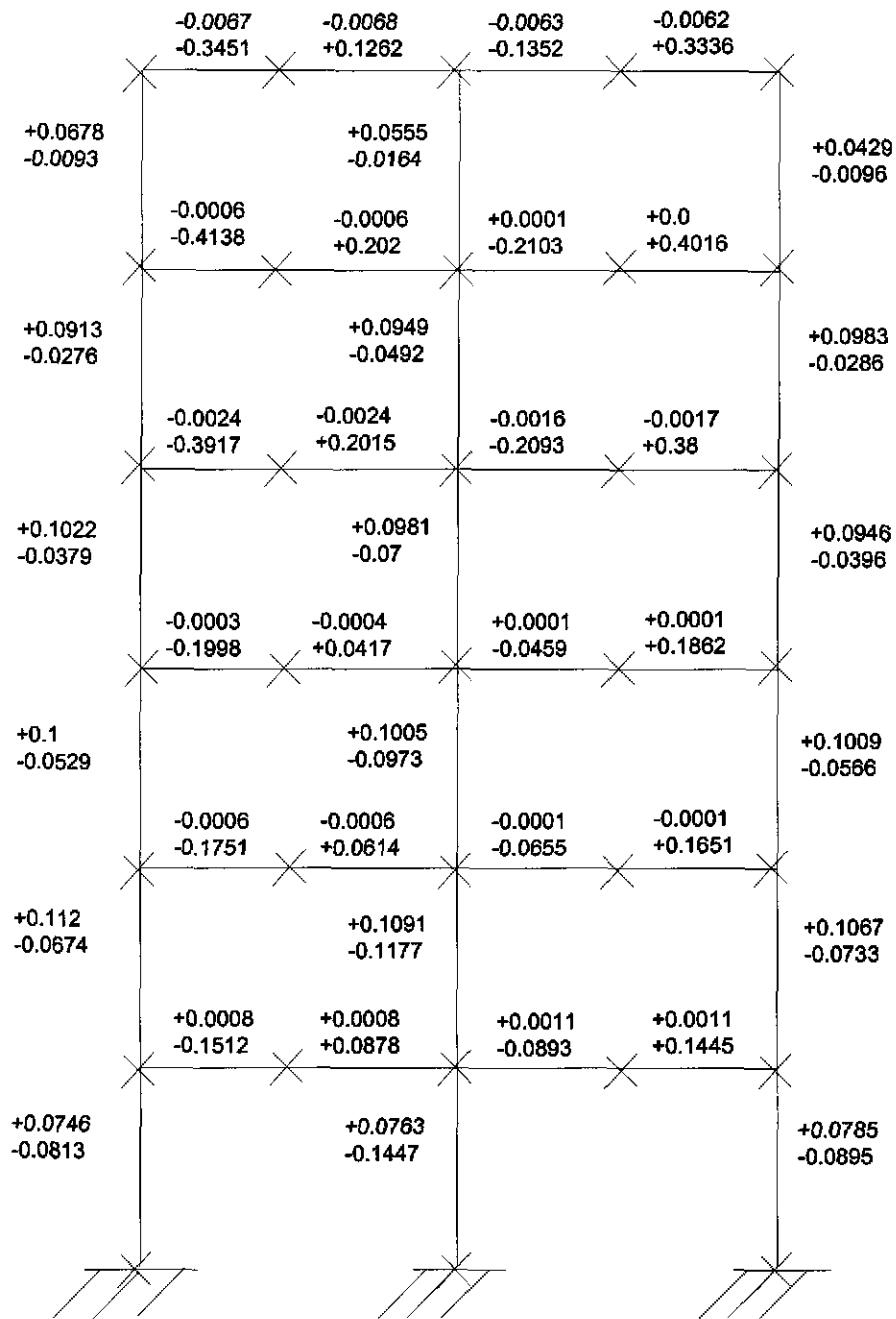


Figure 7.10 Deformation data of the multi-story frame determined by using a first-order analysis (Unit: cm)

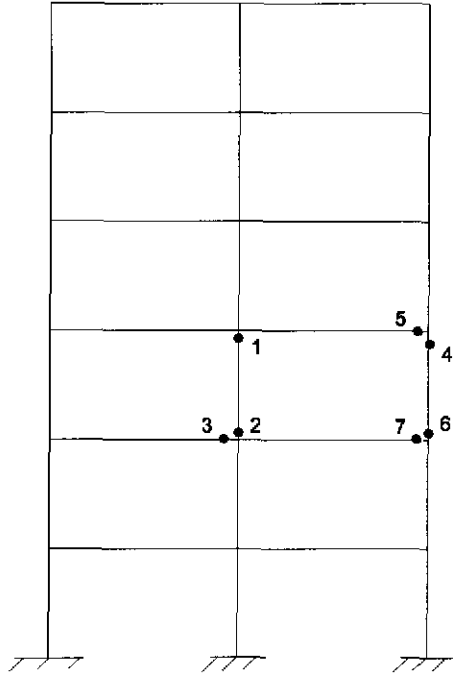


Figure 7.11 Failure mode of the multi-story frame under fire

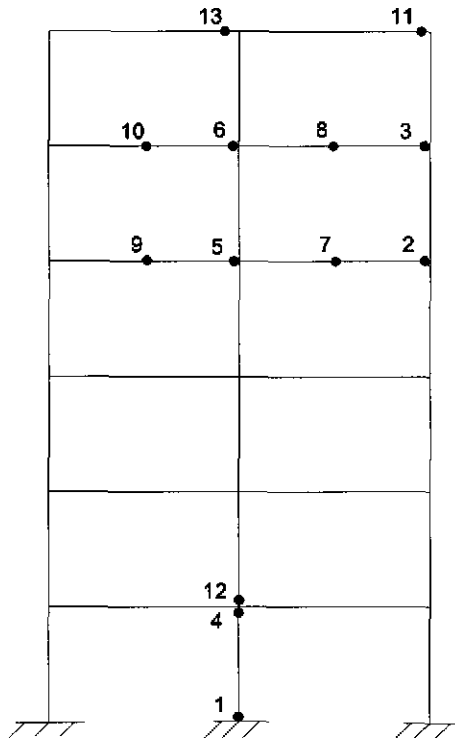


Figure 7.12 Failure mode of the multi-story frame without fire

Table 7.5 Sectional properties of the members of the multi-story steel frame

Section	A (cm ²)	I _x (cm ⁴)	Z _x (cm ³)
IPE 400	84.46	23130	1307
IPE 450	98.82	33740	1702
IPE 600	156.0	92080	3512
HEB 400	197.8	57680	3232
HEB 450	218.0	79890	3982
HEB 500	238.6	107200	4815
HEB 550	254.1	136700	5591
HEB 600	270.0	171000	6425

Table 7.6 Input data of the multi-story steel frame

Multi-story steel frame under fire (Further reduced modulus method)

3	1					
33	3	300				
0	11	0				
0	42	0				
1	84.46	23130.0	1307.0	20500.0	23.5	
2	98.82	33740.0	1702.0	20500.0	23.5	
3	156.0	92080.0	3512.0	7175.0	3.5955	
4	156.0	92080.0	3512.0	20500.0	23.5	
5	197.8	57680.0	3232.0	20500.0	23.5	1
6	218.0	79890.0	3982.0	20500.0	23.5	1
7	238.6	107200.0	4815.0	20500.0	23.5	1
8	254.1	136700.0	5591.0	20500.0	23.5	1
9	270.0	171000.0	6425.0	20500.0	23.5	1
10	238.6	107200.0	4815.0	7175.0	3.5955	1
11	254.1	136700.0	5591.0	7175.0	3.5955	1
1	0.0	375.0	7	1	2	
2	0.0	375.0	7	2	3	
3	0.0	375.0	10	3	4	
4	0.0	375.0	7	4	5	
5	0.0	375.0	5	5	6	
6	0.0	375.0	5	6	7	
7	0.0	375.0	9	8	9	
8	0.0	375.0	9	9	10	
9	0.0	375.0	11	10	11	
10	0.0	375.0	8	11	12	
11	0.0	375.0	6	12	13	
12	0.0	375.0	6	13	14	
13	0.0	375.0	7	15	16	
14	0.0	375.0	7	16	17	
15	0.0	375.0	10	17	18	
16	0.0	375.0	7	18	19	
17	0.0	375.0	5	19	20	

Table 7.6 Input data of the multi-story steel frame (cont.)

18	0.0	375.0	5	20	21
19	300.0	0.0	4	2	22
20	300.0	0.0	3	3	23
21	300.0	0.0	3	4	24
22	300.0	0.0	2	5	25
23	300.0	0.0	2	6	26
24	300.0	0.0	1	7	27
25	300.0	0.0	4	22	9
26	300.0	0.0	3	23	10
27	300.0	0.0	3	24	11
28	300.0	0.0	2	25	12
29	300.0	0.0	2	26	13
30	300.0	0.0	1	27	14
31	300.0	0.0	4	9	28
32	300.0	0.0	3	10	29
33	300.0	0.0	3	11	30
34	300.0	0.0	2	12	31
35	300.0	0.0	2	13	32
36	300.0	0.0	1	14	33
37	300.0	0.0	4	28	16
38	300.0	0.0	3	29	17
39	300.0	0.0	3	30	18
40	300.0	0.0	2	31	19
41	300.0	0.0	2	32	20
42	300.0	0.0	1	33	21
1	1	1	1		
8	1	1	1		
15	1	1	1		
2	0.32704	-1.1784			5
7	0.16368	-0.7608			
9		-2.3568			5
14		-1.5216			
16		-1.1784			5
21		-0.7608			
22		-2.3568			5
27		-1.5216			
28		-2.3568			5
33		-1.5216			

7.3 Seismic Design

Although many buildings designed by the conventional design codes performed well during the recent high magnitude earthquakes in Northridge (1994), Kobe (1995), and Taiwan (1999) in relation to life safety, the level of damage to structures and the cost of

repair were unexpectedly high. To maintain the life safety of a structure and to reduce the cost of repair of damaged structures, performance-based design that specified different levels of performance objectives should be considered. In advanced analysis, the structure is loaded with a predetermined lateral load pattern and is pushed statically. The corresponding deflection can be determined and compared to the target displacement at which performance of the structure is evaluated. In seismic design, the advanced analysis can provide much needed structural information with regards to failure mechanism, locations and sequence of formation of plastic hinges, overstrength factor, and excessive deformation demands. Therefore, the advanced analysis can be readily adapted to perform the performance-based seismic design of steel structures.

7.3.1 Overview

In this section, the ASCE 7-98 [32] and AISC-LRFD 1999 seismic provisions [48] are reviewed. The ASCE 7-98 procedures are followed throughout this section because the prescribed forces are at the strength level which are consistent with the AISC-LRFD design. Since the provisions are briefly summarized here, detailed specifications should be referenced from the applicable codes if necessary.

7.3.1.1 Seismic Base Shear

The seismic base shear in a given direction is determined in accordance with the following equation:

$$V=C_s W \tag{7.1}$$

where

W = total dead load and applicable portions of other loads listed in Section 9.5.3.2, ASCE

7-98

C_s = seismic response coefficient determined as below

$$0.044IS_{DS} \leq C_s = \frac{S_{DS}}{R/I} \leq \frac{S_{D1}}{T(R/I)}$$

where

I = occupancy importance factor as in Table 7.7

R = response modification factor as in Table 9.5.2.2, ASCE 7-98

= 4 for ordinary steel moment frames

= 5 for ordinary steel concentrically braced frames

= 6 for intermediate steel moment frames

T = fundamental period of the structure in the considered direction

$$\leq C_u T_a$$

C_u = coefficient for upper limit on calculated period as provided in Table 7.8

T_a = approximate fundamental period

$$= C_T (h_n)^{3/4} \text{ for all cases}$$

= 0.1 N for moment-resisting frames not exceeding 12 stories that the
story height is at least 10 ft.

where

h_n = height in feet above the base to the highest level of the structure

C_T = 0.035 for steel moment-resisting frames

= 0.030 for steel eccentrically-braced frame acting along or with
moment resisting frames

= 0.030 for reinforced concrete moment-resisting frames

= 0.020 for all other buildings

N = number of stories

S_{D1}, S_{DS} = design spectral response acceleration at a period of 1.0 second
and in the short period range, respectively

$$S_{D1} = \frac{2}{3} S_{M1}$$

$$S_{DS} = \frac{2}{3} S_{MS}$$

where

$$S_{M1} = F_v S_1$$

$$S_{MS} = F_a S_s$$

F_v = site coefficient defined in Table 7.9

F_a = site coefficient defined in Table 7.10

S_1, S_s = mapped maximum considered earthquake spectral response acceleration at a
period of 1 second and at short periods, respectively, as determined in accordance
with Section 9.4.1, ASCE 7-98

Table 7.7 Occupancy importance factors (from Table 9.1.4, ASCE 7-98)

Seismic Use Group	I
I	1.0
II	1.25
III	1.5

* Seismic Use Group is defined in Table 9.1.3, ASCE 7-98

Table 7.8 Value of coefficient C_u (from Table 9.5.3.3, ASCE 7-98)

Design Spectral Response Acceleration at 1 second, S_{D1}	Coefficient C_u
≥ 0.4	1.2
0.3	1.3
0.2	1.4
0.15	1.5
0.1	1.7
0.05	1.7

Table 7.9 Value of F_v (from Table 9.4.1.2.4b, ASCE 7-98)

Site Class	Mapped Maximum Considered Earthquake Spectral Response acceleration at 1-Second Periods				
	$S_1 \leq 0.1$	$S_1 = 0.2$	$S_1 = 0.3$	$S_1 = 0.4$	$S_1 \geq 0.5$
A	0.8	0.8	0.8	0.8	0.8
B	1.0	1.0	1.0	1.0	1.0
C	1.7	1.6	1.5	1.4	1.3
D	2.4	2.0	1.8	1.6	1.5
E	3.5	3.2	2.8	2.4	-
F	-	-	-	-	-

* Site classification is defined in Table 9.4.1.2, ASCE 7-98

Table 7.10 Value of F_a (from Table 9.4.1.2.4a, ASCE 7-98)

Site Class	Mapped Maximum Considered Earthquake Spectral Response acceleration at Short Periods				
	$S_s \leq 0.25$	$S_s = 0.5$	$S_s = 0.75$	$S_s = 1.0$	$S_s \geq 1.25$
A	0.8	0.8	0.8	0.8	0.8
B	1.0	1.0	1.0	1.0	1.0
C	1.2	1.2	1.1	1.0	1.0
D	1.6	1.4	1.2	1.1	1.0
E	2.5	1.7	1.2	0.9	-
F	-	-	-	-	-

Table 7.11 Allowable story drift, Δ_a (from Table 9.5.2.8, ASCE 7-98)

Structure	Seismic Use Group		
	I	II	III
Structures, other than masonry shear wall or masonry wall frame structures, 4 stories or less with interior walls, partitions, ceilings and exterior wall systems that have been designed to accommodate the story drifts	$0.025h_{sx}$	$0.020h_{sx}$	$0.015h_{sx}$
Masonry cantilever shear wall structure	$0.010h_{sx}$	$0.010h_{sx}$	$0.010h_{sx}$
Other masonry shear wall structures	$0.007h_{sx}$	$0.007h_{sx}$	$0.007h_{sx}$
Masonry wall frame structures	$0.013h_{sx}$	$0.013h_{sx}$	$0.010h_{sx}$
All other structures	$0.020h_{sx}$	$0.015h_{sx}$	$0.010h_{sx}$

* h_{sx} is the story height below Level x

7.3.1.2 Lateral Seismic Force

The vertical distribution of seismic forces induced at each level shall be determined from equation (7.2).

$$F_x = C_w V \quad (7.2)$$

where

F_x = lateral seismic force at level x

V = total design lateral force or shear at the base of the building

C_{vx} = vertical distribution factor

$$= \frac{w_x h_x^k}{\sum_{i=1}^n w_i h_i^k}$$

where

w_i and w_x = portion of the total gravity load of the structure located or assigned to level i or x

h_i and h_x = height from the base to level i or x

k = exponent related to the building period

= 1 for structures having a period of 0.5 second

= 2 for structures having a period of 2.5 second

= 2 or determined by linear interpolation between 1 and 2

for structures having a period between 0.5 and 2.5 second

7.3.1.3 Combination of Load Effects

The effects on the structure and its components due to seismic force shall be combined with gravity loads in accordance with the combination of load effects provided in Section 5.3.1. The earthquake-induced force effects shall include vertical and horizontal effects as given by equation (7.3) or (7.4). The vertical seismic effect term $0.2S_{DS}D$ need not be included where S_{DS} is equal to or less than 0.125.

For the load combination in equation (5.2e), Section 5.3.1:

$$E = \rho Q_E + 0.2S_{DS}D \tag{7.3}$$

For the load combination in equation (5.2g), Section 5.3.1:

$$E = \rho Q_E - 0.2 S_{DS} D \quad (7.4)$$

where

D = effect of dead load

Q_E = effect of horizontal seismic force

ρ = reliability factor

$$1.0 \leq \rho = 2 - \frac{20}{r_{\max} \sqrt{A}} \leq 1.5$$

where

r_{\max} = ratio of the design story shear resisted by the single element carrying the most shear force in the story to the total story shear, for a given direction of loading

A = floor area in square feet of the diaphragm level immediately above the story

7.3.1.4 Drift Limitations

ASCE 7-98 requires the design story drift Δ shall not exceed the allowable story drift Δ_a as indicated in Table 7.11 for any story.

7.3.1.5 Spectral Response Acceleration

The spectral response acceleration S_a of a building in the lateral direction is used to define the horizontal ground motion intensity, which may be expressed by a total horizontal base shear force [49]:

$$S_a = \frac{V}{W} g \quad (7.5)$$

where

V = total horizontal base shear

W = total weight of the building

G = gravitational constant

7.3.1.6 Expected Yield Stress

One important factor of brittle fracture of beam-to-column moment connections in the Northridge earthquake is that the actual member yield stresses were generally higher than the specified minimum yield stress F_y , which elevated the connection demand. According to the AISC-Seismic Provisions for Structural Steel Building [48], the required strength of a connection or related member should be determined from the expected yield stress F_{ye} of the connected member

$$F_{ye} = R_y F_y \quad (7.6)$$

where

$R_y = 1.5$ for ASTM A36 steel

= 1.3 for A572 Grade 42

= 1.1 for others

7.3.2 Performance-Based Seismic Design

Serviceability drift limits are often taken as a measure of a building's performance at corresponding load levels. There are four building performance levels specified in FEMA 273 [39]: (1) Operational; (2) Immediate-Occupancy; (3) Life-Safety; and (4) Collapse-Prevention. Most buildings are able to meet or exceed the Operational Level under very low levels of ground shaking. However, it is usually not economically practical to design a structure based on this kind of performance under severe ground motion levels caused by earthquakes. Immediate-Occupancy refers to a very limited structural damage that would occur during an earthquake and minor repairs would not be required prior to reoccupancy. For this level, the building and its elements retain nearly all of their pre-earthquake stiffness and strength. Life-Safety means that significant damage has occurred to the structure after an earthquake. Although structural elements and components may be severely damaged, it will not result in large falling debris hazards. Injuries may occur due to the result of structural damage, but the overall risk of life is very low. The performance level of Collapse-Prevention means the building is on the verge of partial or total collapse. The stiffness and strength of the lateral-force-resisting system reduce greatly and large permanent lateral deformation of the structure has occurred. The structure may not be repaired and is not safe for reoccupancy.

Although the Operational Level is defined, its design criterion is not specified. The design criteria for other performance levels associated with lateral drifts at roof level are tabulated in Table 7.12 [38].

Table 7.12 Design criteria for structural performance levels (from Table 2-4, FEMA 273)

Structural system	Ratio of lateral drift at roof level to building height		
	Immediate Occupancy	Life Safety	Collapse Prevention
Steel moment frames	0.7 %	2.5 %	5 %
Braced steel frames	0.5 %	1.5 %	2 %

7.3.3 Analysis Procedures

The operation procedures of using the advanced analysis method to determine the pushover curve are summarized in the flow chart shown in Figure 7.13. In the analysis, the static-equivalent loading consists of constant gravity loads and monotonically increasing lateral loads. To do this, the scaling number of lateral forces is chosen as a number that is 10 times larger than that of gravity loads. The scaling number for lateral loads is decreased at a constant rate until the structure fails. Once the pushover curve is obtained, the base shear corresponding to each performance level can be identified and the performance level of the structure under specified loading condition can be determined.

7.3.4 One-Bay Two-Story Steel Frame Example

For simplicity, a one-bay two-story steel frame is selected to illustrate the application of advanced analysis to performance-based seismic design. It is noted that accidental torsional effects are not considered in this example, because the magnitude of the effects vary depending on the layouts of lateral resisting frames.

Figure 7.14 shows the one-bay two-story building. All connections are rigid. Preliminary W10×15 is used for roof beam and W10×19 is used for floor beam that are both continuously braced about their weak axes, while W10×19 is chosen for all columns which are bent about the strong-axis. ASTM A36 and A572 Grade 50 are respectively used for beams and columns in this example.

The uniform factored gravity loads and lateral seismic forces on roof and floor levels are listed in Table 7.13. The calculation of lateral seismic forces is based on the processes listed in Section 7.3.1.1 and 7.3.1.2. The constant gravity load intensities are applied on the roof and floor beams, while the lateral seismic forces are incrementally applied at the roof and floor levels. The relationship between the normalized base shear force and the ratio of roof drift to the building height are shown in Figure 7.15 for both the yield stress and the expected yield stress. The normalized base shear force or the spectral response acceleration S_a associated with the performance levels of Immediate Occupancy, Life Safety, and Collapse of the structure can be identified from this figure. It can be obviously seen that the case of yield stress can resist smaller base shear force or earthquake intensity than the case of expected yield stress. Note that the structure has collapsed before the performance level of Collapse Prevention is reached if the base shear force is large enough. The progressive occurrence and extent of plastic behavior are illustrated in Figures 7.16a and 7.16b for both cases of yield stress and expected yield stress, respectively. Note that all plastic hinges are formed at the ends of beam members for the case of yield stress, while some plastic hinges are formed at column ends for the

case of expected yield stress. It prevails that the expected yield stresses should be considered in seismic design to avoid the weak column condition.

For the base shear force and lateral seismic forces listed in Table 7.13, the lateral roof drifts are respectively 16.28 in. and 3.51 in. for the cases of yield stresses and expected yield stress. Thus, the criterion of the performance level of Life Safety is violated for the case of yield stress. On the other hand, the case of expected yield stress cannot meet the performance requirements of *Immediate Occupancy*, but it satisfies the criterion of Life Safety performance level.

Table 7.13 Distribution of lateral seismic forces

Story Level	Total Gravity Load (kips/ft)	w_i (kips)	C_s	V (kips)	C_{vx}	F_x (kips)
Roof	0.864	14.06	0.088	3.3	0.77	2.54
Floor	1.336	23.44			0.23	0.76
Σ	-	37.5	-	-	1	3.3

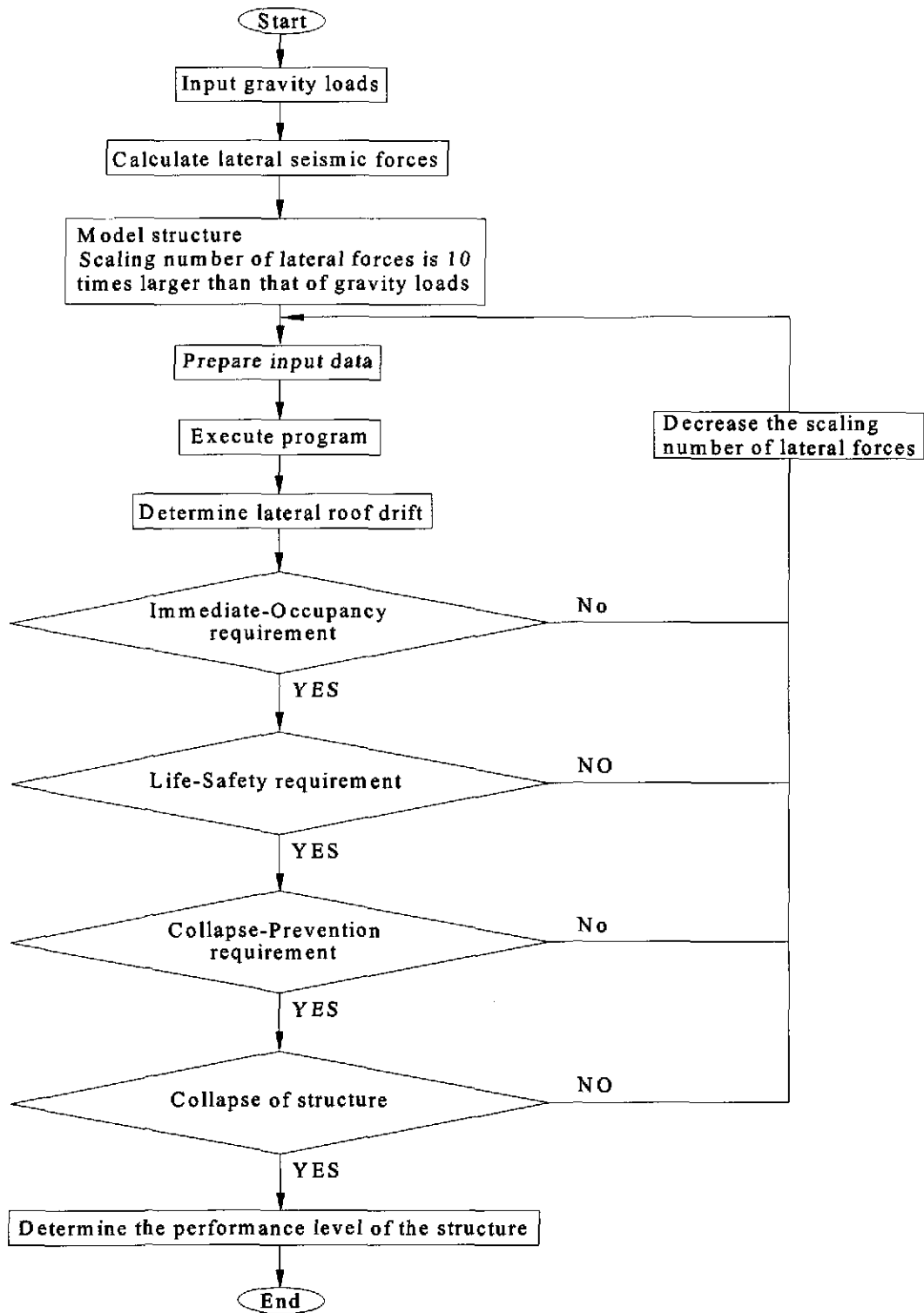


Figure 7.13 Pushover analysis procedure for seismic design using advanced analysis

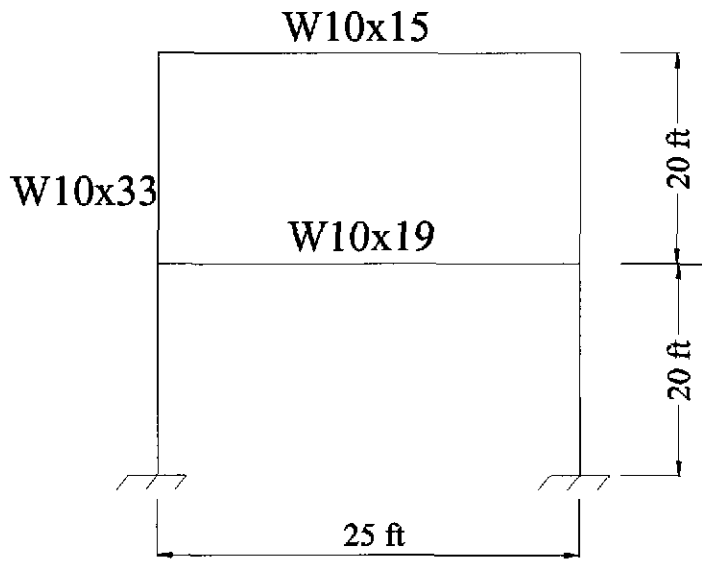


Figure 7.14 Two-story frame for the seismic performance-based design example

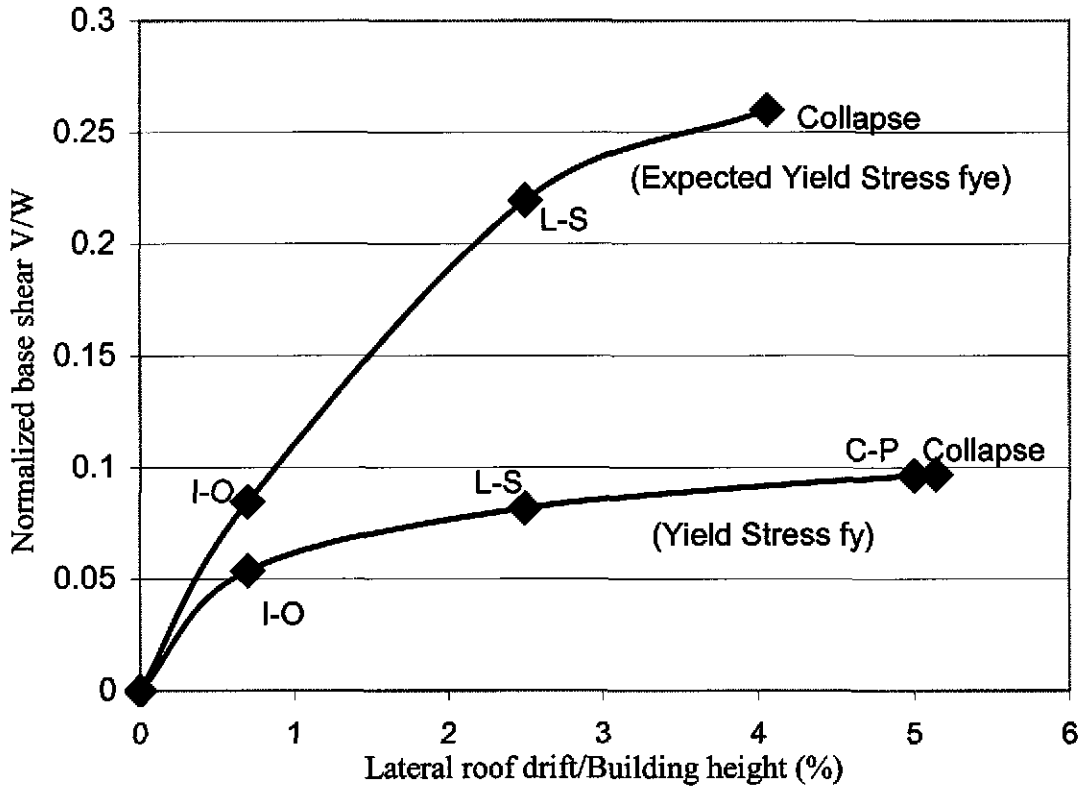


Figure 7.15 Performance curves of the two-story frame

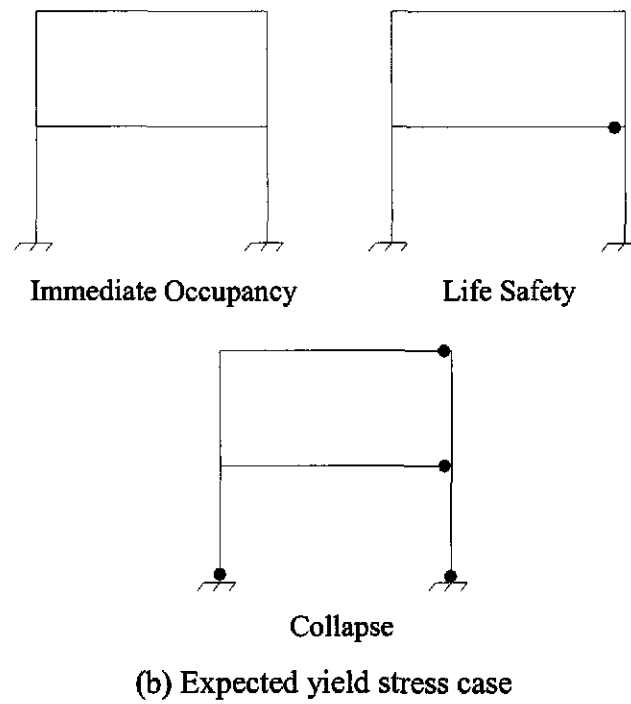
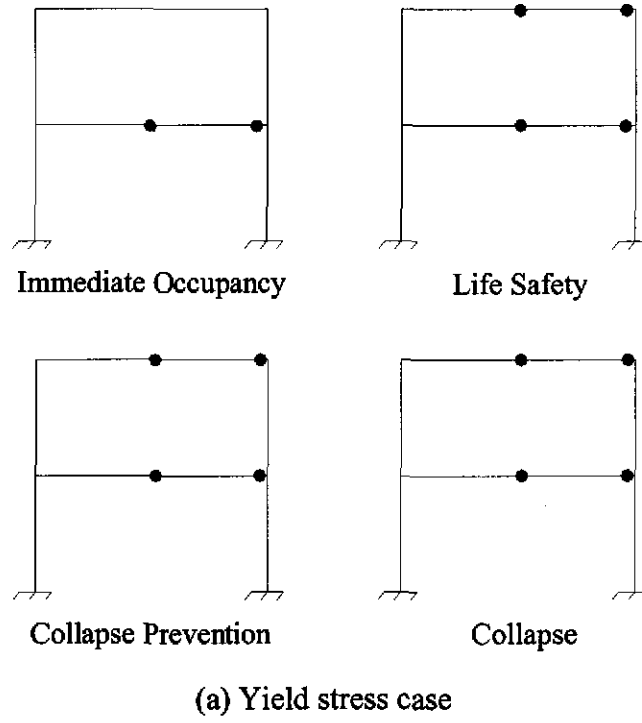


Figure 7.16 Plastic behavior of the two-story frame at different performance level

7.4 Summary

After several disasters such as 1994 Northridge earthquake and 2001 World Trade Center event, the need for performance-based seismic and fire resistance design are emerging. Advanced analysis is a computer-based analysis and design approach which is consistent with the characteristics of performance-based design. The procedures of applying advanced analysis method to the performance-based fire resistance and seismic design are proposed. Two examples are provided to show that advanced analysis is efficient and easy to implement for performance-based design of steel structures.

CHAPTER 8

CONCLUSIONS

The analysis and design method of steel frames indicated in the AISC-LRFD Specification was developed at the time that computer technology was not sufficient. At that stage, only simple calculation could be implemented. Therefore, first-order elastic analysis was adopted and all nonlinear effects were approximately involved in the design equations. In the AISC-LRFD method, the strength of a beam-column member affected by other part of the structural system is adjusted by using the effective length factor K that implicitly involves the effects of nonlinearities. In the direct analysis method, K -factor is set to be equal to unity and equivalent notional loads and/or modified stiffness are introduced to approximate the material nonlinearities and initial out-of-plumbness. For both LRFD and direct analysis methods, structural material remains elastic during the analysis process and the stiffness of the structural system and its members are not affected by the gradual yielding of steel. Therefore, compatibility between the actual inelastic members as examined by specified equations and the elastic system as assumed in the analysis is not satisfied. Since these two methods cannot trace the accurate force-displacement relations and predict the limit strength of a structural system and its members, tedious interaction equations are required to estimate the strength of each member.

For both AISC-LRFD and direct analysis methods, a structure is analyzed as a whole. However, the axial and flexural strength of each member is checked individually

through the design equations. The ultimate strength of the critical member in a structural system is considered as the design criterion and inelastic redistribution of internal forces cannot be involved. Therefore, determined member forces are not correct and a more conservative design result will be obtained. In addition, since member-based design approaches do not provide information about a structural system, it is difficult to implement performance-based design by using these methods.

Computer technology has developed to a stage that the effects of structural nonlinearities can be considered directly in the analysis process. The real structural behaviors can be accurately predicted and the limit state capacity and stability of a structural system and its members can be captured. As a result, the checks of corresponding specification rules and the use of K-factors are not required.

With the computer-based analysis technique, steel frame analysis and design is tending towards more on the overall system response and less on individual member response. Advanced analysis is a state-of-the-art analysis and design method which incorporates the aspects of engineering involving mechanics, material, and computing. Compared with conventional methods, advanced analysis provides more information such as failure mode and overstrength factors and allows inelastic redistribution of internal forces because it is a system-based design approach for steel structures. Thus, advanced analysis is consistent with performance-based design.

In this study, the force-displacement relationship comprising the key factors influencing steel frame behavior is described. Design procedures of using advanced analysis are provided. Selected examples show the ease and convenience of the advanced

analysis method. Design results similar to the AISC-LRFD method are obtained. All these provide structural engineers great confidence in applying advanced analysis to practical steel frame design. The applications of the advanced analysis method to the performance-based fire resistance design and seismic design are also presented in this study.

Although advanced analysis overcomes the drawbacks of member-based design approaches, some limitations are existed in current practice. For advanced analysis to achieve its full potential as a tool for the practical design of steel frames, future work required is to integrate the effects of local buckling of cross sections, lateral-torsional buckling of members, flexibility of connections, and 3-D member behavior into the advanced analysis. Secondary structural elements such as concrete floor slab, composite joists and walls may affect the structural behaviors of the steel frames. These effects should be taken into consideration by developing simple but realistic models that can be incorporated into the advanced analysis in the near future. Because the advanced analysis is efficient and accurate for steel frame design, it should be adopted in the applicable codes to popularize its use.

REFERENCES

1. AISC, *Load and Resistance Factor Design, Manual of Steel Construction*, 3rd ed., American Institute of Steel Construction, Chicago, IL, 2001.
2. AISC, *Allowable Stress Design Specification for Structural Steel Building*, American Institute of Steel Construction, Chicago, IL, 1989.
3. AISC, *Load and Resistance Factor Design, Manual of Steel Construction*, Vol. 1 and 2, 2nd ed., American Institute of Steel Construction, Chicago, IL, 1994.
4. J. Y. R. Liew, D.W. White, and W. F. Chen, " Beam-Column Design in Steel Frameworks-Insights on Current Methods and Trends," *Journal of Constructional Steel Research*, **18**, 269-308 (1991)
5. AISC-SSRC Task Group on Stability, *Draft Provisions on Frame/ Member Stability*, American Institute of Steel Construction, October 25, 2001.
6. S. E. Kim and D. H. Lee, " Second-Order Distributed Plasticity Analysis of Space Steel Frames," *Engineering Structures*, **24**, 735-744 (2002).
7. S. E. Kim, M. H. Park, and S. H. Choi, " Direct Design of Three-Dimensional Frames Using Practical Advanced Analysis," *Engineering Structures*, **23**, 1491-1502 (2001).
8. W. F. Chen, S. E. Kim, and S. H. Choi, " Practical Second-Order Inelastic Analysis for Three-Dimensional Steel Frames," *Steel Structures*, **1**, 213-223 (2001).
9. K. Wongkeaw and W. F. Chen, " Consideration of Out-of-Plane Buckling in Advanced Analysis for Planar Steel Frame Design," *Journal of Constructional Steel Research*, **58**, 943-965 (2002).

10. S. E. Kim, J. H. Lee, and J. S. Park, "3-D Second-Order Plastic-Hinge Analysis Accounting for Lateral Torsional Buckling," *International Journal of Solids and Structures*, **39**, 2109-2128 (2002).
11. S. E. Kim and J. H. Lee, "Improved Refined Plastic-Hinge Analysis Accounting for Local Buckling," *Engineering Structures*, **23**, 1031-1042 (2001).
12. P. Avery, *Advanced Analysis of Steel Frames Comprising Non-Compact Sections*, PhD thesis, School of Civil Engineering, Queensland University of Technology, Brisbane, Australia, 1998.
13. W. F. Chen and S. E. Kim, *LRFD Steel Design Using Advanced Analysis*, CRC Press, New York, 1997
14. W. F. Chen, "Structural Stability: from Theory to Practice," *Engineering Structures*, **22**, 116-122 (2000).
15. T. Kanchanalai, "The Design and Behavior of Beam-Column in Unbraced Steel Frames," *AISI Project No. 189, Report No. 2*, Civil Engineering/Structures Research Lab, University of Texas at Austin, October 1977.
16. N. E. Shanmugam and W. F. Chen, "An Assessment of K Factor Formulas," *Engineering Journal*, **32**, 3-11 (1995)
17. D. W. White and J. F. Hajjar, "Buckling Models and Stability Design of Steel Frames: a Unified Approach," *Journal of Constructional Steel Research*, **42**, 171-207 (1997).
18. L. F. Geschwindner, "A Practical Look at a Frame Analysis, Stability, and Leaning Columns," *Engineering Journal*, **39**, 167-181 (2002)

19. W. F. Chen, *Handbook of Structural Engineering*, CRC Press, New York, 1997.
20. W. F. Chen and E. M. Lui, *Structural Stability Theory and Implementation*, Elsevier, New York, 1987.
21. D. W. White and J. F. Hajjar, "Design of Steel Frames without Consideration of Effective Length," *Engineering Structures*, **19**, 797-810 (1997).
22. T. V. Galambos, *Guide to Stability Design Criteria for Metal Structures*, 4th ed., John Wiley & Sons, New York, 1988.
23. W. F. Chen and S. Toma, *Advanced Analysis of Steel Frames*, CRC Press, West Palm, FL, 1994.
24. S. E. Kim and W. F. Chen, "Practical Advanced Analysis for Braced Frame Design," *Journal of Structural Engineering*, **122**, 1266-1274 (1996).
25. W. F. Chen and I. Sohal, *Plastic Design and Second-Order Analysis of Steel Frames*, Springer-Verlag, New York, 1995.
26. E. M. Lui and W. F. Chen, "Analysis and Behavior of Flexibility Jointed Frames," *Engineering Structures*, **8**, 107-118 (1986)
27. W. F. Chen and T. Atsuta, *Theory of Beam-Columns, Vol. 1, In-Plane Behavior and Design*, MacGraw-Hill, New York, 513pp., 1976.
28. L. Duan and W. F. Chen, "A Yield Surface Equation for Doubly Symmetrical Sections," *Engineering Structures*, **12**, 144-119 (1990).
29. J. Y. R. Liew, D. W. White, and W. F. Chen, "Chapter 2.5: Beam-Column," *Constructional Steel Design, An International Guide*, P. J. Dowling, ed., Elsevier Applied Science Publishers, England, 105-132, 1992.

30. J. Y. R. Liew, D. W. White, and W. F. Chen, "Second-Order Refined Plastic Hinge Analysis for Frame design: Part 1," *Journal of Structural Engineering*, ASCE, **119**, 3196-3216 (1993).
31. N. Kishi and W. F. Chen, "Moment-Rotation Relations of Semi-Rigid Connections with Angles," *Journal of Structural Engineering*, ASCE, **116**, 1813-1834 (1990).
32. J. Y. R. Liew, *Advanced Analysis for Frame Design*, PhD dissertation, School of Civil Engineering, Purdue University, West Lafayette, IN, 1992.
33. ASCE, *ASCE 7-98 Minimum Design Loads for Buildings and Other Structures*, American Society of Civil Engineers, New York, 2000.
34. A. Aminmansour, "A New Approach for Design Steel Beam-Column," *Engineering Journal*, **37**, 41-72 (2000).
35. L. B. Burgett, "Selection of a "Trial" Column Section," *Engineering Journal*, **10**, 54-59 (1973)
36. S. E. Kim and W. F. Chen, "A Sensitivity Study on Number of Elements in Refined Plastic-Hinge Analysis," *Computers and Structures*, **66**, 665-673 (1998).
37. B. Ellingwood, "Serviceability Guidelines for Steel Structures," *Engineering Journal*, **26**, 1-8 (1989).
38. Federal Emergency Management Agency, *NEHRP Guidelines for the Seismic Rehabilitation of Buildings, Rep. FEMA 273*, Washington D. C., 1997.
39. D. Talamona, J. M. Franssen, J. B. Schleich, and J. Kruppa, "Stability of Steel Columns in Case of Fire: Numerical Modeling," *Journal of Structural Engineering*, **123**, 713-720 (1997).

40. American Society for Testing and Materials, *Standard Test Methods for Fire Tests of Building Construction and Materials, Rep. E 119*, PA, 1998.
41. C. G. Bailey, T. Lennon, and D. B. Moore, “ The Behavior of Full-Scale Steel-Framed Buildings Subjected to Compartment Fires,” *The Structural Engineer*, **Vol. 77/No 8**, 15-21 (1999).
42. T. O’Meagher and B. Jones, “ Fire Resistance of Structural Members: A Performance-Based Approach,” *The Structural Engineer*, **79**, No.13, 20-21 (2001).
43. British Steel. *The Behavior of a Multi-Story Steel Framed Building Subjected to Fire Attack- Experimental Data*, Swindon Technology Center, 1998.
44. S. L. Chan and P. P. T. Chui, “ A Generalized Design-Based Elastoplastic Analysis of Steel Frames by Section Assemblage Concept,” *Engineering Structures*, **19**, 628-636 (1997).
45. D. H. Skinner, discussion of “ Effects of Elevated Temperature on Structural Members,” *Journal of Structural Division, ASCE*, **102**, 685-687 (1976)
46. A. Rubert and P. Schaumann, “Structural Steel and Plane Frame Assemblies under Fire Action,” *Engineering Structures*, **13**, 371-382 (1986).
47. S. L. Chan and B. H. H. Chan, “ Refined Plastic Hinge Analysis of Steel Frames under Fire,” *Steel and Composite Structures*, **1**, 111-130 (2001)
48. AISC, *Seismic Provisions for Structural Steel Buildings*, American Institute of Steel Construction, Chicago, 1997.
49. A. K. Chopra, *Dynamics of Structure Theory and Application to Earthquake Engineering*, Prentice Hall, New Jersey, 1995.